NASA Contractor Report
CR-179625
EDR 12909

[redacted]
COPY NUMBER 056

ADVANCED GEARBOX TECHNOLOGY FINAL REPORT

by
N. E. ANDERSON
R. W. CEDOZ
E. E. SALAMA
D. A. WAGNER

ALLISON GAS TURBINE DIVISION
General Motors Corporation

PREPARED
for
NATIONAL AERONAUTICS
AND
SPACE ADMINISTRATION

NASA LEWIS RESEARCH CENTER
CONTRACT NAS3-24341

1. Report No.	2. Government Accession No.	3. Recipient's Catalog No.
CR-179625		

4. Title and Subtitle	5. Report Date
Advanced Gearbox Technology (AGBT) Final Report	June 1987
	6. Performing Organization Code

7. Author(s)	8. Performing Organization Report No.
N. E. Anderson, R. W. Cedoz, E. E. Salama, D. A. Wagner	EDR 12909
	10. Work Unit No.

9. Performing Organization Name and Address	11. Contract or Grant No.
Allison Gas Turbine Division, GM Corp. P.O. Box Box 420 Indianapolis, IN 46206-0420	NAS3-24341
	13. Type of Report and Period Covered Contractor Report Aug. 84 thru Jan. 87

12. Sponsoring Agency Name and Address	14. Sponsoring Agency Code
NASA-Lewis Research Center 21000 Brookpark Rd. Cleveland, Ohio 44135	RTOP 535-03-22

15. Supplementary Notes

NASA Project Manager - D. C. Reemsnyder
Published in part and presented at the June 1987 AIAA/SAE/ASME/ASEE 23rd Joint Propulsion Conference in San Diego, CA

16. Abstract

An advanced 13,000 HP. counterrotating (CR) gearbox was designed and successfully tested to provide a technology base for future designs of geared propfan propulsion systems for both commercial and military aircraft. The advanced technology CR gearbox was designed for high efficiency, low weight, long life, and improved maintainability. The differential planetary CR gearbox features double helical gears, double row cylindrical roller bearings integral with planet gears, tapered roller prop support bearings, and a flexible ring gear and diaphragm to provide load sharing.

A new Allison propfan back-to-back gearbox test facility was constructed. Extensive rotating and stationary instrumentation was used to measure temperature, strain, vibration, deflection, and efficiency under representative flight operating conditions. The tests verified smooth, efficient gearbox operation.

The highly-instrumented advanced CR gearbox was successfully tested to design speed and power (13,000 HP), and to a 115% overspeed condition. Measured CR gearbox efficiency was 99.3% at the design point based on heat loss to the oil. Tests demonstrated low vibration characteristics of double helical gearing, proper gear tooth load sharing, low stress levels, and the high load capacity of the prop tapered roller bearings. Applied external prop loads did not significantly affect gearbox temperature, vibration, or stress levels. Gearbox hardware was in excellent condition after the tests with no indication of distress.

17. Key Words (Suggested by Author(s))	18. Distribution Statement
Advanced Gearbox Gearbox - Turboprop Gearbox - Aircraft	[redacted]

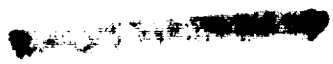

FOREWORD

The Advanced Gearbox Technology (AGBT) program was performed under the direction of Gerald A. Kraft, Advanced Turboprop Project Office, NASA Lewis Research Center. The Allison Gas Turbine Division of General Motors Corporation managed and performed the work reported herein and totally funded the program to test the fully instrumented advanced counterrotation gearbox and slave gearbox. The Allison program manager was R. D. Anderson. D. A. Wagner was the engineering design manager. Primary individuals responsible for the design were N. E. Anderson, R. W. Cedoz, P. V. Cagle, and E. E. Salama.

Other Allison engineering staff specialists performed the component finite element modeling, dynamics analyses, and bearing analyses.

L. Nightingale and L. Miller were responsible for gearbox testing including test equipment design, installation and operation, gearbox buildup, and data reduction.

The support of the NASA-Lewis specialists who contributed in design reviews and evaluations throughout the design process is recognized. In particular, the authors thank D. P. Townsend and J. J. Coy and his staff for the detailed engineering review of the design.

TABLE OF CONTENTS

TABLE OF CONTENTS (CONT)

LIST OF ILLUSTRATIONS

LIST OF ILLUSTRATIONS (CONT)

LIST OF ILLUSTRATIONS (CONT)

LIST OF TABLES

LIST OF TABLES (CONT)

1.0 SUMMARY

The Advanced Gearbox Technology (AGBT) program was conducted by Allison Gas Turbine Division of the General Motors Corporation under contract from NASA Lewis Research Center. The objective was to develop a long-life, low maintenance gearbox suitable for geared propfan propulsion systems for use in commercial airline service.

An advanced 13,000 HP, counterrotating (CR) gearbox was designed and successfully tested to provide a technology base for future geared propfan propulsion systems for both commercial and military aircraft. The gearbox was designed for high efficiency (>99%), 8.33:1 gear ratio, low weight, long life, and improved maintainability. Modern design techniques and advanced gear and bearing materials were used to provide increased reliability. The differential planetary CR gearbox features double helical gears, double row cylindrical roller bearings integral with the four planet gears, tapered roller bearings for prop support, and a flexible ring gear and diaphragm to provide load sharing. Extensive rotating and stationary instrumentation including an internal telemetry system were incorporated in the gearbox design to allow measurement of temperature, strain, vibration, deflection, and efficiency under representative flight operating conditions.

A new Allison CR propfan back-to-back gearbox test facility was constructed. This recirculating power rig loads the test gearbox acting as a speed reducer against the slave gearbox acting as an increaser. Propfan loads were applied to the housings through a series of pneumatic rams to simulate flight load conditions.

The highly-instrumented advanced CR gearbox was successfully tested to design speed and power (13,000 HP), and to a 115% overspeed condition. Estimated CR gearbox efficiency was 99.3% at the design point based on heat loss to the oil. The unique rotating instrumentation operated satisfactorily and verified smooth, efficient gearbox operation.

Parametric tests demonstrated the predicted low vibration characteristics of double helical gearing, proper gear tooth load sharing, low stress levels, and the high load capacity of the prop tapered roller bearings. Vibration and temperature levels were primarily a function of speed. Applied external prop thrust and moment loads did not significantly affect gearbox temperature, vibration, or stress levels.

Gearbox hardware was in excellent condition after the tests with no indication of distress. Successful testing of the full-scale CR gearbox has demonstrated the practicality of advanced technology high-power gearboxes for future propfan aircraft.

2.0 INTRODUCTION

Prop-Fan propulsion system technology was reviewed extensively in the NASA sponsored Advanced Prop-Fan Engine Technology (APET) Definition Studies (Ref 1) performed by three major U.S. gas turbine engine manufacturers--Allison, Pratt & Whitney, and General Electric. All three studies identified the potential fuel savings of Prop-Fan powered aircraft compared to turbofans of the same technology level. As a part of that study, technology needs were evaluated for purposes of defining the technology needs of production model Prop-Fan propulsion systems of the early 1990s. The conclusion from the APET study was that a major gearbox technology project is needed to develop long life, low maintenance gearboxes suitable for commercial airline service. An immediate response to this recommendation was an extension of the APET study to provide an in depth look at single rotation and counterrotation gearboxes and Prop-Fan pitch change systems in the 10,000 shp power class. These preliminary design activities identified design features that would significantly contribute to achieving the long life/low maintenance objectives. This work (Ref 1) became the starting point for major technology verification programs jointly sponsored by NASA and industry.

Allison began the AGBT program with NASA in August 1984 with the goal of testing an advanced technology gearbox in a rig configuration with as many technology features as practical in the initial test hardware. Technology verification was to be accomplished in a full-scale counterrotation gearbox that would have the potential to accommodate various gear train types. The program was structured to allow approximately one year for each phase--design, fabrication, and test.

The gearbox design task was aimed at developing component technologies applicable to large (10,000 to 16,000 shp) turboprop engines. It identified near-term and long-term concepts relative to achieving long life (15,000 to 30,000 hr system mean time between unscheduled removal [MTBUR]), ease of maintenance, and a high level of performance. Near-term advanced technologies (capable of being fabricated in the 1985/1986 time period) were selected and applied in the baseline design.

Testing of the advanced counterrotation gearbox was not part of this NASA contract. Allison funded the testing to verify the advanced technologies implemented in the design. Extensive rotating and stationary measurements were made of temperature, strain, vibration and movement under representative flight operating conditions.

3.0 CONCEPTUAL DESIGN

3.1 SUMMARY AND CONCLUSIONS--CONCEPTUAL PHASE

In the conceptual design, basic requirements for a counterrotating Prop-Fan gear system were established, various schemes analyzed, and specific gear and bearing forms selected. Results of these analyses are summarized in Table 3-I.

Table 3-I.
Summary of conceptual design analysis.

Item	Selected configuration	Advantages
General configuration	Differential planetary	Torque split between props is fixed and nearly equal; compact; lightweight; high mechanical efficiency; good reliability and maintainability
Gears	Double helical	Low vibration; low stress; allows use of high capacity cylindrical planet bearings
Planet bearing	Cylindrical roller	Highest capacity rolling element bearing for given space; easy to manufacture an outer race integral with the planet gear
Prop bearings	Tapered roller bearings	Less space required between bearings; bearing stiffness can be increased with axial preload; eliminates use of three bearings
Gear and planet bearing material	CBS 600	Allows operation up to 500°F; better rolling contact fatigue life compared with AISI 9310
Housing	Aluminum casting	Configuration prevents propeller loads from affecting gears; aluminum eliminates corrosion problems

The gear system selected has met all the design goals established at the start of the design. The long life requirement has been addressed by keeping stresses in bearing and gear contacts low. The planet bearing configuration, for example, uses very high capacity cylindrical roller bearings. The structure surrounding these bearings was selected to prevent operation under misaligned conditions. Advanced bearing and gear materials were selected to extend fatigue life and allow operation at higher temperatures. The selected

configuration represents a comprehensive assessment of the design requirement and incorporates the latest bearing and gear technology into a modern turboprop gear system design.

During the conceptual design, various areas of gear system technology were investigated and found to be promising, but were not selected for the AGBT design. In many cases these items, listed in Table 3-II, represent additional risk or require extensive development effort. In some areas no alternate concepts were deemed viable for the design requirements.

Table 3-II.
Alternate design concepts.

- o Configuration
  - The differential configuration was determined to be ideally suited for Prop-Fan gearbox requirements; no alternatives are recommended.
- o Gears and planet bearings
  - Single helical gears and tapered roller planet bearings
  - High contact ratio spur gears and single row spherical or cylindrical planet bearings
- o Gear and planet bearing materials
  - CBS 1000M
  - M50 NiL
- o Propeller mounting system/prop bearings
  - The tapered roller bearing mounting system was found to have many advantages over cylindrical/ball bearing systems; no alternatives are recommended.
- o Housing
  - Stainless steel welded or cast construction
- o Planet carrier
  - Composite materials
- o Processing that can be implemented in the AGBT gearbox
  - Mirror finishing of gear teeth (ultrasmooth surface finish)
  - Ion implantation of materials to reduce friction on tapered bearing ribs
  - Titanium nitriding of splines (very hard surface coatings)

3.2 DESIGN REQUIREMENTS

The AGBT design requirements are divided into two categories: design goals and specific design parameters. The design goals include increased reliability and maintainability as compared to existing turboprop systems, high efficiency (greater than 99%), and low system weight. These objectives must be met for the geared Prop-Fan system to be competitive with current turbofan engines. Specific design parameters are listed in Table 3-III.

The AGBT gearbox power, input speed, and ratio were selected based on the propeller and engine combination representative of future counterrotation Prop-Fan

aircraft. Best estimates made for these parameters, including anticipated future counterrotating Prop-Fan growth, are in Table 3-IV.

Table 3-III.
Specific design parameters.

- o Power, speed, and gear ratio
- o Design life of 30,000 hr MTBUR
- o Mission profile/duty cycle
- o Prop-Fan aerodynamic loads
- o Flight maneuver loads
- o Prop-Fan interface requirements
- o Installation requirements

Table 3-IV.
Design requirements.

Maximum takeoff power	13,000 hp
Gearbox ratio	8.33
Engine speed	9500 rpm
Prop-Fan orientation	pusher
Propeller speed	1140 rpm

The 13,000 hp gearbox design power level is consistent with NASA requirements (10,000 to 16,000 hp) and with future Prop-Fan propulsion systems. The Allison 578-D (10,000 shp) and 578-E (13,000 hp) engines, both based on propulsion technology developed in the T701 engine program, are representative for this application. The first Prop-Fan systems are expected to operate at 10,000 shp. Selection of the gearbox design power level of 13,000 shp allows future growth of the engine to be consistent with a wide range of aircraft.

The prop size and gear ratio selection is based on the APET study (Ref 1) as well as for the Allison 578-D and 578-E engines which are in the midst of configuration studies. Counterrotation Prop-Fan performance data from Hamilton Standard were used in this assessment. A 6 x 6 configuration with a tip speed of 750 ft/sec was recommended.

In Figure 3-1, meantime between unscheduled removal (MTBUR) for the T56 Series III propulsion system is compared to the AGBT goal of 15,000 to 30,000 hr. Military versions of the T56 gearbox are typically removed after 4000 hr for maintenance while commercial gearboxes have achieved 8000 hr MTBUR. The difference can be explained in maintenance procedures and repair practices. Commercial aircraft are used continuously each day and are subjected to routine

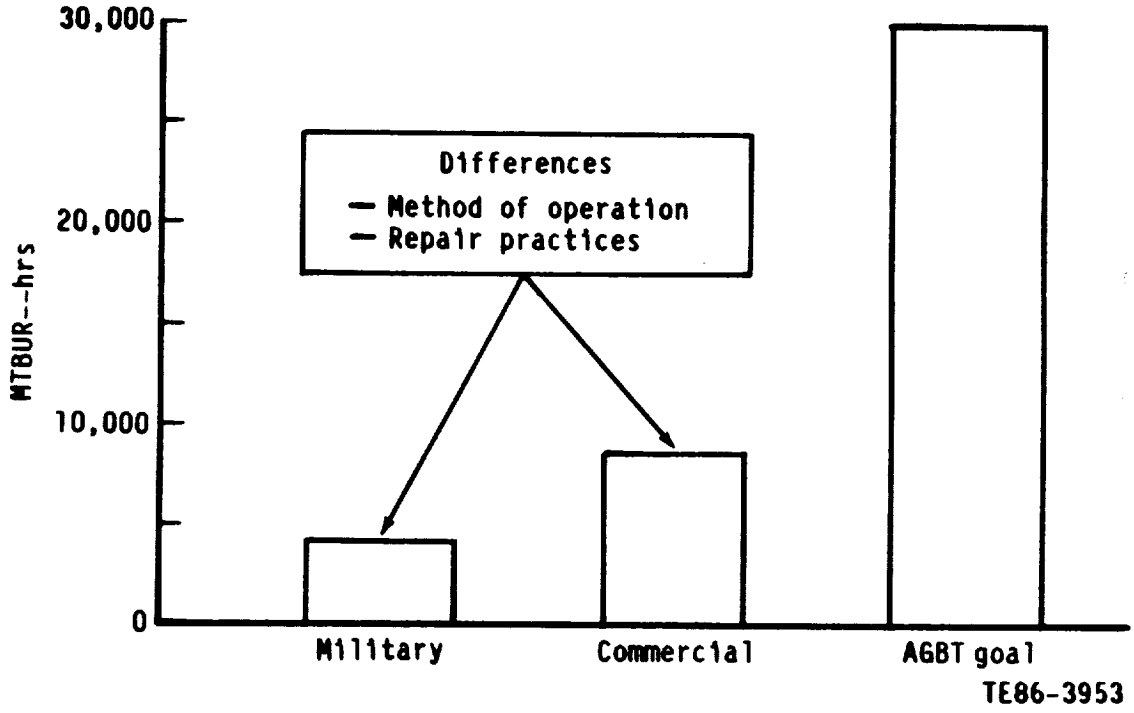

Figure 3-1. AGBT design life compared with T56 Series III experience.

maintenance practices. Military aircraft may stand idle for long periods of time and maintenance is done only when required. The AGBT goal is significantly longer than that currently obtained with the T56 gearbox. Achieving this increase in life requires application of detailed analytical techniques and use of the extensive field data available on the T56 gearbox.

The mission profile used in the AGBT studies is shown in Table 3-V. It is an intercity mission developed for a 150 passenger aircraft. A flight of 62.3 minute duration will cover 300 nautical miles. The mission profile can be transformed into a duty cycle for bearing and gear life calculations by combining this information with steady-state propeller loads. These loads are shown in Figure 3-2 for a 13 ft diameter prop. Loads for smaller diameter props would be lower. The loads shown in Figure 3-2 combine to form a sizable pitching moment (M_P). Maximum loads occur under takeoff conditions where M_P is positive. At cruise conditions both M_P and normal force (F_N) reverse directions and produce a pitching moment in the negative direction of equal magnitude to those loads under takeoff. This has the effect of balancing loads in either direction under the varying flight conditions and does not bias the design for either flight condition. Effects of yaw moment are small in comparison to the pitching moment but are also included in the design. Information on propeller inflow angle including the engine mounting angle is not known at present. Since these angles can affect propeller loads, the values shown in Figure 3-2 must be considered approximate at this time.

In addition to the steady-state propeller loads, flight maneuver loads must also be included in design calculations. In this study the MIL-E-8593A specification modified for commercial turboprops was used. Calculations were made

Table 3-V.
Gearbox mission profile.

Mission phase	Time min	Altitude ft	Velocity M_N	Gearbox input power, hp
Start and warmup	15.0	Sea level	0.0	624
Takeoff	1.0	Sea level	0.0	13,000
First climb	4.0	Sea level to 10,000	0.4	12,500
Second climb	17.1	10,000 to 30,000	0.6	11,000
Cruise	14.7	32,000	0.72*	8,000
Descent	10.5	15,000	0.6	572
Total time	62.3			

*Assumed from the APET studies

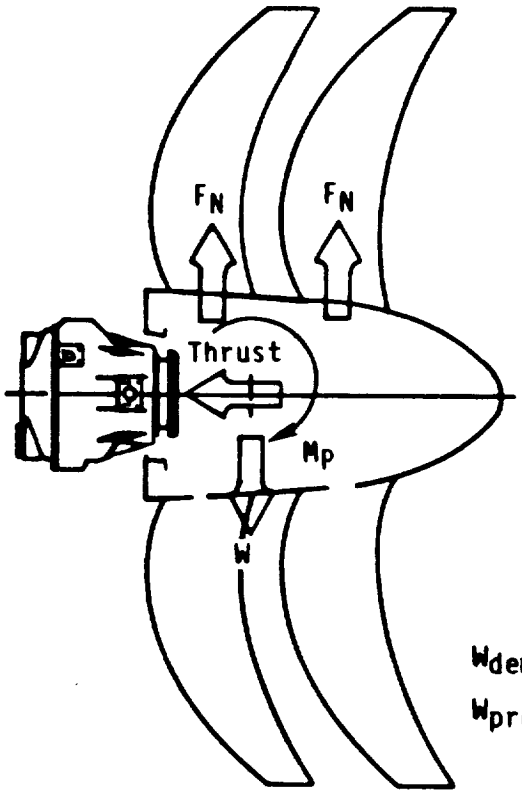

Flight condition	F_N normal load lbf	M_P pitching ft-lbf	M_Y* yawing ft-lbf	Thrust lbf
Warmup	0	0	0	800(1)
Takeoff	3095	10810	±3080	19800
Climb No. 1	2540	5750	±1650	13280
Climb No. 2	2515	4820	±1380	8370
Cruise	-2520	-4290	±1230	4500
Descent	1485	3250	930	-150

*Moment—about a vertical axis

(1)Maximum static thrust = 26,600 lbf

W_{demo} = 2670#

$W_{production}$ = 2220#

TE86-3954

Figure 3-2. Steady-state Prop-Fan loads for pusher gearbox configuration.

to determine the worst combination of aerodynamic and maneuver loads. A 10G down inertia load combined with steady-state cruise loads was found to produce the largest total load. This point was chosen as the housing and prop shaft design load. Normally an aircraft manufacturer would specify maneuver loads for their airframe. Since this information is not available, the information shown in Figure 3-3 was used for sizing purposes.

Loads used for gearbox component sizing are shown in Table 3-VI. Gears are designed for the takeoff power level of 13,000 hp. Bearings were designed for the mean cubic power level resulting from the steady-state propeller loads and the mission profile. The propeller shaft was designed for worst case maneuver inertia loads and cruise propeller load, simultaneously. This stress level was set to be the high cycle fatigue endurance limit. The prop shaft would have infinite life at these stress levels. The housing was designed for the same combination of loads but limiting stress was set to be the three sigma elastic limit. This will allow additional capability for any load above this level. All components were designed for a static overload of 1.5 times the maximum normal load.

Table 3-VI.
Loads used to size gearbox components.

Component	Design point	Source of value
Gears	Takeoff power level	13,000 hp
Bearings (for life calculations)	Mean cubic power level	Steady-state propeller loads and mission profile
Prop shaft	Cruise aero loads with 10Gs down, 2Gs forward, and 1G side force; stress limit = high cycle fatigue endurance limit	Steady-state propeller loads with MIL-E-8593E (AS) inertia loads (modified for commercial turboprops)
Housing	Same as prop shaft but stress limit = 3σ elastic limit	Steady-state propeller loads with MIL-E-8593 (AS) inertia loads (modified for commercial turboprops)
Carrier	Takeoff power level	13,000 hp
All components--static overload	1.5 x maximum normal external load	MIL-E-8593E (AS)

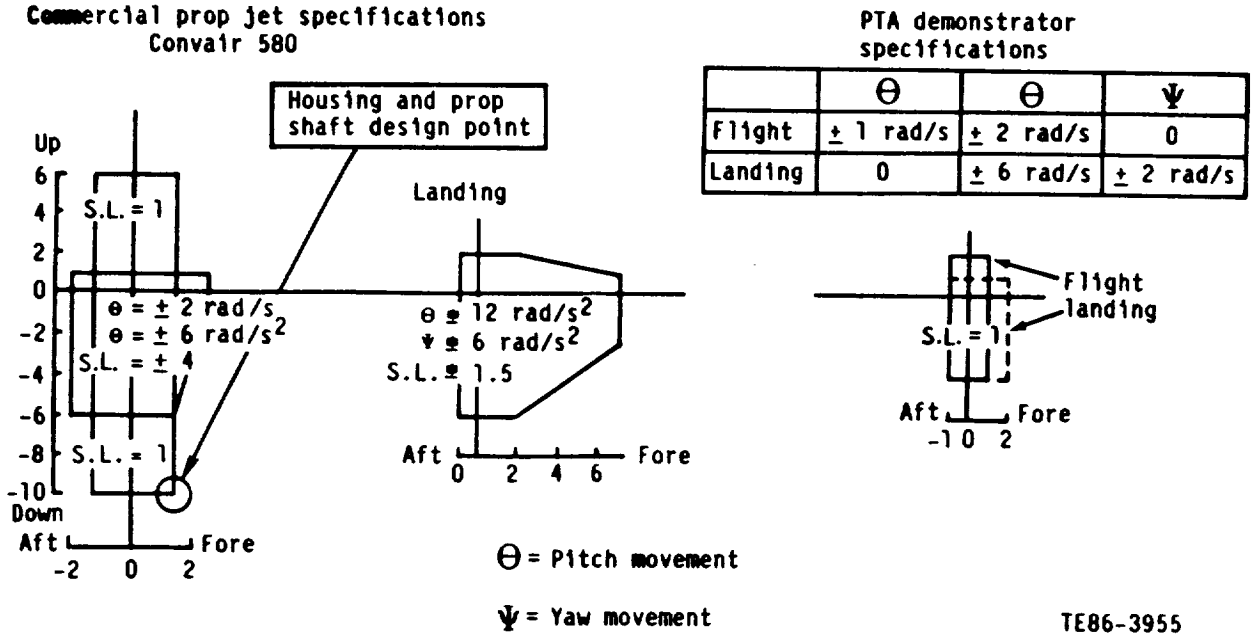

	Θ	Θ	Ψ
Flight	± 1 rad/s	± 2 rad/s	0
Landing	0	± 6 rad/s	± 2 rad/s

Figure 3-3. Flight maneuver inertia loads (Gs).

Gearbox/Prop-Fan interface requirements were sought from Hamilton Standard and integrated into the gearbox design. These requirements are listed in Table 3-VII. The entire prop assembly will be bolted to a flange on the propeller shaft. Although a curvic coupling was considered for this connection point, a bolted flange to facilitate removal and installation was preferred. The aft prop will be driven through a spline internal to the bolted flange. Oil will be supplied to the prop through a tube at the centerline of the gearbox. This oil is also used to cool the Prop-Fan. Oil is returned to the gearbox at the bolted flange i.d.

Table 3-VII.
Gearbox Prop-Fan interface requirements.

Mechanical
- Torque split: front prop--56%, rear prop--44%
- Front prop connection--bolted flange
- Rear prop connection--Spline internal to prop hub
- Oil supply tube required at drive centerline

Lubrication
- 3.75 gpm oil at 180°F, 100 lb/in.^{2} gage
- Heat transferred to oil--15 hp at takeoff, 8 hp at ground idle

A space allocation was made in the conceptual design for equipment required for flight. Items such as a safety coupling, a propeller brake, oil pumps, and a power takeoff (PTO) for future accessories were sized and space allocated for this equipment. Components were designed to be modular and easy to remove and replace. Mounting pads on the housing casting were designed.

3.3 CONFIGURATION STUDY

One of the first considerations in designing a counterrotating Prop-Fan gearbox is the general arrangement of the engine, gearbox, and Prop-Fan on the aircraft. Studies have shown that there are advantages for both tractor and pusher arrangements, depending on the application. Examples of both are shown in Figures 3-4 and 3-5. Although these figures illustrate a fuselage mounting, wing mounted Prop-Fans are also being considered. The impact of having this large number of potential configurations on the conceptual design of the gearbox is surprisingly minor. In each case, the Prop-Fan is nose-mounted from the gearbox housing and the gearbox is suspended from the engine. Apart from detail on the engine to gearbox mounting arrangement, the basic gearbox design requirements are the same. The conceptual design study presented applies to both tractor and pusher arrangements. Section 3.6 discusses specific differences between the two arrangements.

A configuration study was conducted to select the best gear arrangement for the Prop-Fan system. Six candidate gearsets were considered in the configuration study. Four of these provided speed control of the two output shafts while the other two maintained a constant torque split. The torque control

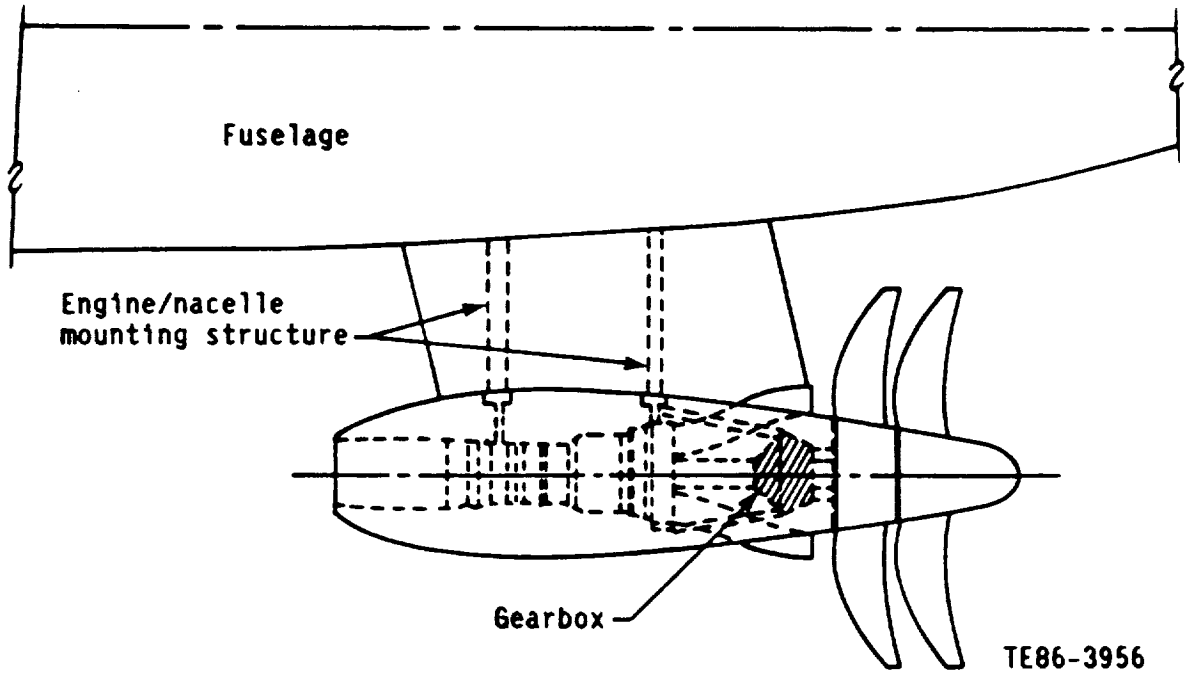

Figure 3-4. Gearbox installation in a pusher arrangement.

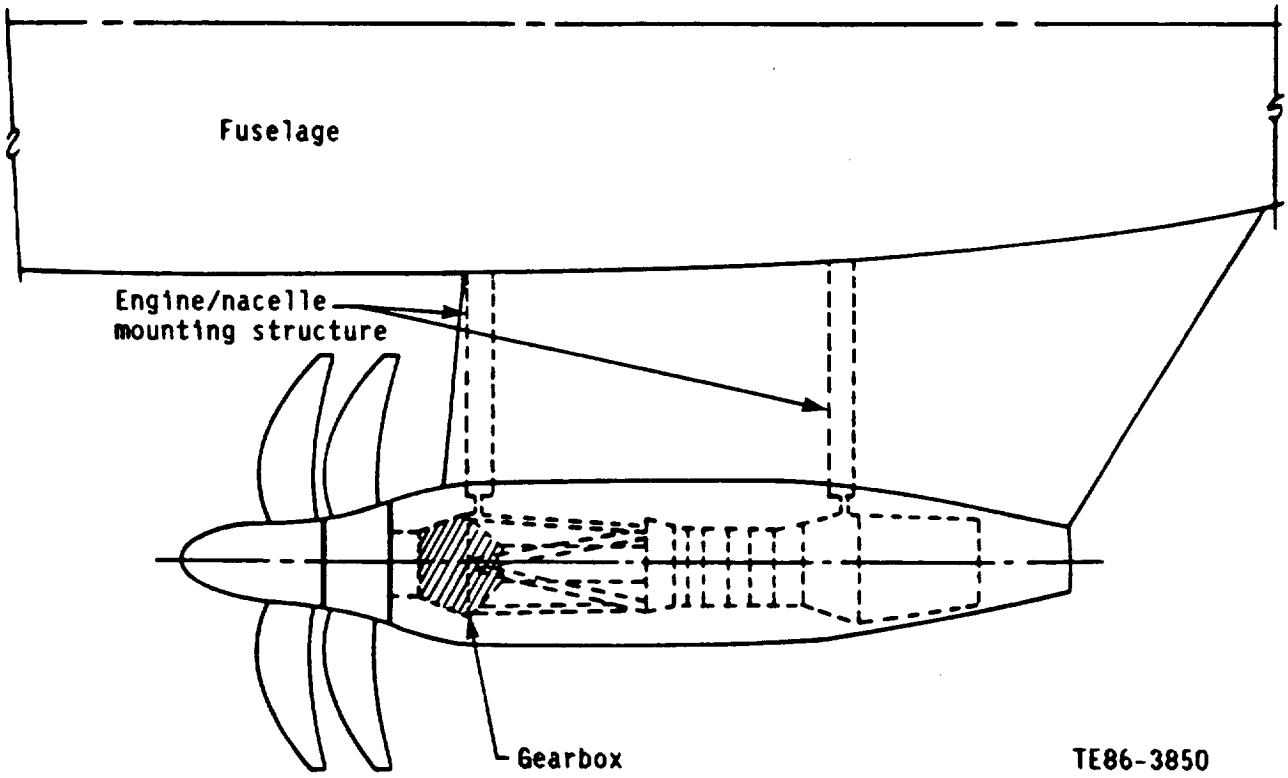

Figure 3-5. Gearbox installation in a tractor arrangement.

gearsets include the differential planetary and the differential epicyclic gear trains. The six configurations are shown in Figure 3-6. At the time of this study, there was no requirement for speed or torque control. All gearsets were considered on their own merit assuming that either could be used. The selection process consisted of three phases. The initial phase considered part count, as shown in Table 3-VIII. The split path planetary was eliminated here. Next, a forced decision technique was used to reduce the number of candidates from five to three, as shown in Table 3-IX. Reliability and efficiency were given high weight factors. In this phase the differential epicyclic was eliminated due to the large diameters required at reduction ratios greater than 4:1. Of the remaining four, the differential planetary and compound planetary ranked high. The two remaining gearsets had similar ratings. Of these two, the split path parallel offset gearset was selected over the triple compound idler due to its better maintainability and possible size advantage. Sketches of these three gearsets were made and a final weighted decision analysis was performed. The results are shown in Table 3-X. Again, reliability and efficiency were weighted heavily. Of the three remaining gearsets, the differential planetary received the highest rating. Apart from this, the differential planetary was the only torque control gearset left in the evaluation. The Hamilton Standard recommendation was for a torque splitting gearset. Thus, from two standpoints the differential planetary was selected.

Table 3-VIII.
Selection step 1: major part count comparison of six gearing configurations.

Gearing configuration	Planet bearings	Bearings	Gears	Bearings and gears	Power paths
Differential planetary	8	13	6	19	4
Compound planetary	8	13	11	24	4
Split path parallel offset (inline)	0	12	8	20	2
Triple compound idler	0	10	12	22	3
Differential epicyclic	6	10	8	18	3
Split path planetary*	8	19	11	30	4

*Deleted

Table 3-IX.
Selection step 2: forced decision comparison of five gearsets.

Category	Weight factor	Differential planetary	Compound planetary	Split path parallel offset	Triple compound idler*	Differential epicyclic*
Reliability	25	75	50	25	0	100
Efficiency	22	88	66	22	44	0
Maintenance	18	36	18	72	54	0
Cost	16	64	48	0	32	16
Weight	12	48	36	12	24	0
Size	7	17.5	17.5	28	7	0
		328.5	235.5	159	161	116

*Deleted

The differential and compound planetaries are similar gearsets. In the differential planetary there is no torsional reaction force to ground. A torque balance is achieved by balancing input and output torques. Since this reaction to ground is missing, the gearbox does not control speed. Pitch of the Prop-Fan blades will determine the speeds of the output shafts.

The compound planetary provides the torsional reaction force needed to control speed by connecting the compound planet gear to a stationary ring gear. In this arrangement, the speeds are always known but torque may divide in any fashion through the ring gear and carrier. The Allison T40 gearbox was designed as a compound planetary system.

The selection of torque versus speed splitting gearbox must be consistent with the Prop-Fan pitch change mechanism. If the pitch change mechanism can be

Table 3-X.
Selection step 3: weighted decision to reduce three gearing configurations to one.

Category	Weight factor	Compound planetary*	Differential planetary	Split path parallel offset*
Reliability	18	18.0	18.0	18.0
Efficiency	17	16.8	17.0	16.7
Maintenance	13	8.2	9.6	13.0
Initial cost	12	11.5	12.0	9.0
Pitch control	12	12.0	12.0	12.0
Weight	11	10.5	11.0	7.3
Technical risk	6	4.5	4.8	6.0
Ease of scaling	5	5.0	5.0	4.4
Spacial envelope	4	4.0	4.0	1.5
Propeller brakes	2	2.0	1.0	2.0
		92.5	94.4	89.9

*Deleted

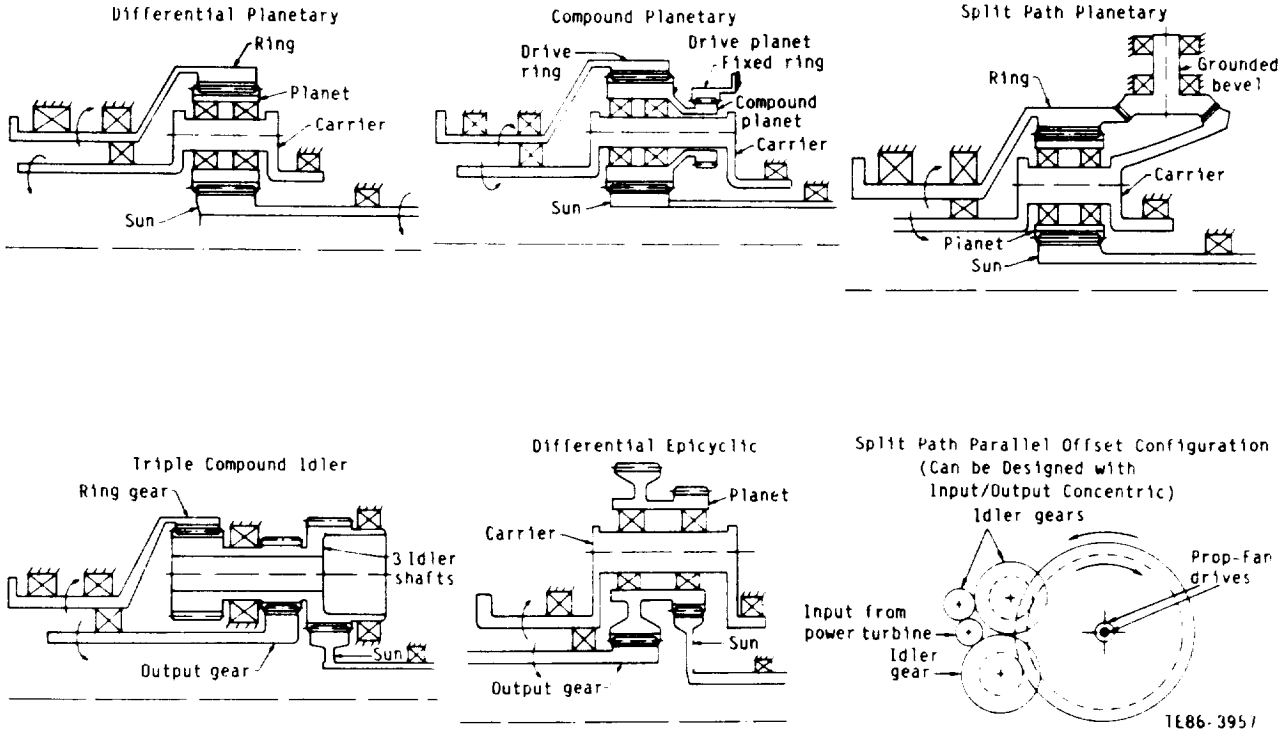

Figure 3-6. Candidate gearset configurations.

coordinated more accurately via speed control, the differential planetary should be selected. From a gearbox standpoint, both gearboxes are the same except for the additional weight and complexity of the compound planet.

3.4 COMPONENT TECHNOLOGY SCREENING

Gear and Bearing Type Selection

Various types of commonly manufactured parallel axis gears were considered in the gear selection process. This included both high and low contact ratio spur, helical, and double helical gears. Calculations were performed for high contact ratio spur, single helical, and double helical gears to determine their relative advantages and disadvantages within the AGBT design envelope. Center distance and face width were fixed while other gear parameters were varied to obtain the best compromise for each gear type. The gears were evaluated for contact stress, bending stress, and flash temperature. Results are shown in Figure 3-7. The single helical and double helical gears were very similar in each category. High contact ratio gears did not show an advantage in any of the three categories. The commonly assumed load reduction of the high contact ratio gear did not compensate for the loss of strength that is found with the thinner teeth. The higher sliding velocities found in the high contact ratio gear increased the flash temperature considerably above either the single or double helical gear. Thus, the advantages commonly cited for the high contact ratio spur gears were not found in this study.

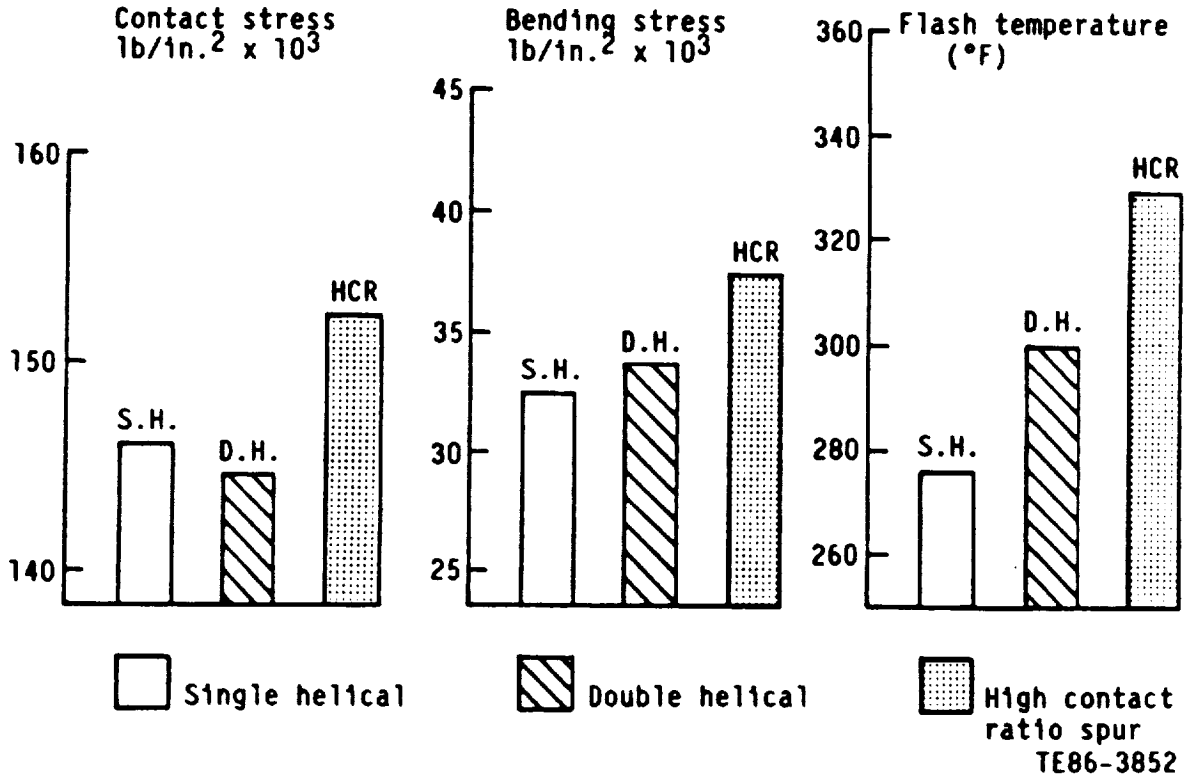

Figure 3-7. Comparison of helical and high contact ratio spur gears.

All three of the gear types studied increased load sharing between the teeth. High contact ratio gears increase the path of contact so that more teeth can share the load and reduce the unit load. Helical and double helical gears also increase contact ratio through use of the helix angle. This load sharing reduces vibration and increases load capacity. Results of comparative testing of gear types at Allison in the T56-A18 gearbox are shown in Figure 3-8. Vibration levels at each gear mesh are substantially reduced from that of the spur gearset. A T56-A18 gearbox, a two-stage gearbox, included herringbone gears in the first stage and single helical gears in the second stage planetary mesh. These low vibration levels help increase reliability of the gearbox due to lower dynamic structural loads on the gearbox components.

In Table 3-XI all six candidate gear types were evaluated for six criteria, the most important being load capacity or life. Vibration was also an important selection criteria. Double helical gears had the highest weighted total. Single helical gears had nearly the same rating. High contact ratio versions of any of these gears were rated low due to both development risk and power loss considerations.

Table 3-XI.
Gear type evaluation.

Selection criteria in order of importance	Weight factor	Spur	HCR spur	Single helical	Double helical	HCR single helical	HCR double helical
Load capacity (life)	4	2.0	4.0	4.0	4.5	4.5	5.0
Vibration, noise	3	1.5	3.5	4.5	5.0	4.0	4.0
Development risk	2	5.0	3.3	5.0	4.0	3.3	3.0
Power loss	2	3.8	2.5	4.3	5.0	3.0	3.3
Ease of manufacture	1	5.0	4.5	5.0	4.0	4.0	3.3
Weight, size	1	2.0	4.0	4.0	3.8	4.5	4.3
Weighted totals		37.1	46.6	57.1	58.8	51.1	52.2

Rating system:

Excellent	5
Good	4
Average	3
Below average	2
Poor	1

Six planet bearing configurations were studied in the conceptual design. They included cylindrical roller bearings, ball bearings, fluid film bearings, both single and double row spherical bearings, and tapered roller bearings. Bearing lives were calculated for each at a given bearing envelope size. Results are shown in Figure 3-9. Fluid film bearings, when properly designed, would have nearly infinite life and are not shown. Ball bearings could not be used due

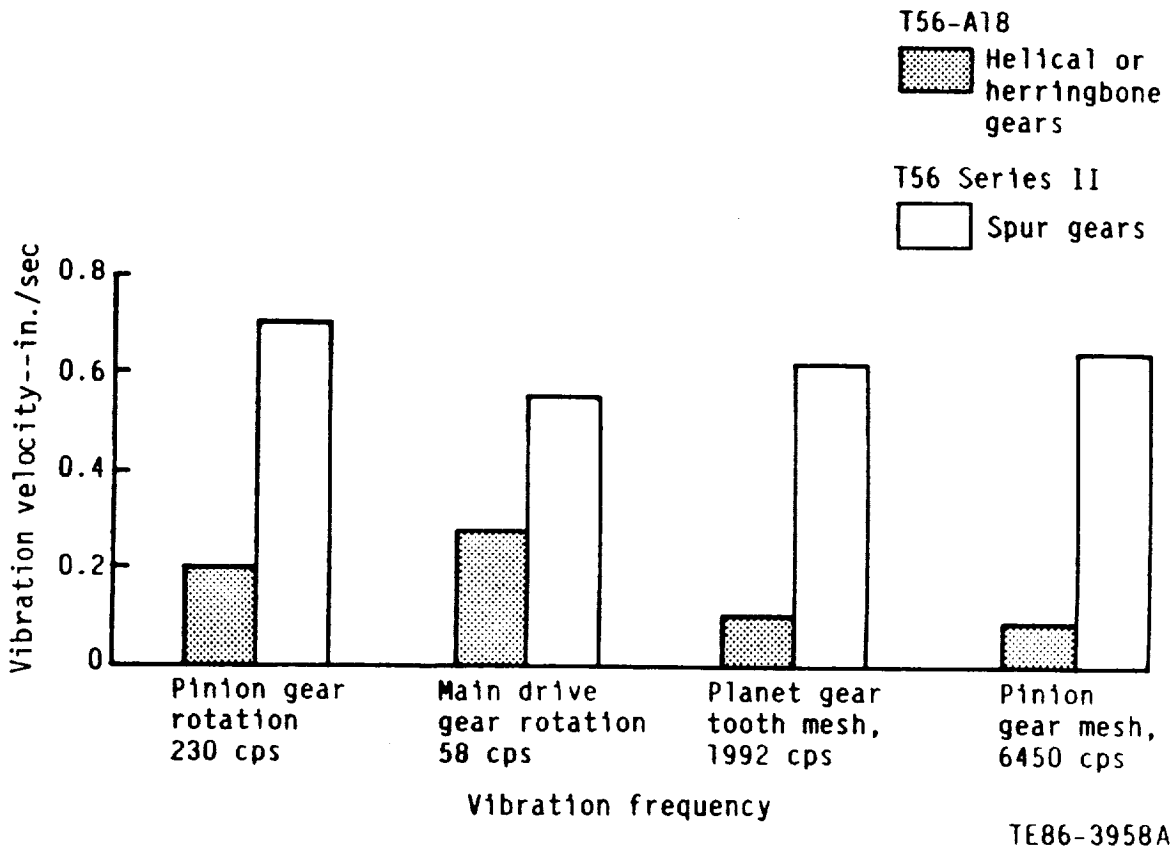

Figure 3-8. Advantages of helical gearing demonstrated in the Allison T56-A18 gearbox.

to their low load capacity in this size range. Cylindrical bearings have the highest capacity of any rolling element type bearing that might fit in the given envelope. The cylindrical bearing had 60% higher life than the nearest competitor. A further evaluation was done to rate these types of bearings for each selection criteria, as shown in Table 3-XII. Load capacity was given the highest priority. The cylindrical bearing was clearly superior to any other bearing type for this application. The combination of the double helical gear and cylindrical planet bearing provides the potential for a very long life gearbox. These two components are ideally suited to work in conjunction with each other. The double helical gear requires axial movement capability that can be provided by the cylindrical roller bearing. The cylindrical roller bearing is also the easiest bearing to manufacture.

Gear and Planet Bearing Material Screening

In the last ten years several new gear and bearing materials have been developed that show promise in the areas of both rolling contact fatigue and hot

Table 3-XII.
Planet bearing type evaluation.

Selection criteria in order of importance	Weight factor	Cylin-drical	Fluid film	Single row spherical	Tapered roller	Double row spherical	Ball
Load capacity (life)	4	4.4	4.4	3.8	4.2	3.2	2.0
Speed capability (DN)	2	5.0	5.0	2.8	3.6	4.0	5.0
Development risk	2	4.0	2.2	2.6	3.0	4.4	3.6
Tolerance to mis-alignment	2	2.4	1.8	5.0	2.4	5.0	4.0
Ease of manufacture (integral with gear)	1	4.6	4.0	3.0	3.0	3.2	3.8
Weight, size	1	4.0	4.6	3.8	3.4	3.2	2.6
Power loss	1	4.6	1.6	3.0	3.0	3.6	4.6
Oil off capability	1	3.4	1.0	2.6	2.0	3.0	3.6
Weighted totals		57.0	46.8	48.4	46.2	52.6	47.8

Rating system:

Excellent	5
Good	4
Average	3
Below average	2
Poor	1

hardness retention without sacrificing bending strength, fracture toughness, or wear resistance. Material requirements for this application are:

- o carburizing grade steel
- o contact fatigue strength above AMS6265
- o bending fatigue strength equal to AMS6265
- o improved hot hardness
- o good fracture toughness
- o good scuff/wear resistance

The materials that can provide these requirements are EX-53, CBS 600, CBS 1000M, Vasco X2, and M50-NiL.

The hot hardness capability required of these materials is limited by lubricants of today. Considering the lubricant capabilities, it is expected that surface hardness must be retained only to temperatures of 500°F. All of these materials have adequate surface hardness at 500°F, as shown in Figure 3-10. For comparison 9310 is also shown in this figure. This superior hot hardness will aid in an oil loss or scoring situation. Data was collected from many sources on rolling contact fatigue. This type of comparison was very difficult due to the numerous sources and the various heat treat techniques employed on each material. The results of these studies are shown in Figure 3-11 where a life improvement factor is shown for each material as compared to the 9310

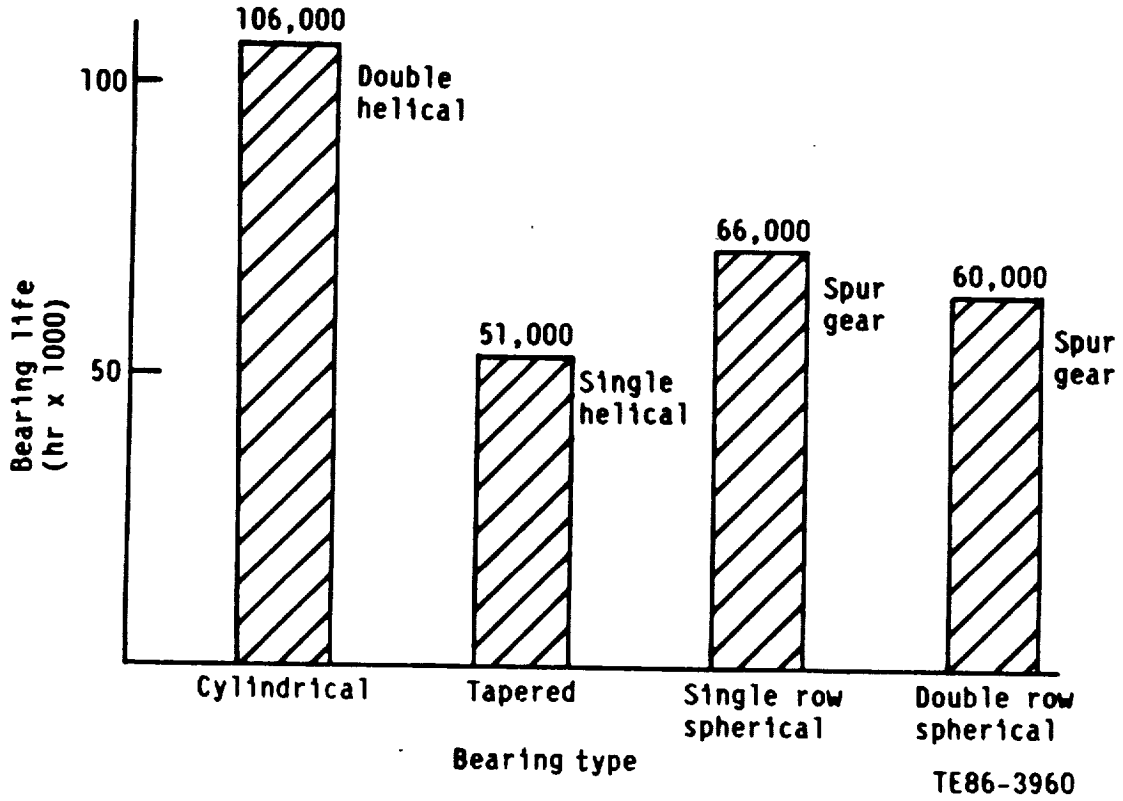

Figure 3-9. Bearing life for various planet types.

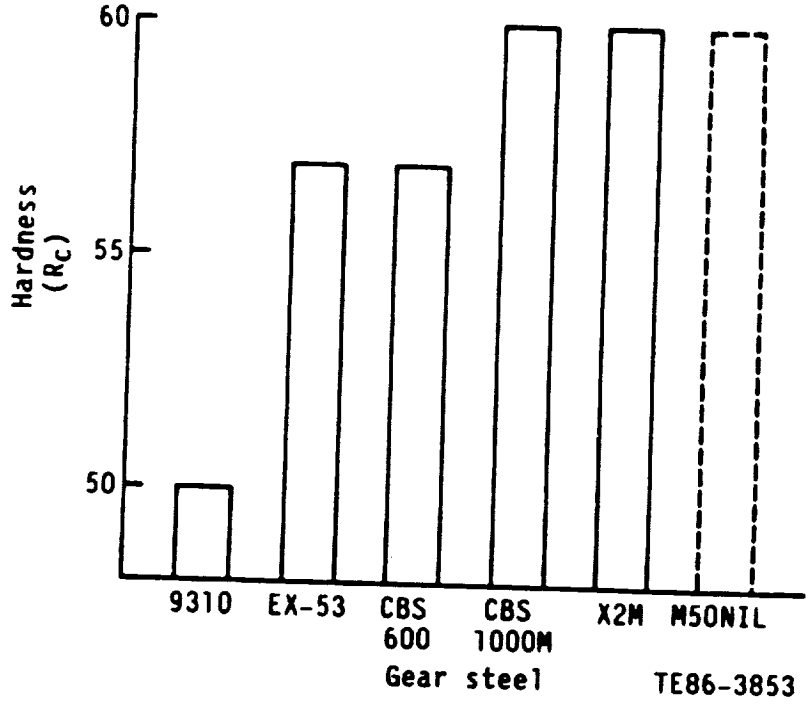

Figure 3-10. Surface hardness at 500°F (all parts at 62 R_C at 70°F).

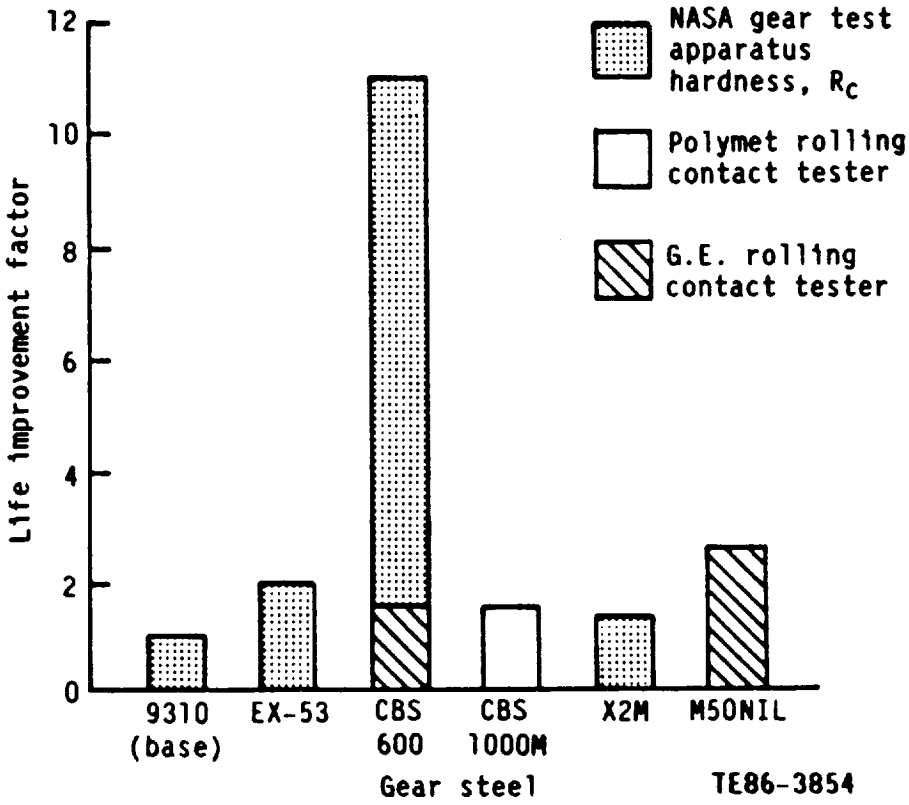

Figure 3-11. Life improvement factors for rolling contact fatigue.

baseline. Three types of machines were used for life improvement factor determination. These include the NASA gear test apparatus and both Polymet and General Electric rolling contact fatigue testers. In the rolling contact fatigue tester, the M50-NiL showed the greatest life improvement over 9310. Life of all other materials was somewhat less than the M50-NiL but they were roughly equivalent to each other. The NASA gear test apparatus, however, showed an 11 times life improvement factor for the CBS 600 material. These results indicate that CBS 600 may have superior capability for use as a gear material.

A weighted evaluation was performed on these gear materials and the results are shown in Table 3-XIII. CBS 600 was chosen as the best. All materials except for Vasco X2M were considered to be viable alternatives as well. A summary of the material screening is shown in Table 3-XIV. CBS 600 was selected since it most closely matched the program requirements. EX-53, however, was also an excellent candidate. Both CBS 1000M and M50-NiL are very promising materials for the future. Not enough data was found, however, to choose either of these materials. Allison's past experience with Vasco X2 was not favorable. Heat treating difficulties prevented evaluation of this material.

Propeller Mounting System

This section discusses the approach taken to support the Prop-Fan and the loads it generates on the gearbox. The main structural components involved--housing,

Table 3-XIII.
Gear material evaluation.

Selection criteria in order of importance	Weight factor	EX-53	CBS 600	CBS 1000M	Vasco X2M	M50-NiL
Rolling contact fatigue	3	3	5	3	3	4
High hot hardness	2	3	3	5	5	5
Manufacturability	2	4	4	3	2	3
Fracture toughness	2	5	4	3	2	2
Bending fatigue	1	3	3	3	3	3
Weighted totals		36	40	34	30	35

Rating system:

Excellent	5
Good	4
Average	3
Below average	2
Poor	1

Table 3-XIV.
Summary.

Material	Rating	Basis for rating
CBS 600	Selected	Most closely matches program requirements
EX-53	Runner up	Excellent candidate--minimum retained austenite of 10% is unusually high
CBS 1000M and M50-NiL	Very promising materials	Not enough data available at present to choose either of these
Vasco X2M	Not recommended	Allison experience with heat treating this material was very poor

prop shaft, carrier, and their support bearings--must work together to prevent overloading in any given area. Design of the structural components within this gearbox was influenced by experience with the T56 system. In a long life gearbox, the gears and bearings within the planetary gearset must be isolated from propeller loads. The housing, planet carrier, and prop shaft must be designed with this in mind. Figure 3-12 illustrates how these loads are handled in the AGBT gearbox. The loads, shown at the prop shaft flange, travel directly

through the prop shaft bearings, into the housing, and out through the housing/engine attachment point. Two attachment points are shown. The final mount location was not resolved in the conceptual design phase. In either case, however, the heavy propeller loads are carried to the mounts directly so that bearings and gears are not affected. The housing has a heavy cross section only in the vicinity of the prop bearings to keep stresses and deflections low.

Tapered roller bearings were selected for support of the propeller shaft in this gearbox. These bearings can be mounted close together yet provide the same kind of support obtained in much larger ball and roller bearing support systems. This is illustrated in Figure 3-13 where an Allison T40 counterrotating system is compared to the AGBT design. Propeller loads are comparable in both systems, yet the AGBT bearings require only half the axial space. This is due to the ability of the tapered roller bearing to project its effective bearing spread to the centerline of its mounting shaft. In addition, mounting stiffness or resistance to movement can be increased simply by increasing bearing preload. This is not possible with a combination of ball and roller bearings. The more common combination of two roller bearings and one ball thrust bearing increases the part count and overall cost since only two tapered bearings are required.

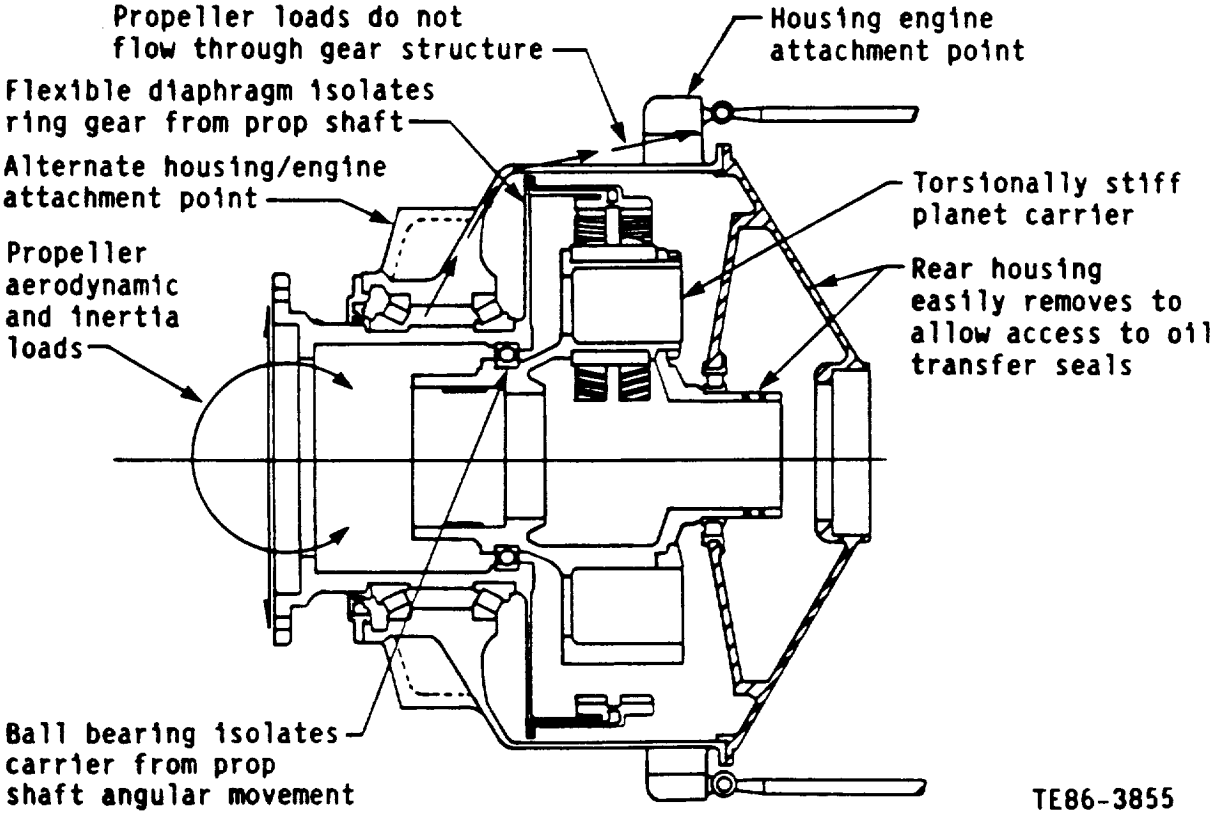

Figure 3-12. Gearbox structural features.

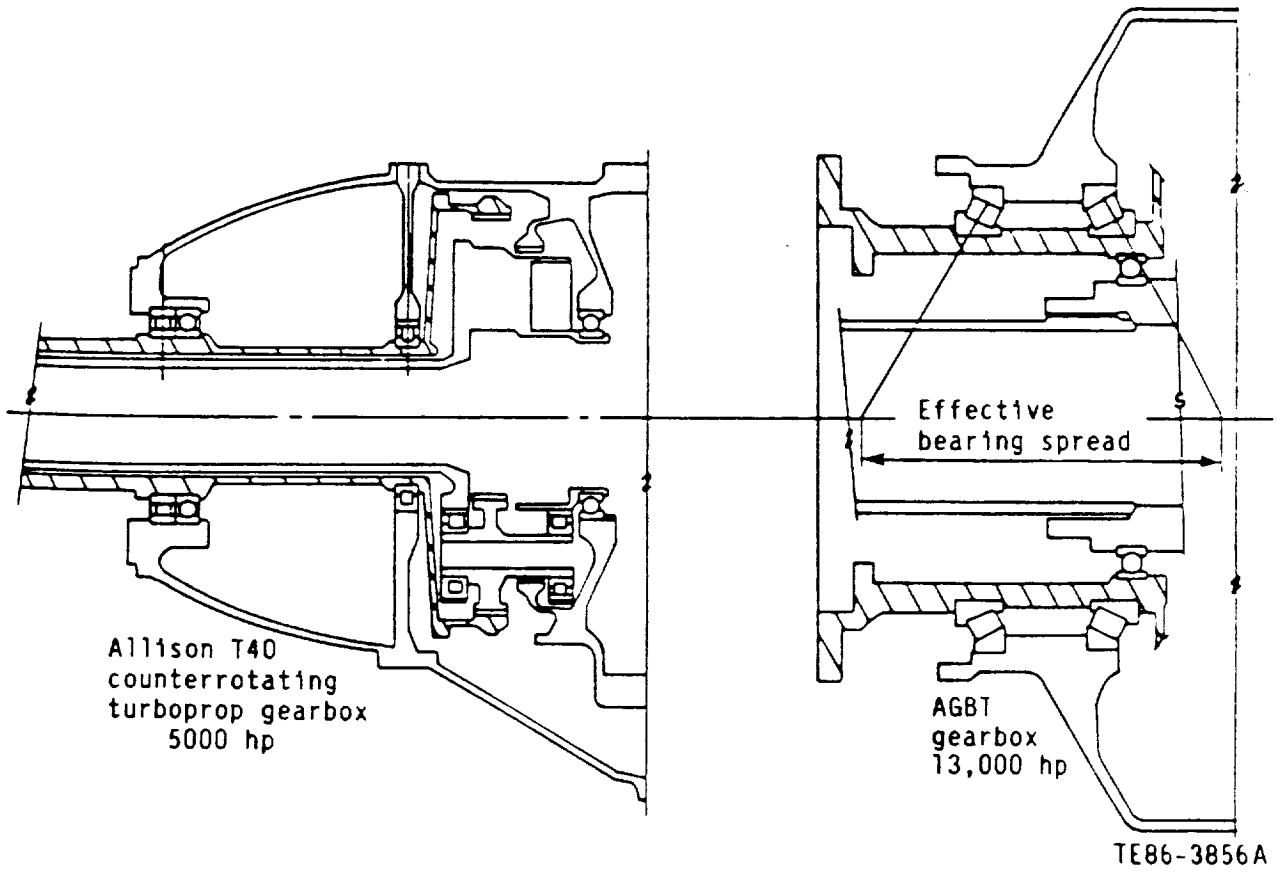

Figure 3-13. Reduced housing length with tapered roller prop bearings.

The mounting of the propeller on a prop shaft can become a major problem in service. Fretting between the bearing inner race and the shaft and between axial mating surfaces is a common problem. Since the propeller loads are unidirectional, a stress cycle is seen between the series of clamped surfaces for each revolution of the shaft. The stress cycles produce minute movements that lead to fretting. Four prop shaft configurations were studied during the conceptual design (see Figure 3-14). These techniques are based either on applying a heavy press fit between the prop bearing and the shaft or on the use of axially clamped wedges that lock the propeller to the shaft. In each case, the assembly requires a large axial clamp force provided either by a series of bolts or a large spanner nut.

The four techniques were evaluated for stress, fretting, maintainability, stiffness, and size, as shown in Table 3-XV. The best configuration was found to be the spline and flange with the bolted diaphragm. It was decided that the wedge technique was not required here. The use of a series of bolts to apply the axial lock up of the assembly was chosen over use of a large prop nut. Securing a single large prop nut would be very difficult in the field.

Referring again to Figure 3-12, a ball bearing is used to support the carrier from the prop shaft. The prop shaft is expected to bend under the heavy

Table 3-XV.
Prop shaft type selection.

Selection criteria in order of importance	Weight factor	Internal wedges with integral diaphragm	External wedges with integral diaphragm	Spline and flange with bolted diaphragm	Spline and flange with internal prop nut
Stress (life)	4	2.0	3.0	4	2.8
Fretting	3	3.0	3.0	3	2.0
Maintainability	2	3.0	2.8	4	2.5
Stiffness	1	3.5	3.3	4	4.0
Size (weight)	1	3.0	2.5	3	3.0
Weighted totals		29.5	32.4	40	29.2

Rating system:

Excellent	5
Good	4
Average	3
Below average	2
Poor	1

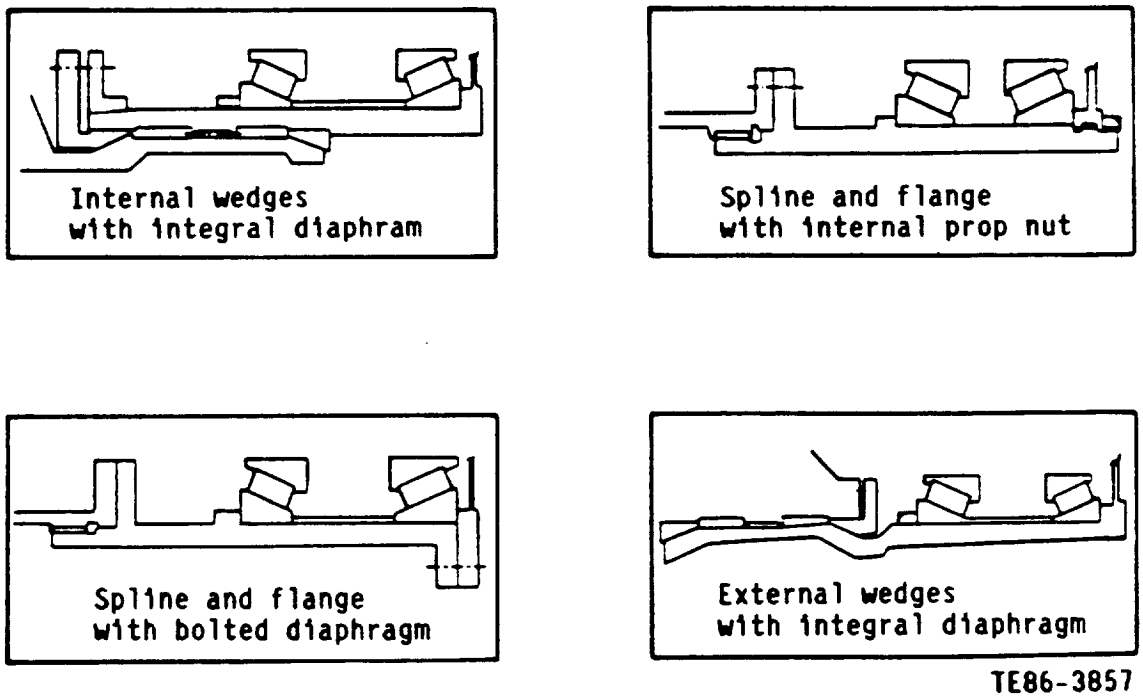

Figure 3-14. Prop shaft configuration study.

propeller loads, and the ball bearing is expected to accommodate the misalignment. Similarly, prop shaft bending is prevented from affecting the gearset through the use of the flexible diaphragm. The diaphragm can handle the torque load easily but is free to deflect under axial loads.

The planet carrier is a rigid structure that establishes the radial location of the gears and planet bearings. In this area good alignment is necessary. Essentially, the planetary gearset will operate on precise axes while the housing and prop shaft deflect around it.

Double Helical Gear Load Sharing

Another important consideration in this gearbox design is the method to allow load sharing between planets and between the two rows of helical gear teeth. The techniques used in this design are based on those used in the T56 where load sharing was found to be within 2%. One method that will be employed is to locate the planet gears exactly on the planet carrier by machining the carrier trunnions accurately. The ring gear will also be allowed to float radially to locate itself around the planets. Load sharing requirements in this gearbox include load sharing between four planets and also between two rows of teeth. This results in eight meshes at the sun planet contact and eight meshes at the planet ring contact that must share the load as equally as possible. The method used is to build in flexibility in all directions except for two: 1) the sun gear is fixed in the axial direction, and 2) the planet gears are fixed in the radial direction. All other components are free to float in the radial and axial directions. Figure 3-15 shows the results of a study that allowed flexibility at either the sun gear or ring gear through the use of splines or a flexible diaphragm. Assuming a friction coefficient of 0.15, the spline at the sun gear location would allow approximately 70/30 load share between the two rows of double helical gears. Load sharing accomplished with the spline at the ring gear is not much better. In fact, this indicated that splines at these two locations are nearly locked. In order to obtain the 50/50 load split between the two rows, the ring gear must be mounted on a flexible diaphragm. This thin diaphragm is stiff in the torsional direction so that it can transmit loads but flexible in the axial direction to allow load sharing.

Lubrication System

The conceptual design of the AGBT system is shown in Figure 3-16. This is a two pressure system that minimizes oil pump power requirements. Since all shafts are rotating within a differential system, an oil transfer system must be designed to allow oil to move from the stationary structure into the rotating shafts. High pressure oil is sent only to the areas that require it: the sun gear mesh and the oil to the pitch change mechanism. All other areas are supplied with lower pressure oil at 50 $lb/in.^2$. Under race lubrication will be provided to the planet bearings and the front carrier support. All other bearings will be jet lubricated. Oil churning losses will be minimized due to the high centrifugal forces within the differential system. Oil that is supplied to the bearing and gear surfaces will be cast away from these components due to centrifugal force. This also ensures that oil is used only once. As the oil is cast out to the housing, a deaeration effect occurs. Oil will drain back down the housing walls and be pulled back into an oil conditioning module

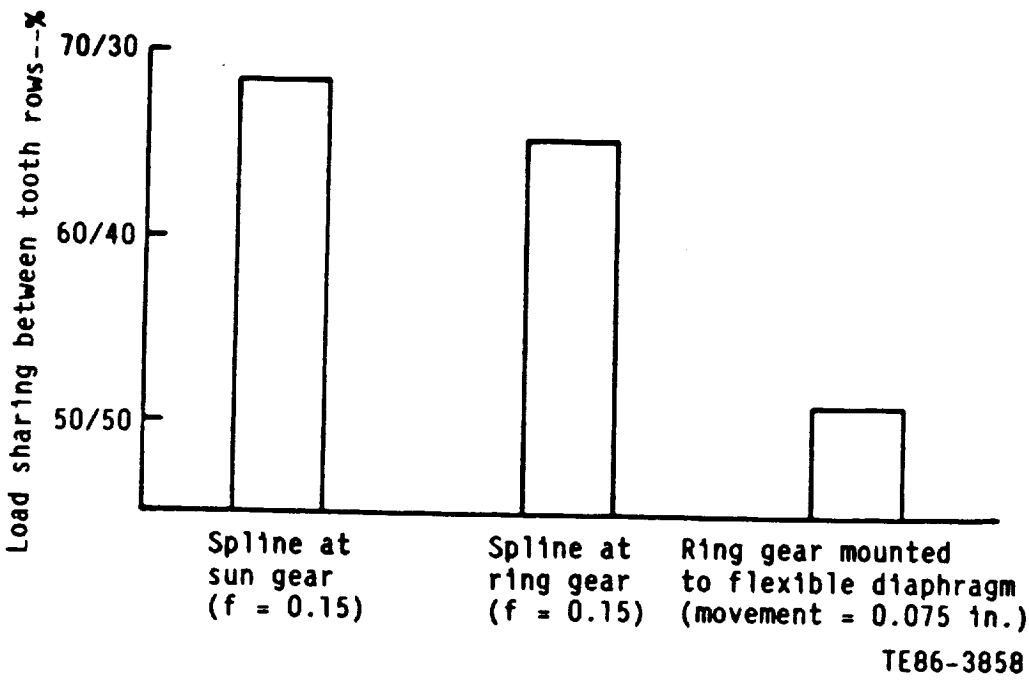

Figure 3-15. Effectiveness of load sharing between tooth rows for double helical gearing.

by two scavenge pumps. Oil is returned from the pitch change mechanism at the inside diameter of the mounting flange. Centrifugal force will be used to feed it back into a collection area. Table 3-XVI lists some of the features of the lubrication system.

Table 3-XVI.
Lubrication system features.

- Oil in temperature 180°F
- Oil flow rates will be selected so that the cooling oil will remove all heat generated at takeoff conditions
- Lubricant MIL-L-23699; system also compatible with advanced gearbox oils
- Filtration: 3 micron absolute
- Oil condition monitoring: Tedeco QDM system

Modulated flow was considered for the lubrication system in the AGBT gearbox. Modulated flow would decrease the amount of oil supply to the bearings and gears at lower power levels where cooling is not required. In many gearboxes this will result in a lessening of churning losses. In a properly designed planetary or differential gearbox, churning losses are minimized by allowing

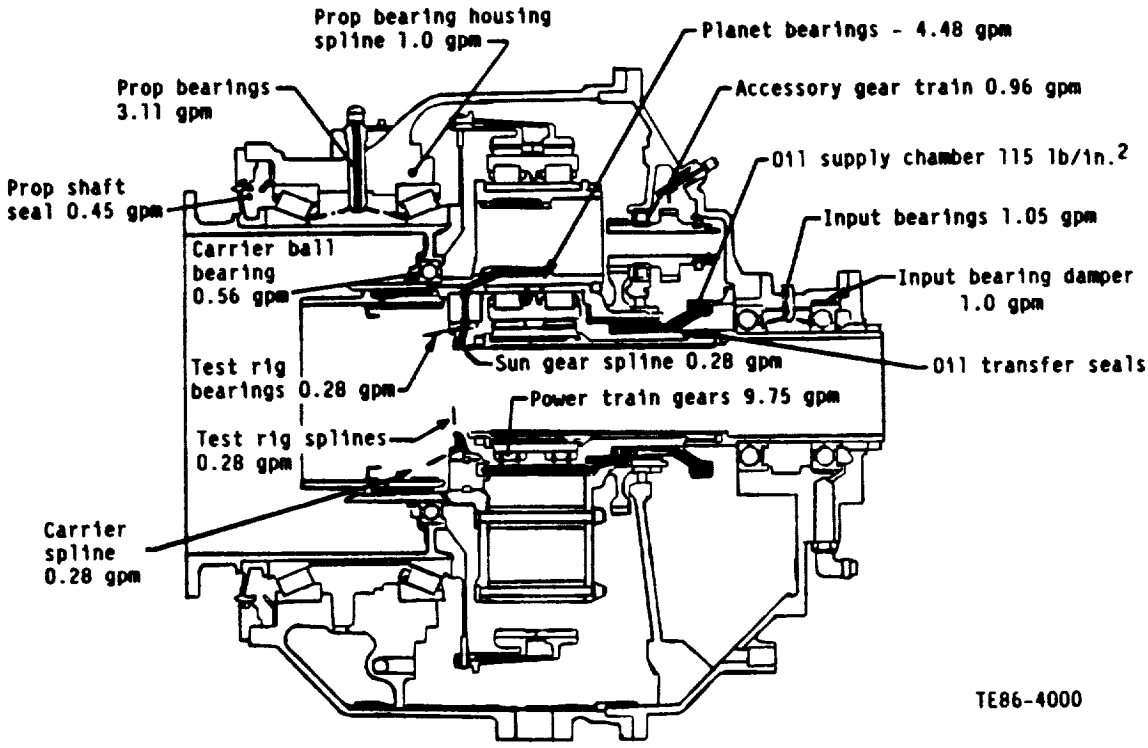

Figure 3-16. AGBT gearbox lubrication schematic.

oil to exit from bearing and gear meshes as rapidly as possible. It is anticipated that churning losses will be minimal in this gearbox, thus the potential benefits of modulated flow will probably not be realized. The problems associated with obtaining a modulated flow system might at some point cause failure of oil flow. This could lead to serious damage to the gearbox and possible failure. Instead of modulated flow, the system uses two pumps at two pressure levels. This minimizes power required for the oil pumps. It also provides some degree of redundancy if one oil pump fails.

3.5 ACCESSORY DRIVES

A conceptual design was performed for an accessory gear train for the AGBT gearbox. The accessory train provided a PTO shaft, oil pump drives, and a prop brake. These accessories are expected to be modular and easy to maintain, remove, and replace. A prop brake allows a connection to be made between the input shaft and the carrier. In a flight gearbox this would allow the propellers to be stopped completely. In a test gearbox, this has the effect of fixing the speed between the two output shafts.

3.6 TRACTOR/PUSHER CONSIDERATIONS

Although the conceptual design of the AGBT gearbox was planned for a tractor application, it can be used as a pusher gearbox with minor modifications. As shown in Figure 3-17, the direction of the gearbox rotation will change. This will require redirecting sun gear oil jets to maintain out-of-mesh lubrication.

All sun and planet gears can be used in either arrangement. A ring gear will be required with a reversed attachment point since the orientation of the propeller is on the opposite side of the ring gear. The pusher application will require careful analysis of the thermal environment of the gearbox. Cooling air may be required to prevent gearbox temperatures from rising above 300°F. This may also increase the cooling requirements for the pitch change mechanism. Attachment points on the gearbox housing may also be different. Unless the thermal environment and the pusher application are substantially different than the tractor arrangement, the modifications described are not significant.

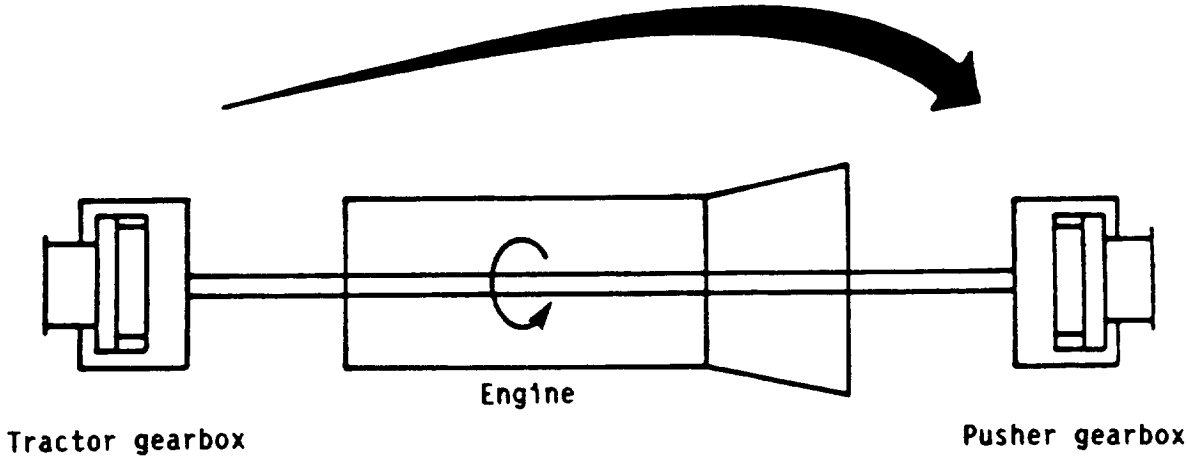

- Direction of rotation changes ⟶ redirect sun gear oil jets
- Blade location relative to gearset changes ⟶ change location of ring gear attachment points

TE86-3859

Figure 3-17. Changing direction of gearbox rotation.

4.0 PRELIMINARY DESIGN

In the preliminary design phase the design criteria was established, the general arrangement was fixed, and some specific details of the component designs were worked out.

4.1 GENERAL ARRANGEMENT

The gearbox general arrangement is shown in Figure 4-1. The arrangement is based on several key features: a differential planetary gear train, a straddle-mounted planet carrier, a flexible mounted sun gear, and close coupled, tapered roller prop shaft bearings. The gearbox is driven at its input shaft, which is supported by two split inner ring ball bearings. These input shaft bearings are preloaded against each other by a pair of disk springs. The input shaft drives the sun gear shaft, which in turn drives the sun gear. The sun gear shaft is connected to both the input shaft and the sun gear with a pair of splines.

The sun gear drives four planet gears, which in turn drive the ring gear. The reaction on the planet from the ring gear and sun gear meshes applies force to the planet carrier through the planet bearing and drives the carrier. The planet carrier is driven in the same direction of rotation as the sun gear, while the ring gear rotates in the opposite direction. The gears are double helical with involute tooth form. The planet gears are free to move axially on cylindrical roller planet bearings. The ring gear is two-piece to facilitate assembly, while the sun and planet gears are one-piece.

The planet carrier is straddle-mounted on two bearings and drives the prop farthest from the engine. One of the carrier support bearings is a split inner ring ball bearing that locates the planet carrier with respect to the prop shaft, while the other is a cylindrical roller.

The prop shaft supports the Prop-Fan with a bolted flange connection. The prop shaft is supported in the housing by a pair of indirect mounted, tapered roller bearings. The housing is four piece, 3-aluminum, 1-steel, and sealed at all joints by O-rings.

4.2 DESIGN CRITERIA

Design criteria for the AGBT gearbox are based on the requirements for future long life gear systems. Many high power aircraft gear systems in use today were designed more than 20 years ago. While those gear systems are good designs that provide good service, today's systems require longer life and higher reliability to be competitive with turbofan engines. Therefore, the goal of future gear system designs and this test gearbox will be to minimize the impact of the gearbox on the Prop-Fan propulsion system. The gearbox will be designed for 30,000 hr mean time between unscheduled removal (MTBUR) and for improved maintainability by assembling it in a modular fashion. Repairing one area of the gearbox will not require a complete disassembly. Accessories, such as oil pumps, will be modular and line replaceable. Replacement will take minutes instead of hours.

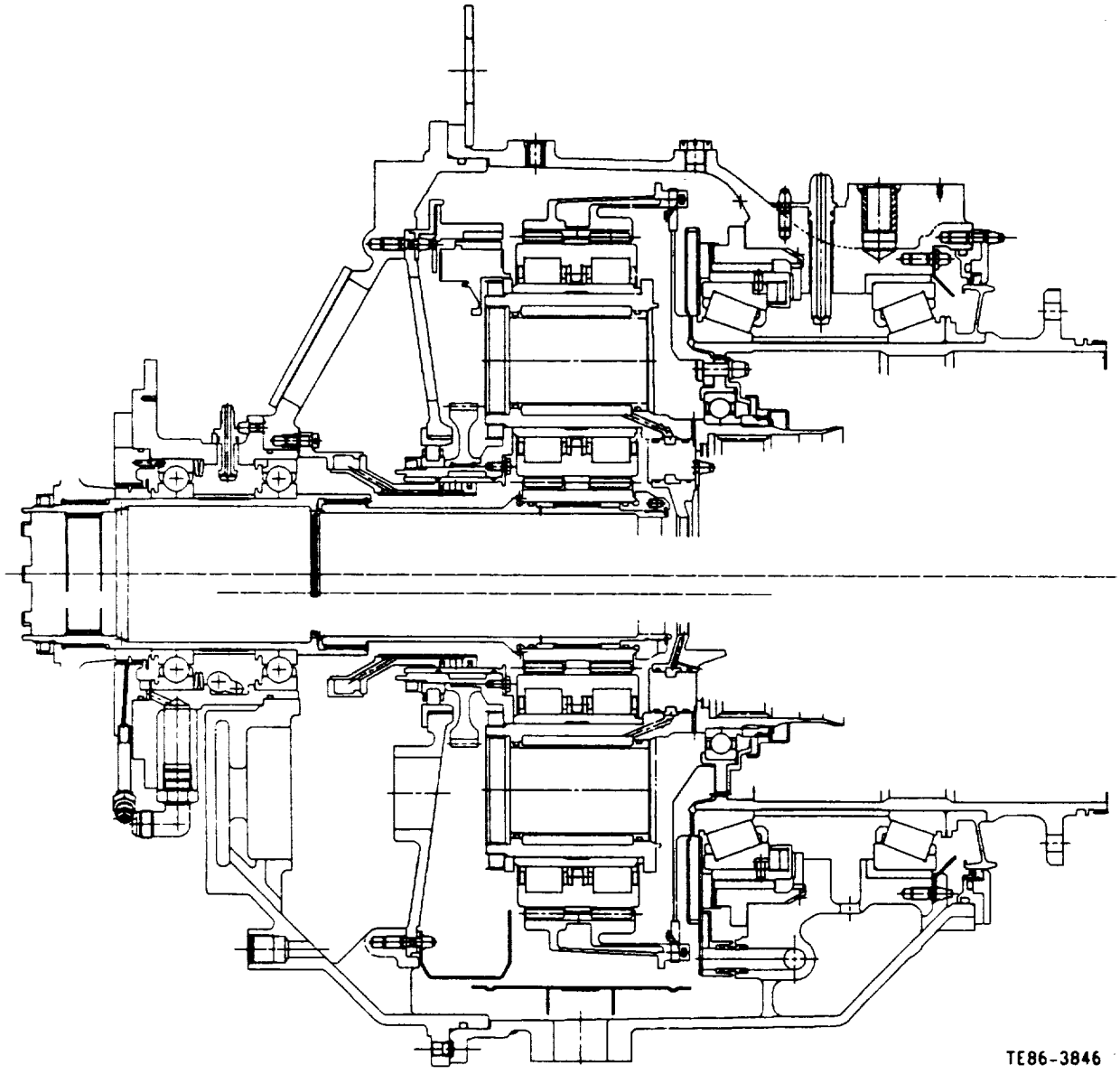

Figure 4-1. Gearbox general arrangement.

The design point of the AGBT gearbox is shown in Table 4-I. The mission is based on that studied in the Advanced Prop-Fan Engine Technology (APET) report. The speed ratio is based on the two propellers turning at equal speed in opposite directions.

The gearbox is designed for maneuver loads discussed in subsection 3.2 and shown in Figure 4-2. The gearbox is also designed to operate up to 55,000 ft and at attitudes described in Figure 4-3.

Table 4-I.
Design point.

Takeoff power	13,000 hp
Input speed	9500 rpm
Speed ratio	8.33:1
Mission length	300 nautical mile
Oil inlet temp	180°F

The design lives of the individual components of the gearbox are based on a desired life of the gearbox of 30,000 hr MTBUR. Modular design of the accessories improves maintainability but also removes these accessories from consideration of gearbox life since they do not cause a removal of the gearbox.

Material selection is based on reliability and cost. Materials with consistent performance--fatigue life, wear resistance, etc--are important for long life and high reliability.

Table 4-II lists the candidate materials to be used for the AGBT gearbox.

Table 4-II.
Materials.

Gears	CBS 600, EMS 64500
Bearings	CBS 600, M50
Shafts	4340, EMS 64500
Seals	Viton, Teflon, carbon
Housing	Aluminum C355-T6
Oil	MIL-L-23699, MIL-L-7808
Fasteners	A286, INCO 718

Gears for the AGBT must be designed for long life, high reliability, and low vibration. To maximize gear life, advanced materials will be used. Smooth tooth surfaces will be obtained to promote good oil film thickness. The advanced gear steels selected, CBS 600 and EMS 64500, have improved fatigue life over current steels and will be clean (VIMVAR) for improved reliability.

Low gear mesh induced vibration is important to long life and reliability of the gearbox and all parts connected to the gearbox. To lower the mesh vibration, the AGBT gears will be helical with a face overlap greater than 1.1. At least two teeth will be in contact with a mating gear at all times. The gears will be double helical so that the induced thrust load from the helical gears will be counteracted.

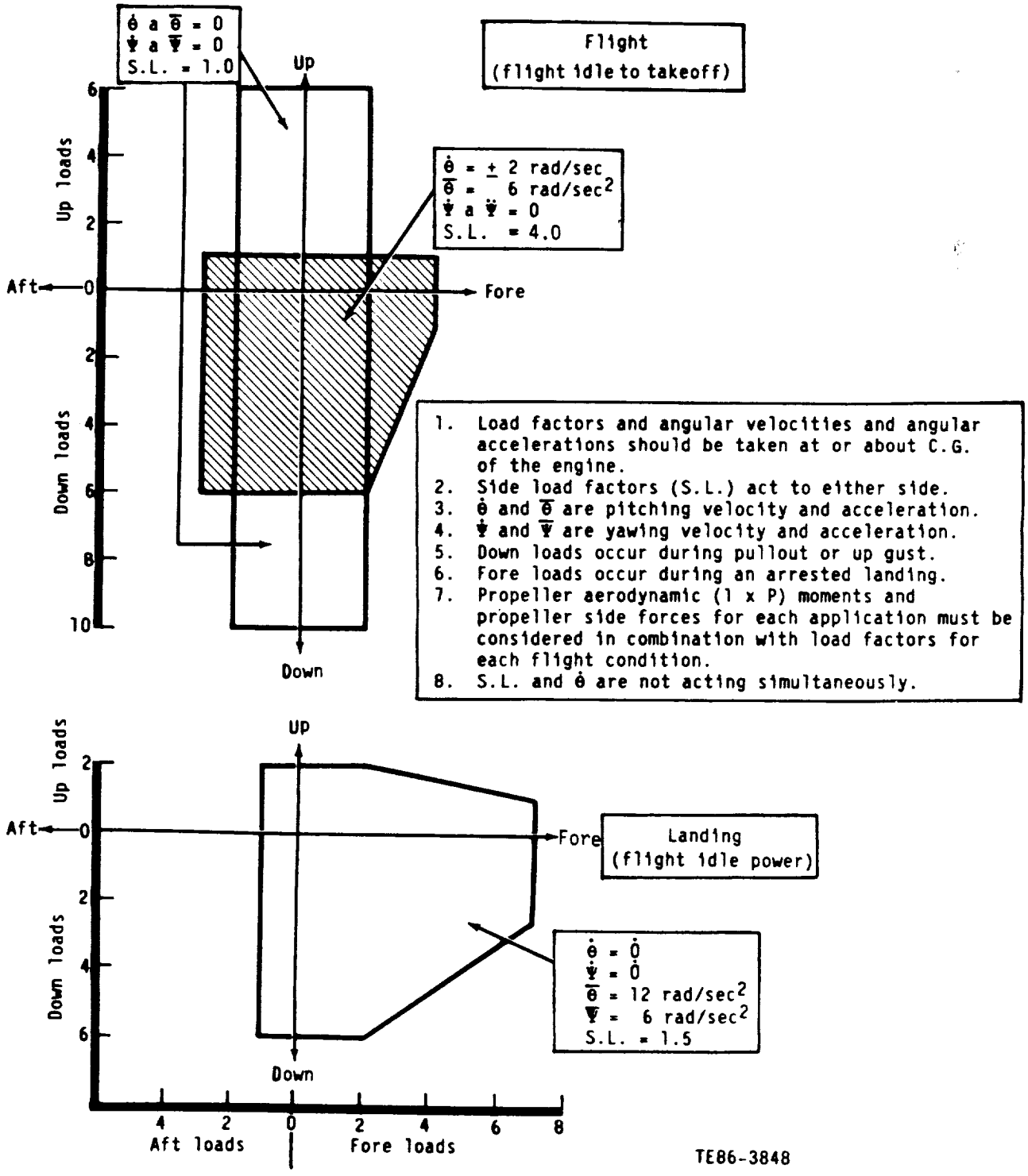

Figure 4-2. Estimated performance of AGBT--flight maneuver load diagram.

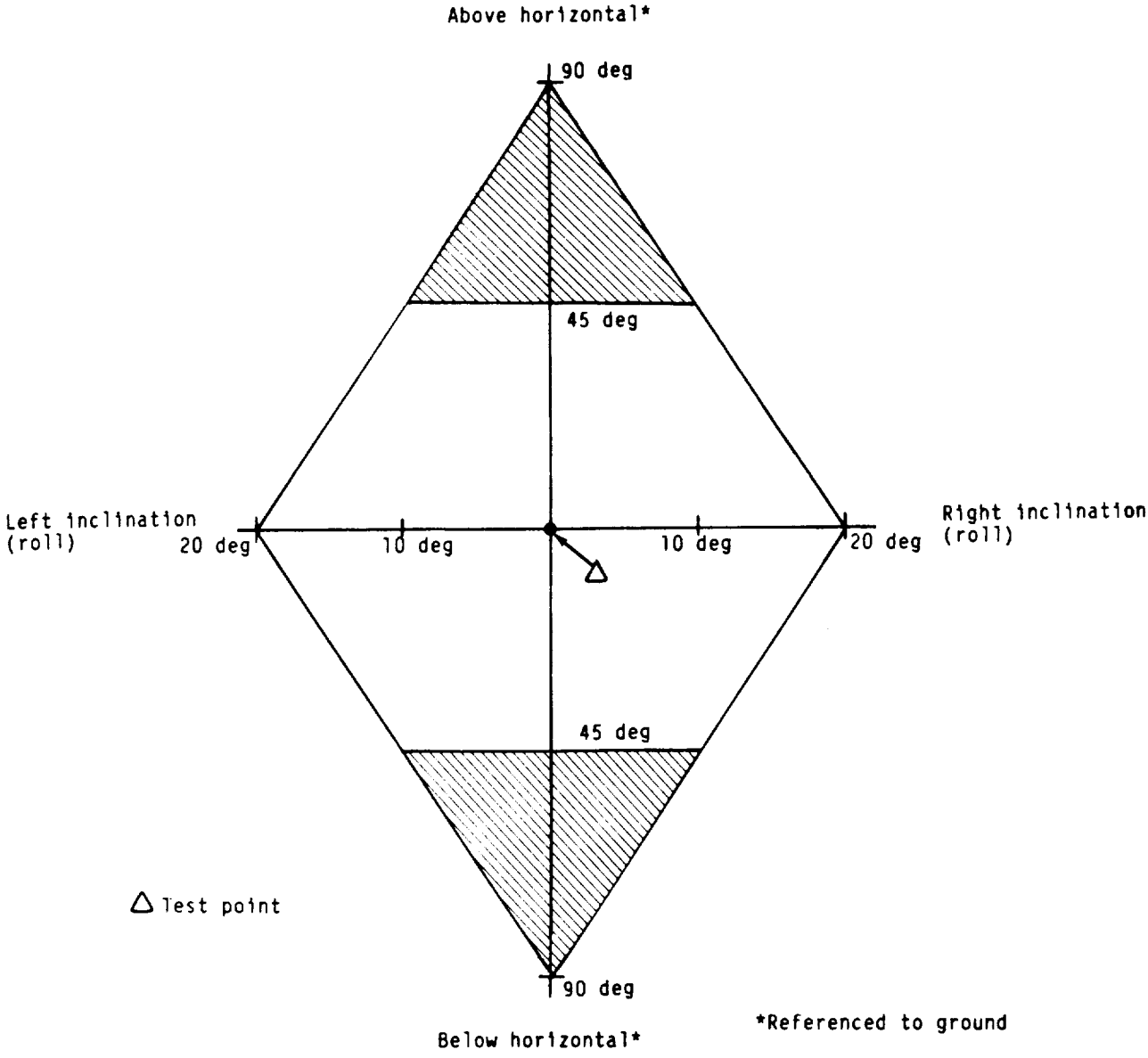

Notes:

(1) The engine will be capable of operating at all possible acceleration conditions; however, for the purpose of defining the direction of acceleration vector from the engine CG, the figure assumes no acceleration other than gravity.
(2) Engine centerline perpendicular to plane of paper.
(3) Continuous operation in clear area.
(4) Ten second operation in shaded area.

TE86-3847

Figure 4-3. Design attitude limits.

The materials selected for the gears have improved hot hardness. The material will retain its hardness at higher operating temperatures than is currently possible. This will improve the scoring resistance of the gears and improve the capability of the gears to run with an oil interruption.

Bearings for the AGBT gearbox are designed for long life per the design life criteria. The bearings will also be designed for high reliability by designing against nonpredictable or secondary type failures. The inner and outer rings will be clamped, bolted, keyed, or pressed to their mating parts to prevent spinning. Bearing materials will retain their hardness to a minimum of 500°F to prevent scuffing. All bearing separators will be one piece machined steel and silver plated for good strength and wear resistance.

The lubrication system for the AGBT gearbox is based on current technology that would be used for a flight gearbox. The lube system will be mounted separately from the gearbox with all oil lines externally plumbed.

The lube system will supply sufficient oil to remove the heat generated in the gearbox. A dry sump will minimize the heat generated by the churning of oil. The scavenge pumps are designed for at least twice the capacity of the lube pump to account for aeration of the oil. A Lubriclone (Tedeco trade name) will be used for deaeration of the oil as well as to track the cleanliness of the oil with a quantitative debris monitoring system.

5.0 DETAIL DESIGN

5.1 GEARING

The gearset for the AGBT rig was designed using the following techniques:

- o The structures were analyzed with finite element analysis (FEA).
- o A mesh generation routine, originally prepared by Boeing Vertol for NASA, of spur and helical gear teeth for finite element modeling (FEM) was used.
- o Each gear was modeled with a full ring of teeth to correctly analyze gear stiffnesses.

5.1.1 Geometry Selection

The AGBT gearset is a differential planetary system. This type of gear system has two outputs with the torque relationship between these outputs fixed and the speed relationship variable. For the Prop-Fan, a differential system is being used to simplify the prop control and improve gearbox reliability, as follows:

- o A differential system fixes the torques but requires a control system to determine the speeds.
- o A nondifferential gear system fixes speeds, but requires a control system to handle the torque.
- o Speeds are easier to control than torque.
- o A differential system has fewer gears and is more reliable.

For a differential planetary gearset, the output torques are fixed at different values. Figure 5.1-1 shows a free body diagram of a planet gear with forces that establish the differential action. The two forces at the sun-to-planet mesh and the planet-to-ring mesh must be equal at constant speed. The planet bearing reaction is the sum of the two mesh forces. The gear diameters are fixed by the gear ratio. Therefore, for a differential planetary system, the torque out the carrier drive is

$$Tc = \frac{R + 1}{2R} To$$

and the torque out the ring gear drive is

$$Tr = \frac{R - 1}{2R} To$$

where R is the gearset ratio for equal but opposite output speeds and To is the total output torque.

The gear design for the planetary system was based on double helical gearing with cylindrical roller planet bearings. The basic size of the planet was determined by the planet bearing. The details of the bearing design are discussed in subsection 5.4.3.

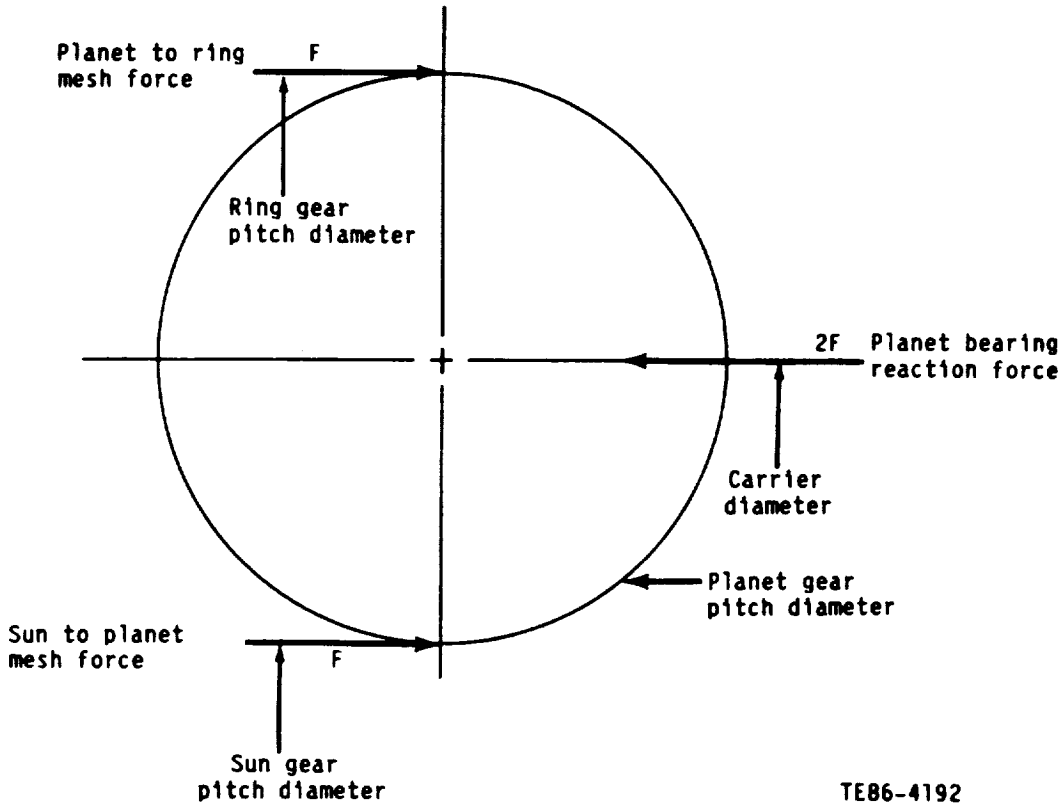

Figure 5.1-1. Planet gear free body diagram.

Assembly of a planetary gearset must be considered at the time the numbers of teeth are selected. The sum of the numbers of sun gear and ring gear teeth must be an integer multiple of the number of planets (four in the case of AGBT, the maximum that will fit at this ratio). For a double helical planetary, it is also necessary for one of the gears, ring gear for AGBT, to be two-piece so that it may be assembled axially.

Double helical gears use high helix angles, 20 to 30 deg, to maximize row-to-row load sharing. In this range the normal pressure angle of the gear teeth should not be greater than 22.5 deg, which is a standard, to prevent the top lands of the teeth from becoming too small. Figure 5.1-2 shows the results of varying the normal diametral pitch on the sun gear root bending stress. In the ratio range of this gearset, the sun gear is the smallest gear and has the highest bending stress.

Using a standard form of seven normal diametral pitch and 22.5 deg pressure angle, the number of teeth were selected to give a proper ratio. The helix angle was adjusted to give a one tooth depth wall thickness between the gear tooth root diameter and the bearing outer raceway. The resulting gearset geometry is shown in Table 5.1-I. The final ratio is 8.33:1.

Gear face width is sized from the spacing of the planet bearing rollers and the manufacturing space necessary to grind the gear teeth. The two tooth rows

Table 5.1-I.
Gear geometry.

Number of teeth

Sun	36
Planet	48
Ring	132
Normal diametral pitch	7
Normal pressure angle	22.5 deg
Helix angle	26 deg

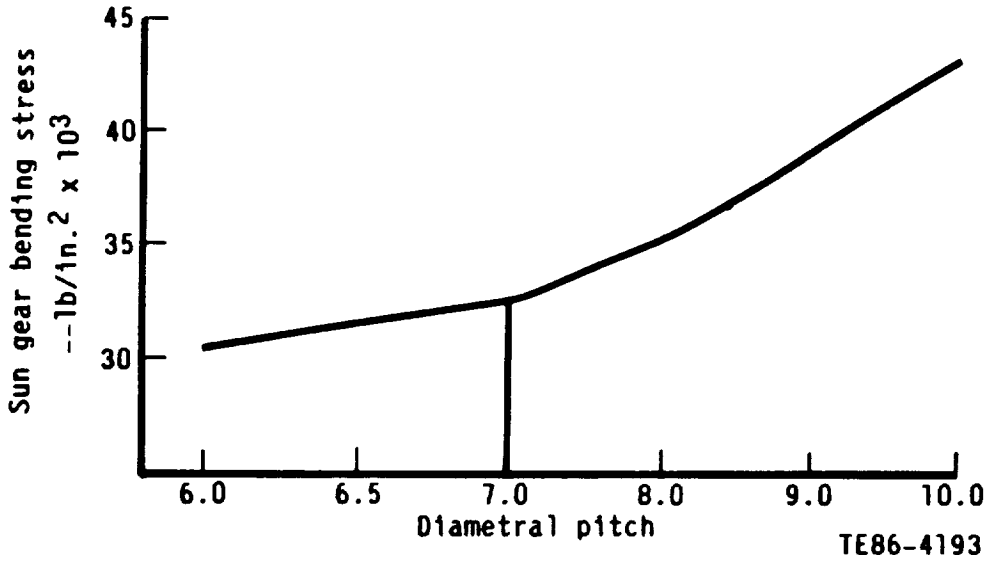

Figure 5.1-2. Double helical diametral pitch.

are placed far enough apart to grind the teeth with a 3 in. diameter wheel. The teeth are also placed directly over the rollers to minimize skewing of the roller raceway. The backlash of the gearset is large enough to ensure adequate clearance at -65°F.

Long life gear systems require prevention of pitting fatigue and scoring failures. Bearing manufacturers are trying to improve the surface finish of the roller and raceways. This improvement would provide a thicker lubricating film for improved pitting fatigue life and a more stable film for scoring resistance.

5.1.2 Geartooth Stresses and Deflections

Table 5.1-II lists the AGBT planetary gearset operating data at maximum power. Aircraft gears are typically designed for takeoff power rather than duty cycle because the stress vs. number of cycles (S/N) curve for pitting fatigue life

Table 5.1-II.
Gear operating data.

Contact stress (AGMA 218.01)		
Sun-to-planet	=	143,000 lb/in.^{2}
Planet-to-ring	=	79,500 lb/in.^{2}
Bending stress (AGMA 218.01)		
Sun	=	29,900 lb/in.^{2}
Planet	=	31,700/32,900 lb/in.^{2}
Ring	=	2740 lb/in.^{2}
Profile overlap	=	1.31
Face overlap	=	1.18
Oil film lambda ratio		
Sun-to-planet	=	1.6
Planet-to-ring	=	2.4
Flash temperature index		
Sun-to-planet	=	287°F
Planet-to-sun	=	202°F
Pitch line velocity	=	12,520 fpm
Tooth loading	=	3239 lb per in. of face width

is so shallow that only the highest stress point is critical. This is also true of the AGBT gears.

The gear tooth contact and bending stresses were analyzed by the techniques published in AGMA 218.01 and are low. This shows that the gearset design is planet bearing driven. The gear tooth overlaps and contact ratios are normal for this type of gear. Even at maximum center distance variation from machining error, temperature, and deflection, the profile overlap is not less than 1.2.

Gear tooth helical windup of the sun and ring gears is caused by ordinary shaft torsion. This torsion changes the helix angle of the gear teeth. The planet gear does not change since it is an idler gear. The sun and ring gears were machined with a slight error in their helix angles so that at full power the teeth would be aligned properly.

The tooth profile of aircraft gears is typically modified from a true involute form so that the gears will mesh smoothly with tooth deflections and spacing errors. The maximum profile modification required was 0.0009 in.

The oil film thickness, lambda ratio, is excellent. This was expected from the fine surface finish on the gears. The flash temperature is moderate and within Allison experience so scoring should not be a problem. The pitch line velocity is moderate for aircraft gearing as is the tooth loading. Heat generation should be reasonably low. (See subsection 5.6.2 for further details.)

5.1.3 Ring Gear Support

The ring gear for the AGBT gear system is a two-piece, axially split gear, so that it may be assembled with the planets. The induced thrust from the internal helical gear teeth forces the two pieces together, thus they do not operate with axial clearance.

The ring gear is driven by the four planet gears, which drives the prop shaft and in turn drives the forward prop. The connection between the ring gear and the prop shaft is a flexible structure that provides freedom of movement for the ring gear while transmitting power from the ring gear to the prop shaft. This attachment structure is shown in Figure 5.1-3.

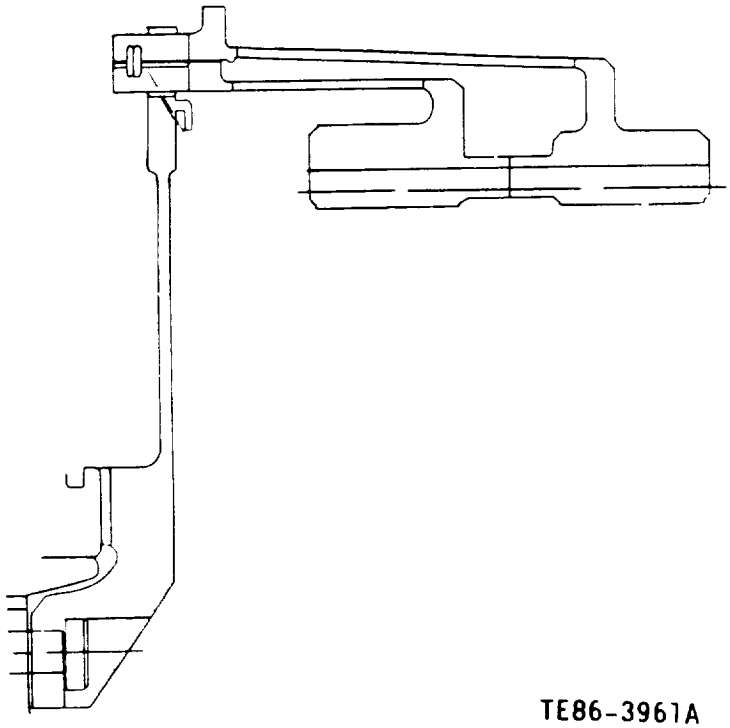

TE86-3961A

Figure 5.1-3. Ring gear attachment.

The complex problem of prediction of the deflection of the ring gear was solved by finite element analysis. Figure 5.1-4 shows views of one of the ring gear 3-D sector models. The geometry of the model was adjusted many times until the deflections were uniform between the two gear halves, with minimal twisting of the teeth. The models included the gear teeth, as can be seen in the figure. Results of the final geometry are shown in Figures 5.1-5 and 5.1-6. The radial deflections are even to within 0.002 in. between the two halves and side-to-side so load sharing will be consistent. Since tangential deflections are consistent, side-to-side edge loading will not occur.

Because a planetary gearset is designed for flexibility, critical natural frequencies can be a problem. There may be many modes of the ring gear and its support in the operating range because of the flexibility required for good load sharing. Only a few of these modes have the potential for being excited due to the unique aspects of a planetary gearset (Figure 5.1-7).

5.1.4 Planet Gear Stiffness

The planet gear of the AGBT gearset is a dual function part. The outside of the ring is a double helical gear while the inside of the ring is a pair of cylindrical roller bearing raceways. A planet gear is a type of idler gear. This means the force on the driving gear teeth is reacted by a force on driven gear teeth. A free body diagram (FBD) of these forces for the AGBT planet gear is shown in Figure 5.1-1. This FBD shows the forces that cause or are caused

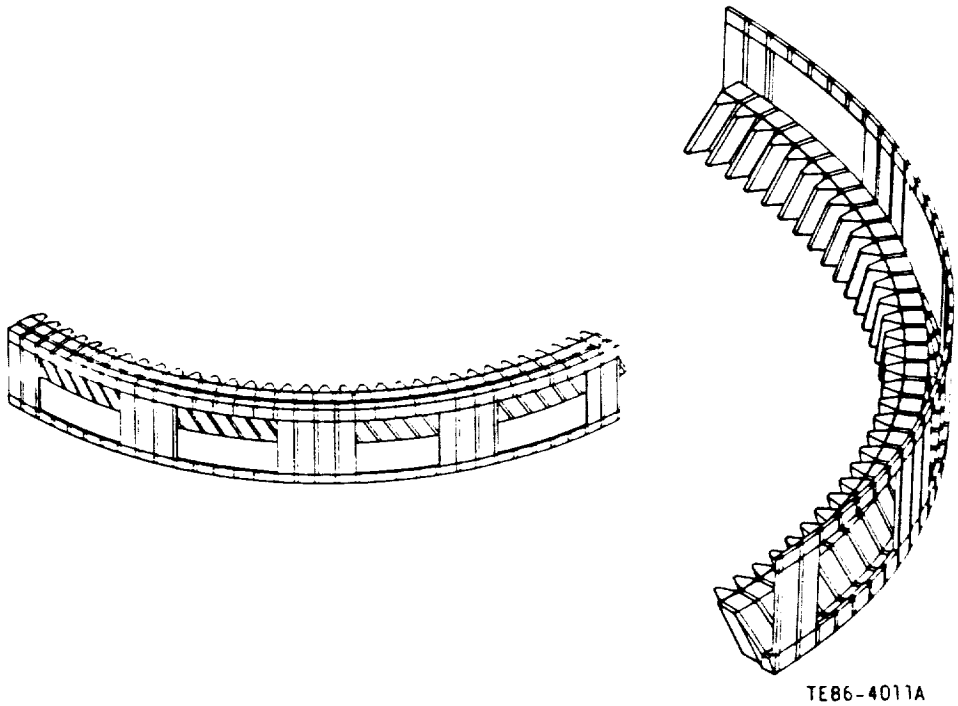

Figure 5.1-4. 3-D finite element models of ring gear geometry.

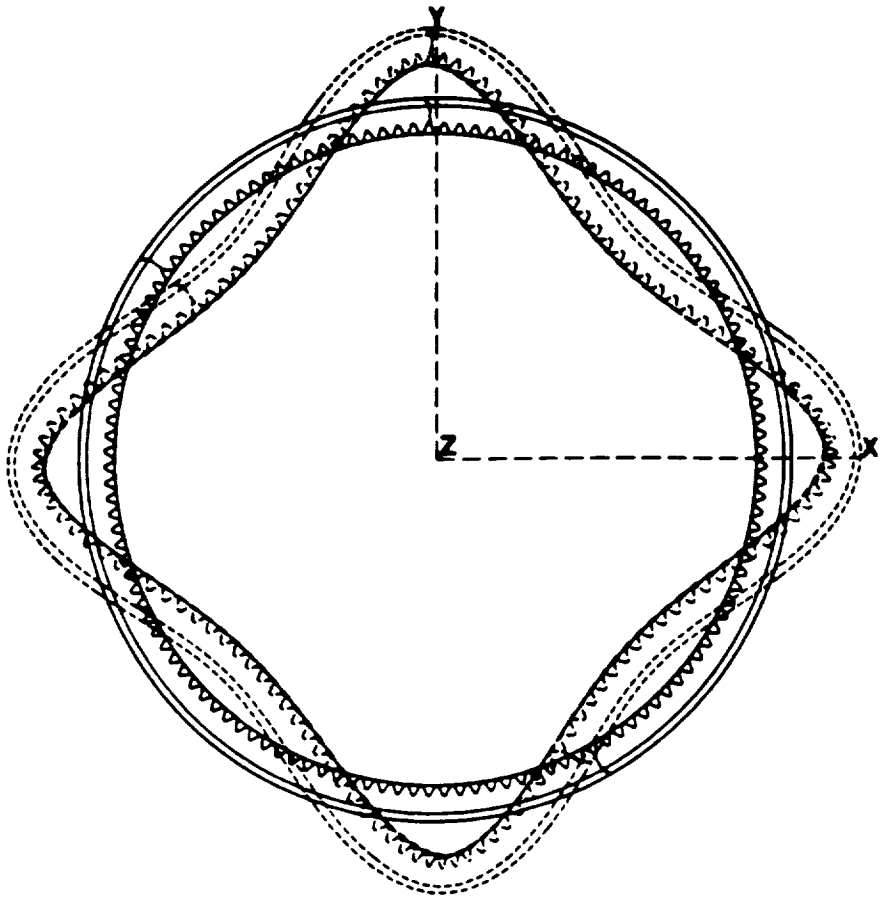

TE86-4010A

Figure 5.1-5. Typical ring gear radial deflection.

by rotation. The separating forces in this type of planet gear cause a pinching load that results in a two point out-of-round bearing raceway. This out-of-round condition can help or hurt the bearing depending on its magnitude. The stiffness of the planet gear was analyzed to control the effect of the pinch loads.

To define the planet gear stiffness and its result on the bearing, a finite element model of the planet gear and bearing was made. This model included the gear with its helical teeth, bearing rollers, bearing internal clearance, gear mesh forces, and gear centrifugal force. Two versions of the gear model are shown in Figure 5.1-8 and a description of the full model is shown in Figure 5.1-9. One side of the double helical planet gear is modeled as a complete ring. The rollers are modeled as three springs in parallel.

The results of the finite element analysis predicted the individual planet bearing roller loads. These loads are shown graphically (see Figure 5.1-10) in a polar plot, which also shows the bearing load zone. The rollers on one side of the bearing (180 deg) are loaded and the other rollers are coasting.

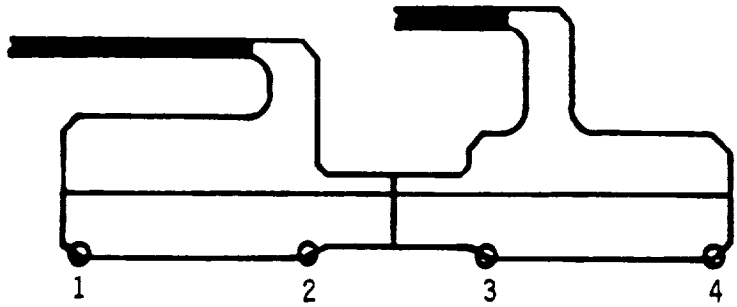

	1-2	3-4
Radial mismatch	0.0020	0.0010
Tangential mismatch	0.0010	0.0015

TE86-4012A

Figure 5.1-6. Calculated ring gear deflections.

5.1.5 Sun Gear Stiffness

Helical gear teeth can cause a skewing or twisting of a part due to its angular load line across the face of the tooth. This twisting can cause misalignment between pairs of teeth in a gear mesh. A finite element analysis of the AGBT sun gear was completed to determine the total misalignment produced by the gear deflections. Figure 5.1-11 shows the finite element model and the loads applied. The resulting deflections showed only 0 deg 0 min 24 sec misalignment at full torque.

5.1.6 Load Sharing

One of the key elements in the design of a double helical planetary gearset is enabling each planet to carry an equal load. For a three planet system where the loads are statically determinate, this is done by fixing either the ring gear, one of the planet gears, or the sun gear in the axial direction and one gear in the radial direction. For planetary systems with four or more planets, parts must be designed with flexibility.

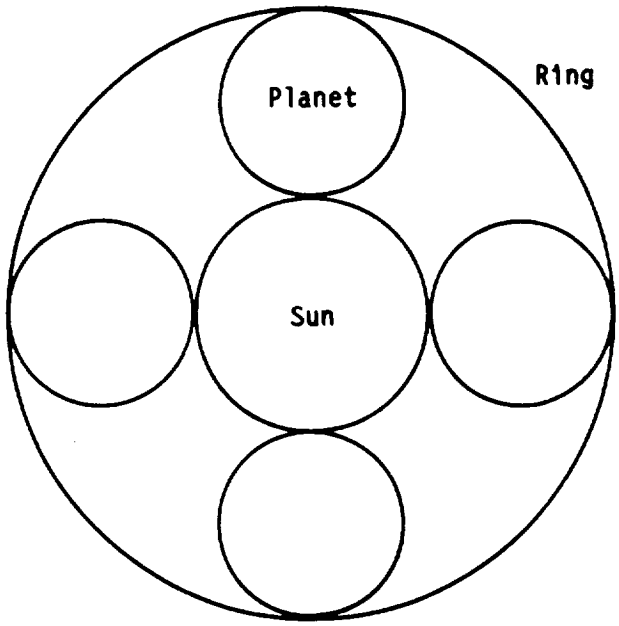

Critical Modes Identification

Ring gear --Multiples of 4-D
Planet gear--Multiples of 2-D
Sun gear --Multiples of 4-D TE86-4201

Figure 5.1-7. Unique aspects of planetary system.

The AGBT planetary gearset has four planet gears. The sun gear and ring gear are free to move in the radial direction for planet-to-planet load sharing. The planet gears and ring gear are free to move in the axial direction for tooth row-to-row load sharing.

Figure 5.1-12 shows the worst load sharing error expected, based on ring gear movement. The highest loaded mesh pushes the ring gear, which moves and causes the other three meshes to pick up more load. The mesh at the sun gear carries the same load as the mesh at the ring gear and the load at other meshes is adjusted.

Figure 5.1-13 shows total mesh-to-mesh predicted load error. Row-to-row load error, from movement of the flex diaphragm (see subsection 5.1.3), is added to planet-to-planet load error. The value is reasonable without selective assembly.

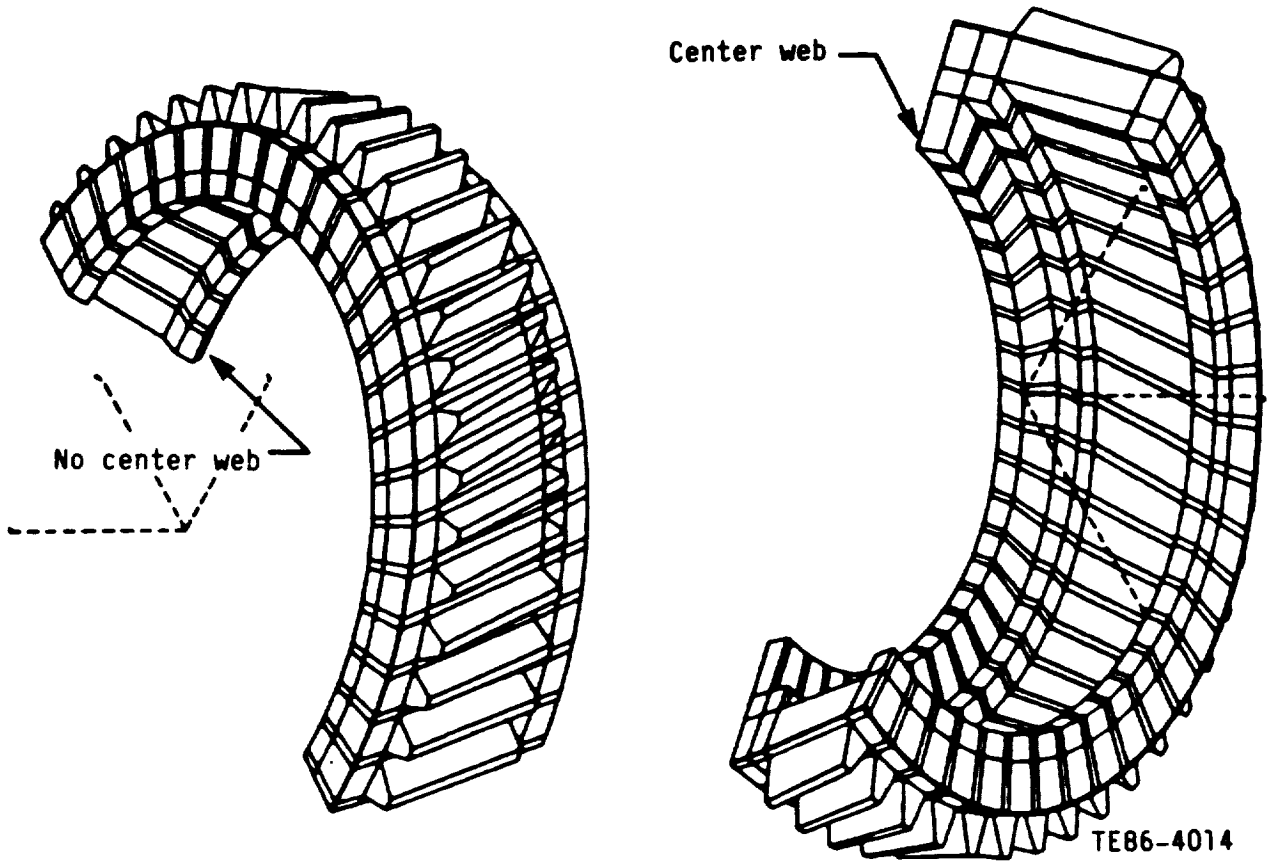

Figure 5.1-8. Finite element models of planet gear.

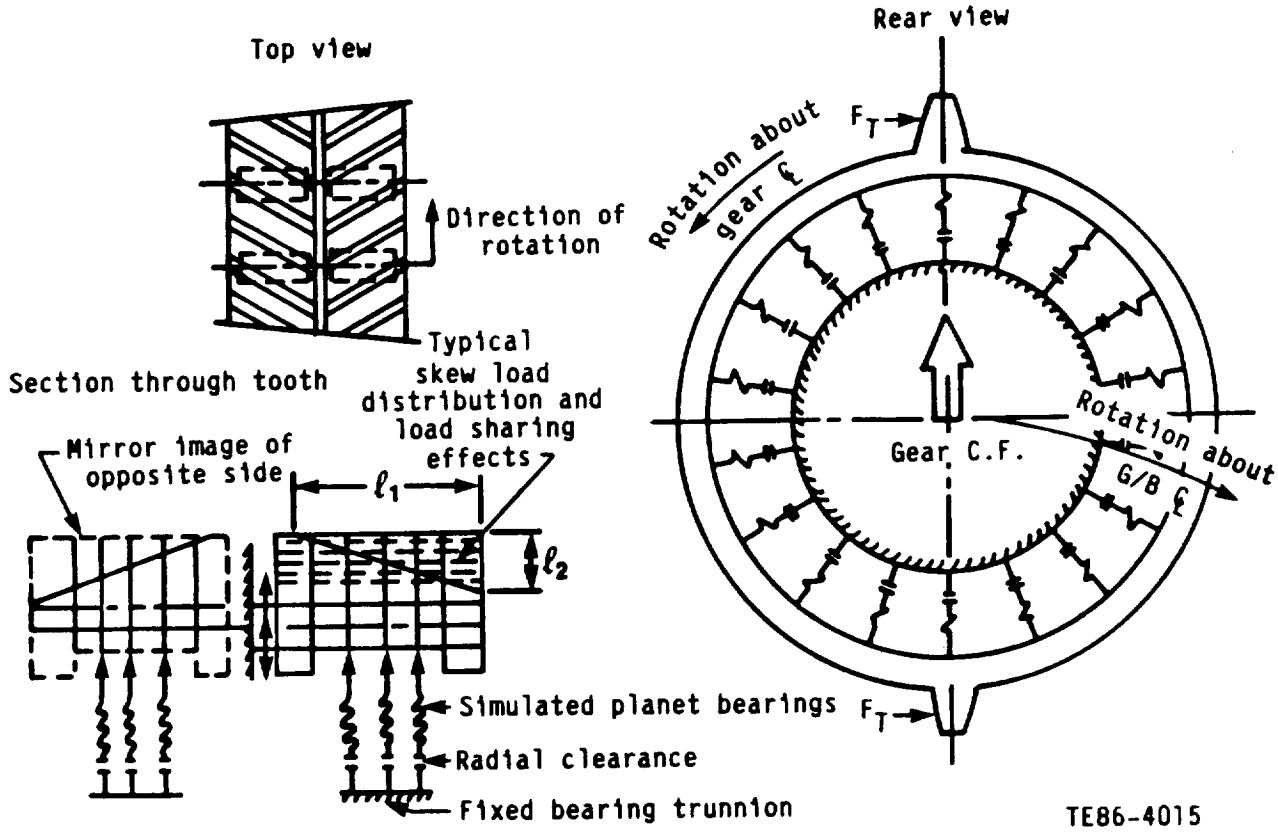

Figure 5.1-9. Procedure used in determining bearing load distribution.

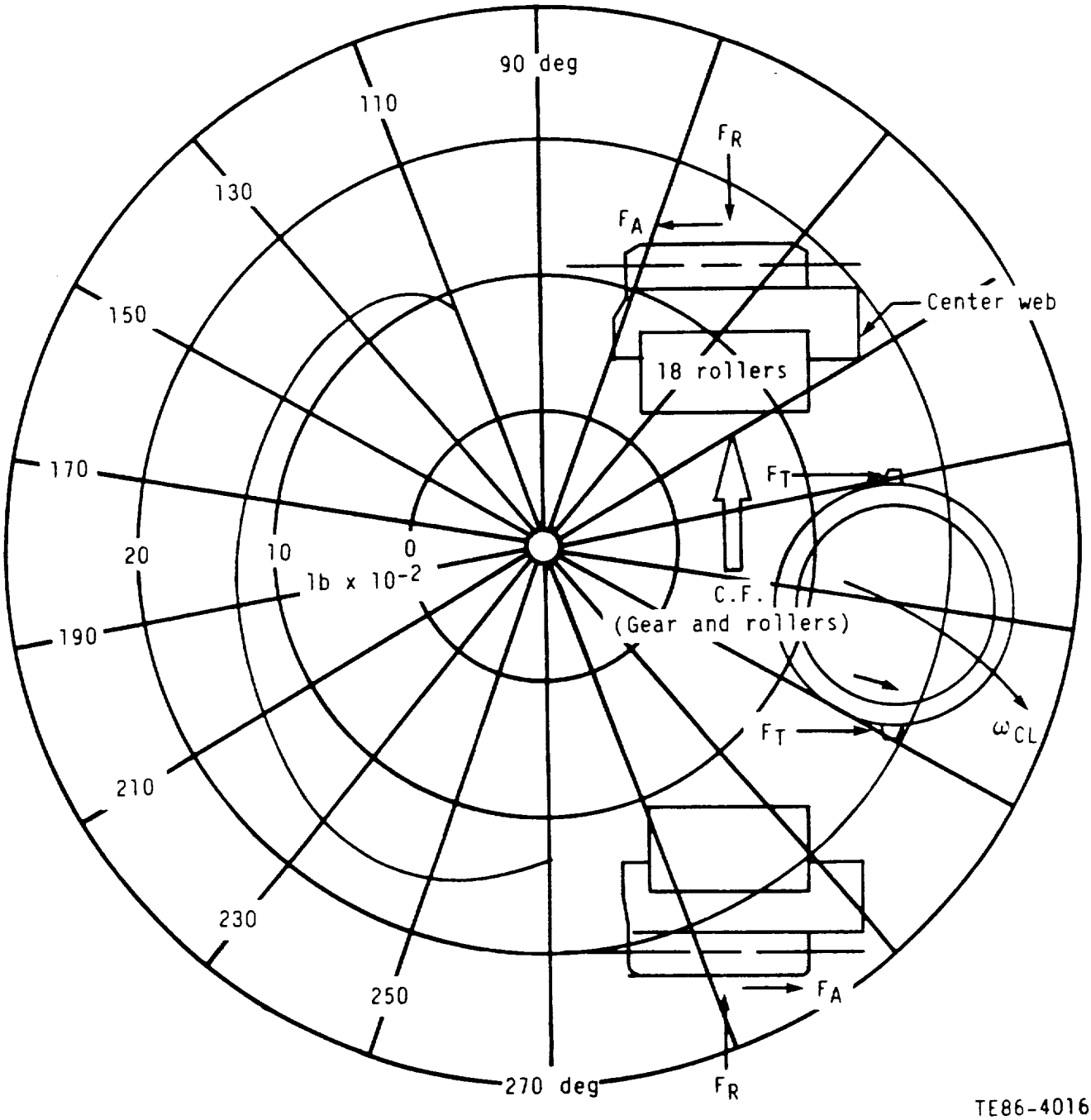

Figure 5.1-10. AGBT planet gear bearing reaction loads.

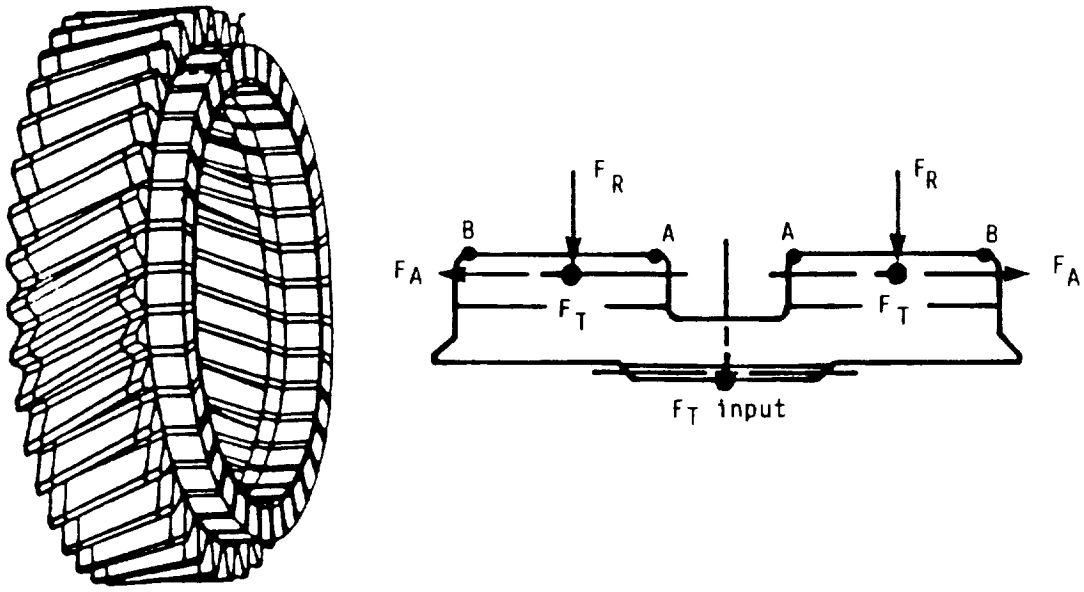

TE86-4018B

Figure 5.1-11. Sun gear deflection.

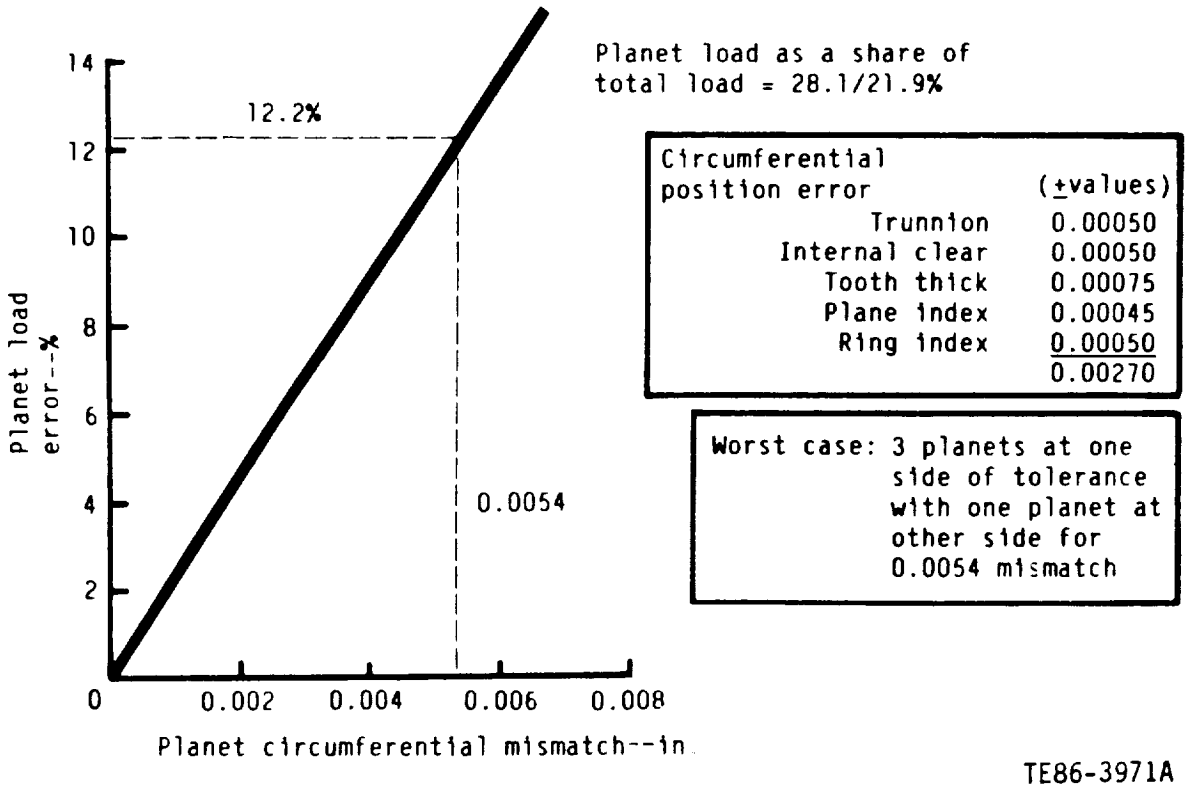

TE86-3971A

Figure 5.1-12. Planet-to-planet load error.

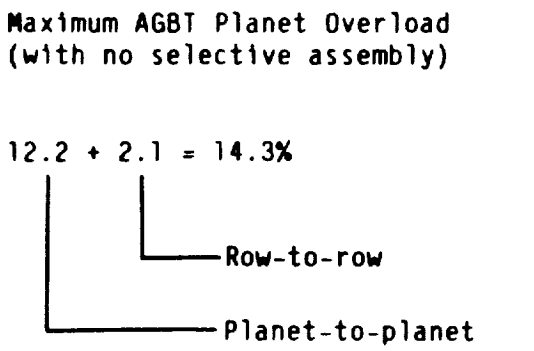

Figure 5.1-13. Load sharing.

5.2 CARRIER

5.2.1 Design Approach

The planet carrier performs several functions in the AGBT differential planetary gearbox.

1. It reacts planet bearing loads.
2. It transfers power from the gearset to the aft prop drive shaft.
3. It establishes radial location of the gearset.
4. It establishes the centerline of the main power gear assembly.
5. It transfers oil to several locations.

These requirements lead to the need for an accurately machined piece of hardware that is highly resistant to trunnion deflection under load.

5.2.2 Structural Analysis

Carrier sizing was accomplished by performing a 3-D finite element model (FEM) analysis of the entire assembly. The carrier model was created by combining several less complicated substructures (see Figure 5.2-1). CAD facilities were used to generate meshes for the two carrier plates and the spacer. The trunnions were generated with a cylinder preprocessor. All substructures were joined as if they were one piece to create the complete model. The model was loaded by applying the planet bearing load distribution, determined in the planet bearing analysis, to nodes corresponding to the roller locations. These forces were reacted by the carrier spline. One point was used to fix the carrier position in space in the radial plane (a node on a trunnion).

Results of the stress analysis are shown in Figure 5.2-2. The maximum bending stress occurs in the trunnion side back plate between the trunnion and spacer. The overall maximum stress was 45,000 lb/in.^{2} at the oil feed holes. This stress results from the stress concentration due to an axial hole drilled in the plate. All stresses are less than the 102,000 lb/in.^{2} allowable for AISI 4130 material. This value reflects a three sigma confidence level at 400°F.

Deflections obtained from this model are shown in Figure 5.2-3. The exaggerated plot shows that most of the movement occurs in the back plates while very little occurs in the trunnion itself. Much of the overall torsional windup occurs in the carrier spline. The important windup is that which misaligns the trunnion centerline relative to the undeflected centerline. This value is estimated to be 0 deg - 2 min. There is also some very minor radial deflection of the trunnion.

5.2.3 Carrier Fasteners

Trunnion Nut

The carrier model was analyzed as if it was a welded or one piece construction. The fasteners used to hold the assembly together were sized to apply the loads found in this model. The trunnion nut clamp load was selected to prevent relative movement between the two carrier halves.

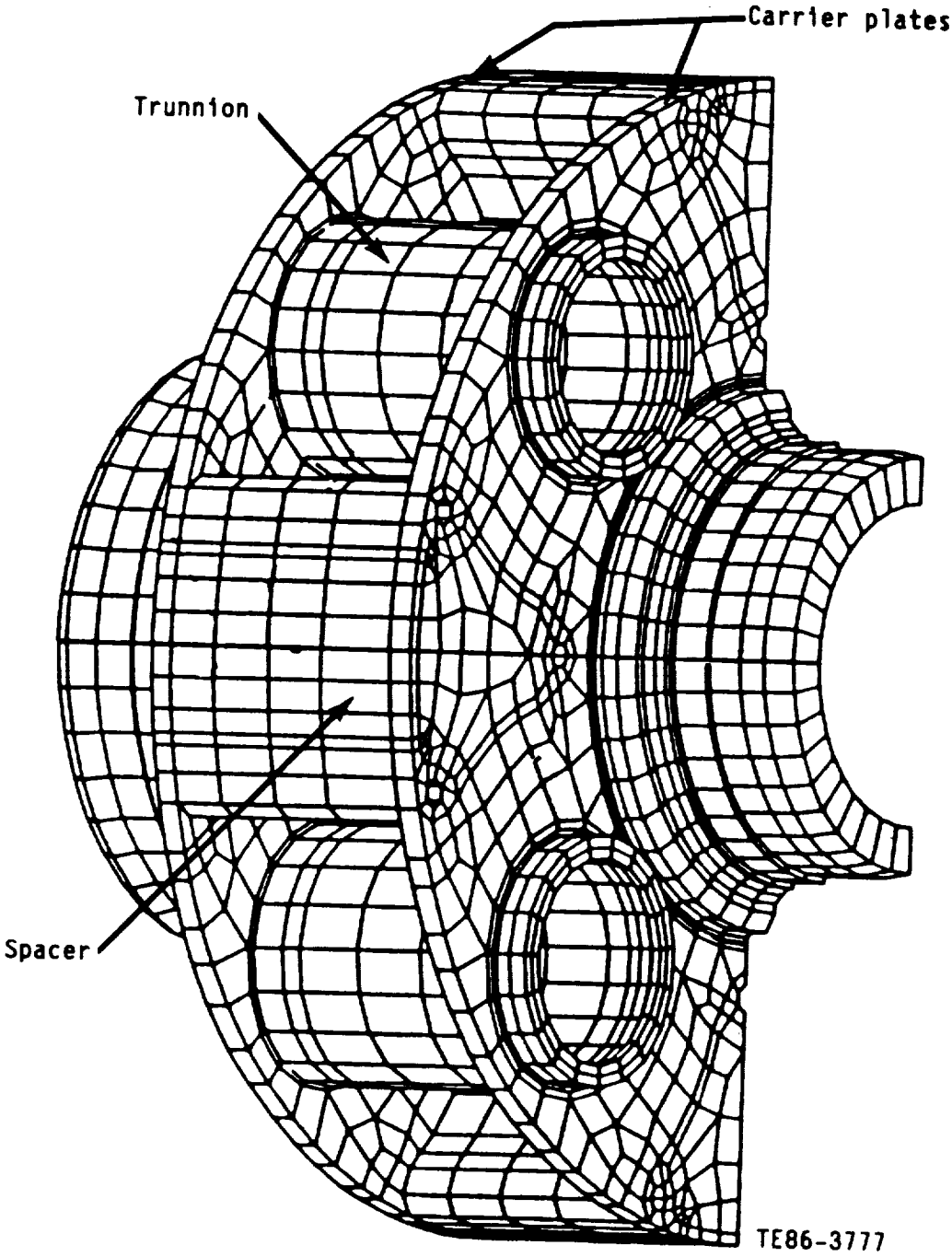

Figure 5.2-1. Planet carrier FEM model.

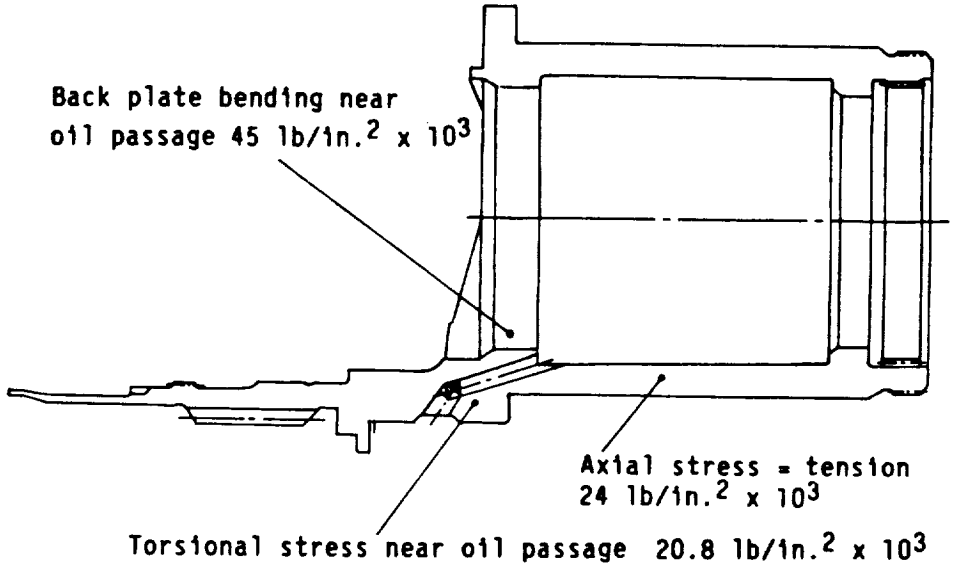

TE86-3845

Figure 5.2-2. Planet carrier stresses.

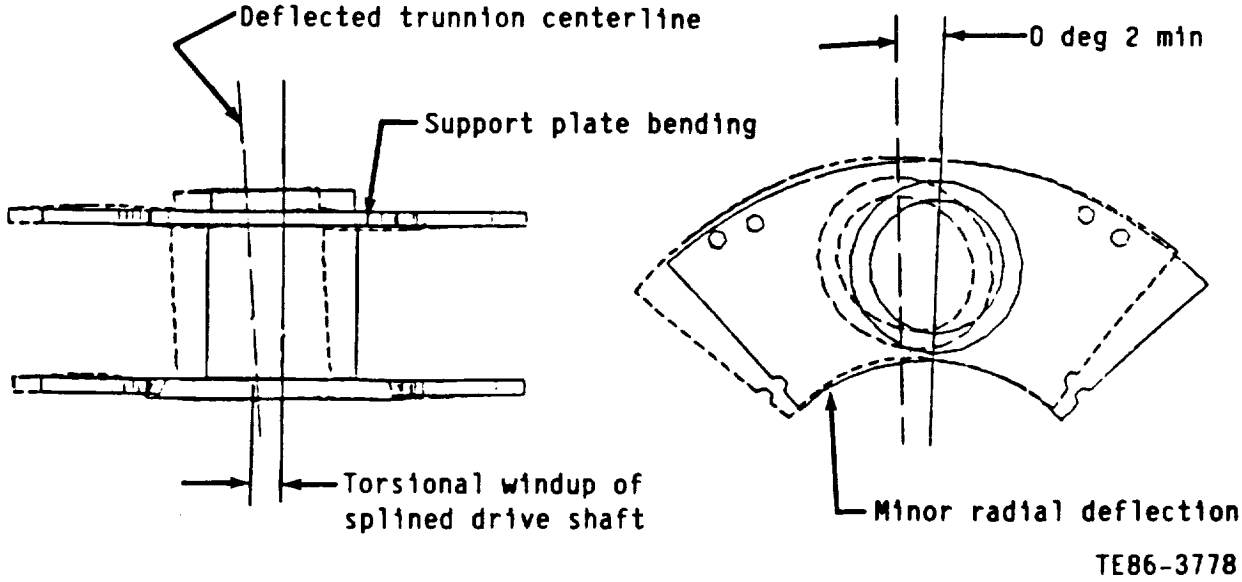

TE86-3778

Figure 5.2-3. Carrier trunnion deflection.

A shear force of 5506 lb must be transmitted between the carrier halves at each trunnion (see Figure 5.2-4). In order to prevent movement, the locknut must generate a friction force equal to this shear force. Assuming a worst case friction coefficient of 0.1 for lubricated steel on steel and noting that there are two friction faces that will resist this shear force:

$$F_{clamp} = \frac{5506}{0.1} \times (0.5) = 27{,}530 \text{ lb}$$

To ensure that at least 27,530 lb is applied by the locknut, a thread friction coefficient of 0.15 was selected. The torque required is 1550 ft-lb. If the friction coefficient is actually at the low limit, f = 0.10, and the 1550 ft-lb is applied, F_{clamp} will be greater than required (F_{clamp} = 40,994 lb). This is the design load used to calculate stress in the locknut.

A Patran FEM analysis was performed on the locknut since handbook calculations showed that stresses could be high. The model is shown in Figure 5.2-5 and the results in Figure 5.2-6. The thrust face is relieved to reduce the moment created by the axial thread force. The thread loads result primarily in tensile hoop stress with the highest value at the inner diameter of the thrust face. The assumed thread load distribution concentrates the load near the thrust face. The 109,000 lb/in.^{2} stress is not enough to yield AISI 4140 steel (yield strength 130,000 lb/in.^{2}), but it does indicate that if the loads on the first several threads are higher than those assumed, local yielding can result. A subsequent calculation showed that the maximum locknut stress drops to 78,000 lb/in.^{2} if all threads share the load equally. Based on these results, the locknut design was determined to be satisfactory.

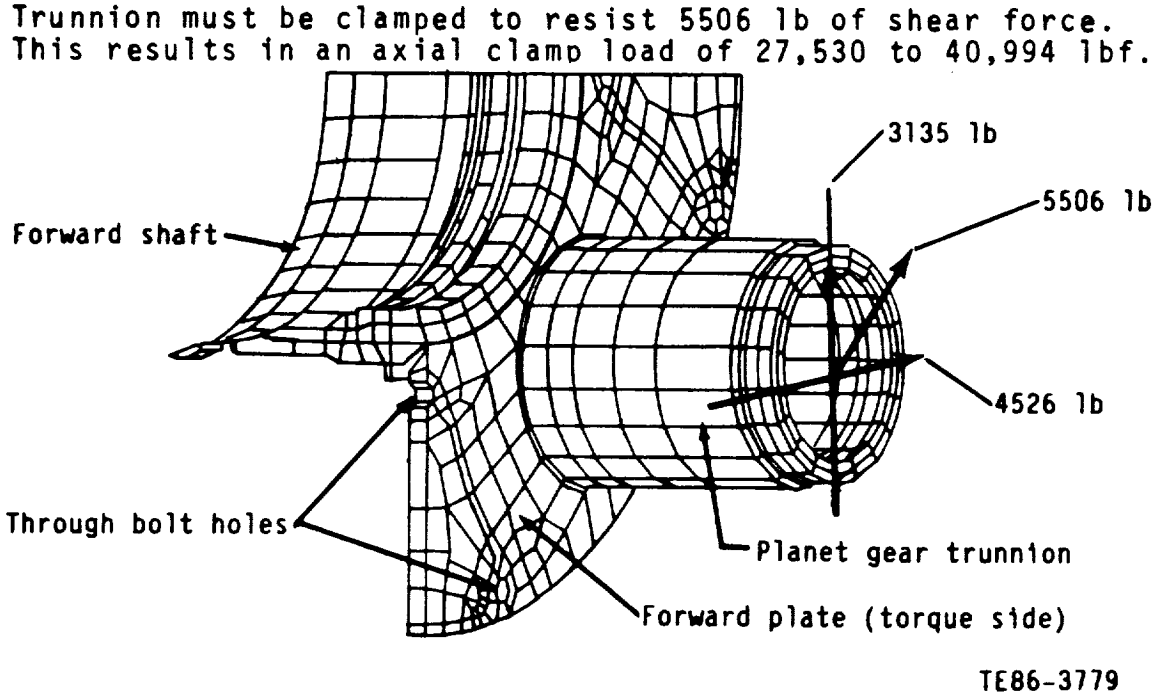

Figure 5.2-4. Carrier trunnion clamp load.

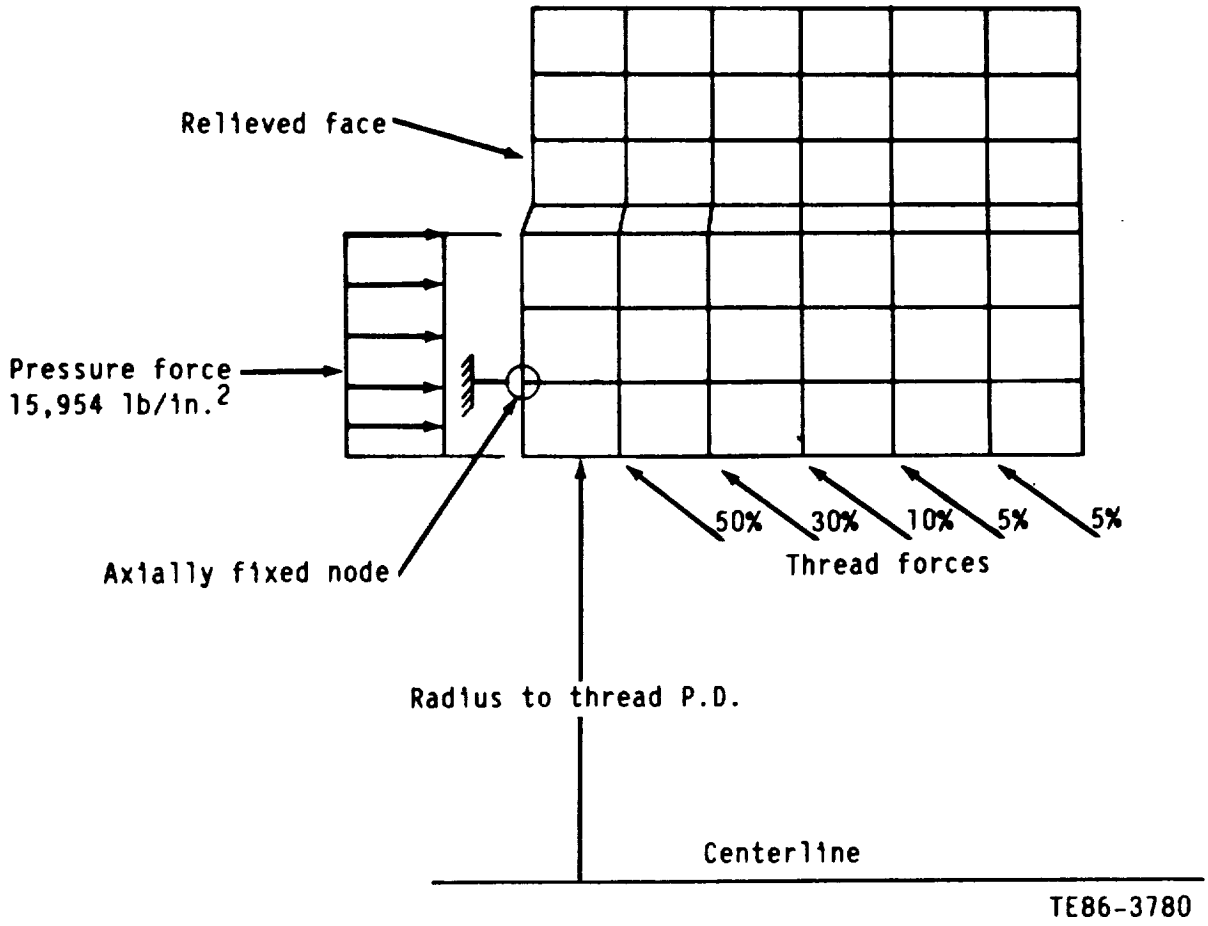

Figure 5.2-5. Patran model of AGBT trunnion locknut.

Spacer Bolts

The spacer bolt load required to prevent movement of spacers relative to the carrier plates is 8500 lb per bolt as determined by the FEM analysis (see Figure 5.2-7). At full load, an additional tensile force of 2000 lb per bolt will be developed. Thus, the bolts must be able to withstand 10,500 lbf. This load could be carried by a high strength three-eighths bolt at a thread stress of 122,000 lb/in.^{2}. A seven-sixteenths bolt diameter was selected, however, to provide a substantial factor of safety so that initial clamp load could be increased, if necessary. The bolt is made of AMS 5662 CRES (inconel) and heat treated to provide a yield stress of 190,000 lb/in.^{2} and a tensile stress of 220,000 lb/in.^{2}. At a thread stress of 190,000 lb/in.^{2}, this bolt can produce 23,000 lbf.

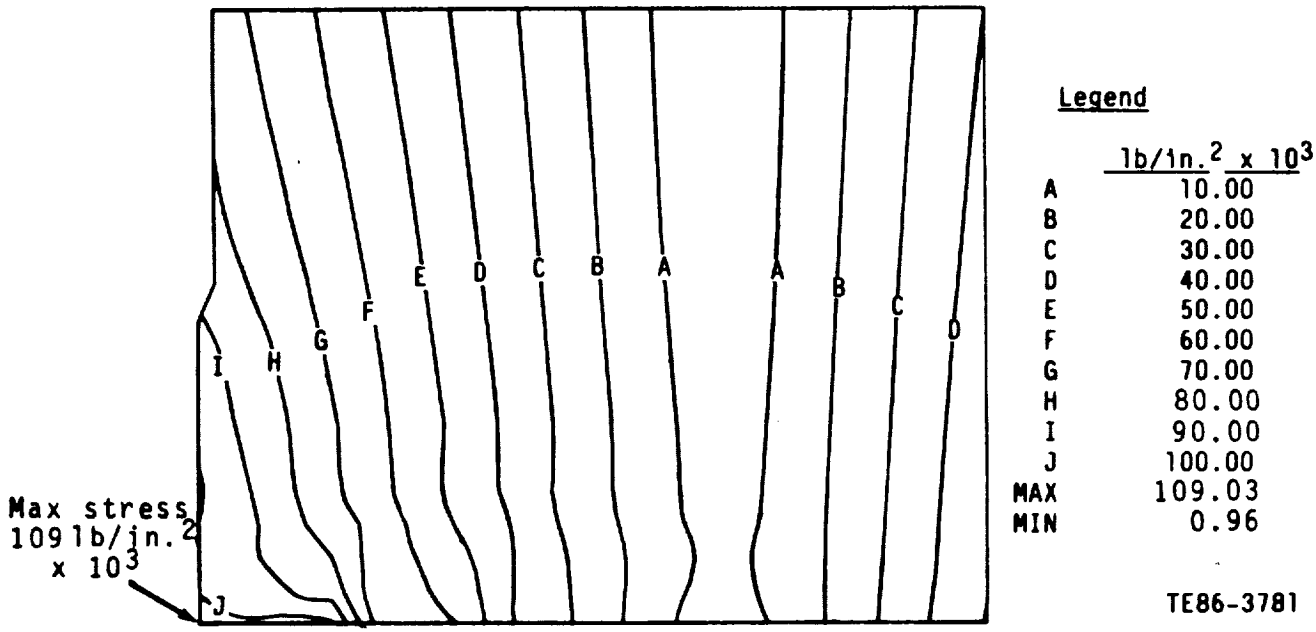

Figure 5.2-6. Locknut equivalent stress.

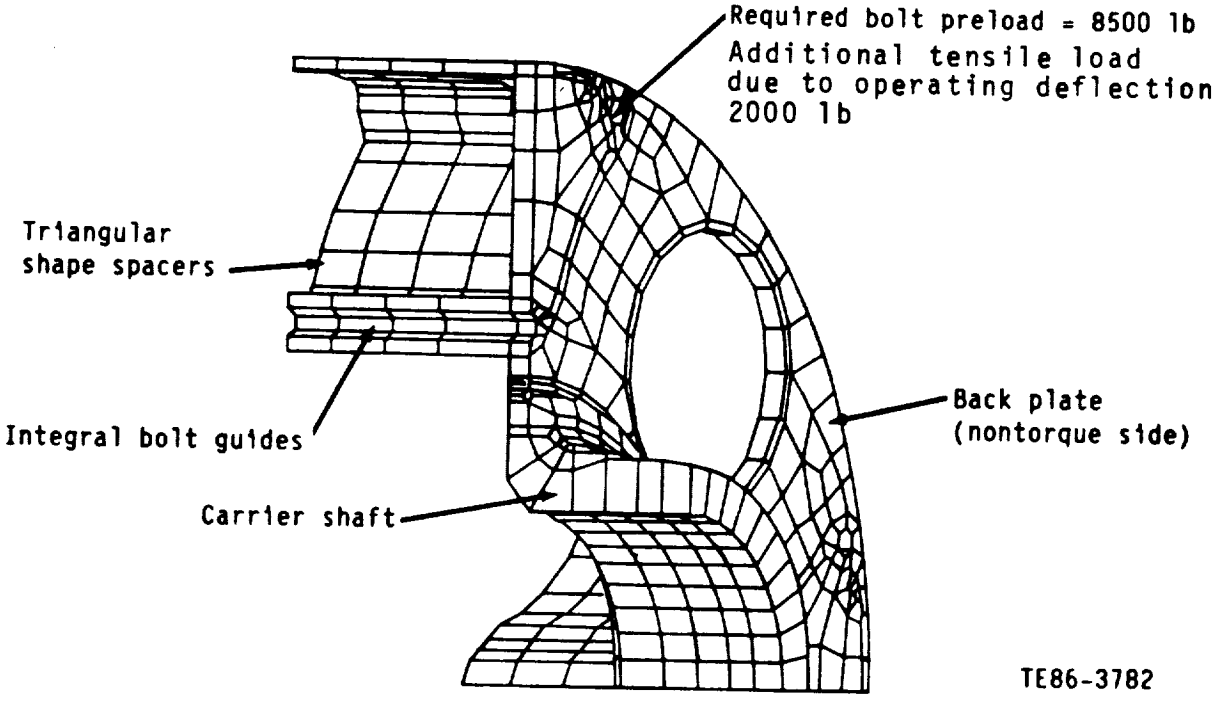

Figure 5.2-7. Carrier spacer bolt clamp loads.

5.3 SHAFTING AND SPLINES

5.3.1 Prop Shaft

The AGBT prop shaft was designed to support a 13,000 hp Prop-Fan using loads and geometry from Hamilton Standard. The prop shaft area is shown in Figure 5.3-1. The shaft is a cylindrical piece supported in the housing by two tapered roller bearings. At each end of the shaft there is a bolt flange. The flange at the left (Figure 5.3-1) supports the Prop-Fan; the other flange connects to the flex diaphragm, which supplies power from the ring gears.

The prop shaft connection to the prop is held concentric with a close fitting pilot diameter. An O-ring seals the joint and a spline locks it to prevent bolts from carrying the torque load. The clamp load is designed to keep the prop shaft from separating under moment loads or slipping under torque and shear loads. The worst case for moment loads is cruise and the worst case for torque is takeoff. The bolts are Inconel 718 material.

The prop shaft is connected to the flex diaphragm with a ring of bolts. These bolts provide an axial clamp load across the tapered roller bearing inner rings and seal runner that prevents fretting under high moment loads. The bolts are made from Inconel 718 and the nuts from Waspaloy for high strength and corrosion resistance.

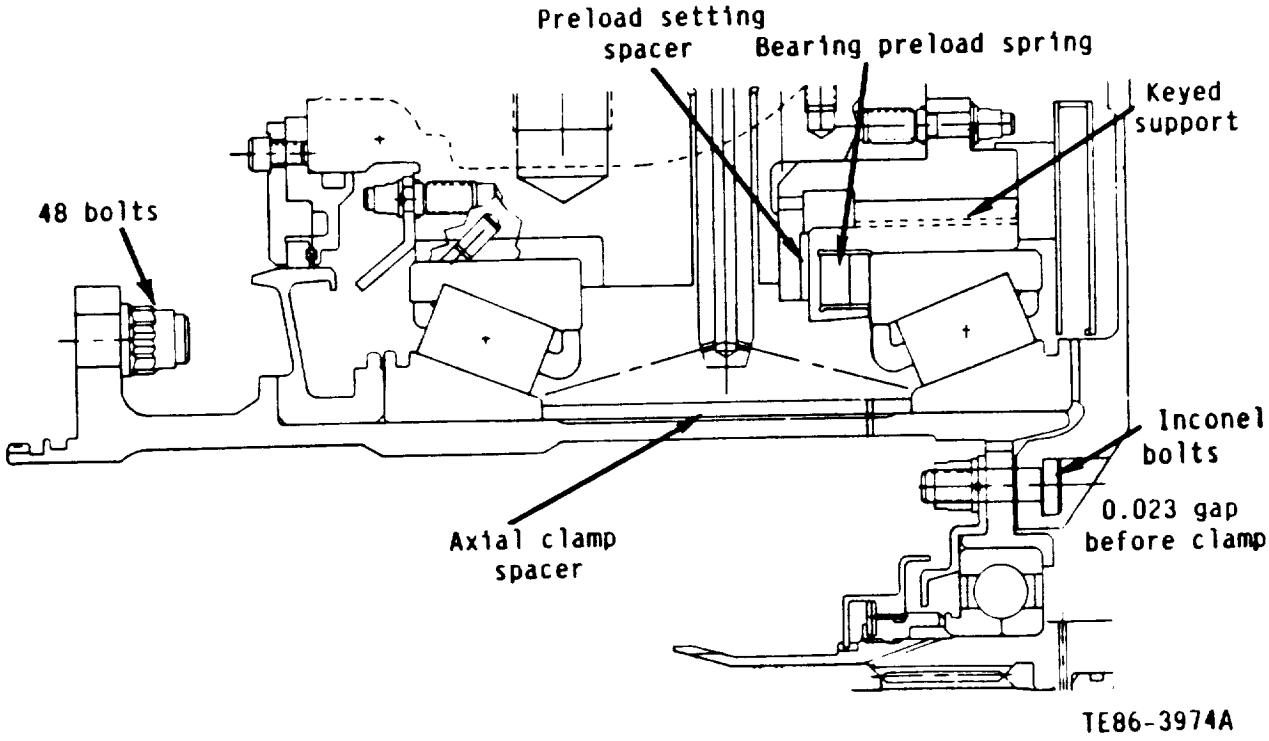

Figure 5.3-1. Prop shaft.

The proper axial load is set by controlling the gap between the prop shaft flange and the flex diaphragm before bolt clamping. This gap is controlled by measuring the parts and grinding the axial clamp spacer to the proper length. The tapered roller bearings are set similarly by grinding the preload setting spacer (see subsection 5.4.1).

Strength of a prop shaft is critical to the reliability of the engine. Because of high loads from the prop and its nonuniform shape, the stress analysis of the prop shaft was done by finite element models (FEM). A three-dimensional (3-D) sector FEM was used to analyze prop loads and stresses. A two-dimensional (2-D) FEM was used to analyze the prop shaft stresses and deflection caused by the axial clamp. These two models are shown in Figure 5.3-2.

The stress analysis on the prop shaft was a combination of the results of the two models. The 2-D model gave the stresses in the shaft due to the axial clamp load. These stresses were taken as mean or nonalternating. The prop loads were applied to the 3-D model and the resulting stresses were assumed to be alternating stresses. Figure 5.3-3 shows the propeller loads that were used in the 3-D model. These are worst case loads. The aerodynamic loads are at high speed cruise and supplied by Hamilton Standard. The inertia loads are generated by maneuvers and wind gusts. These loads are additive and result in the total load shown in Figure 5.3-3. The prop shaft was designed for infinite fatigue life at these loads.

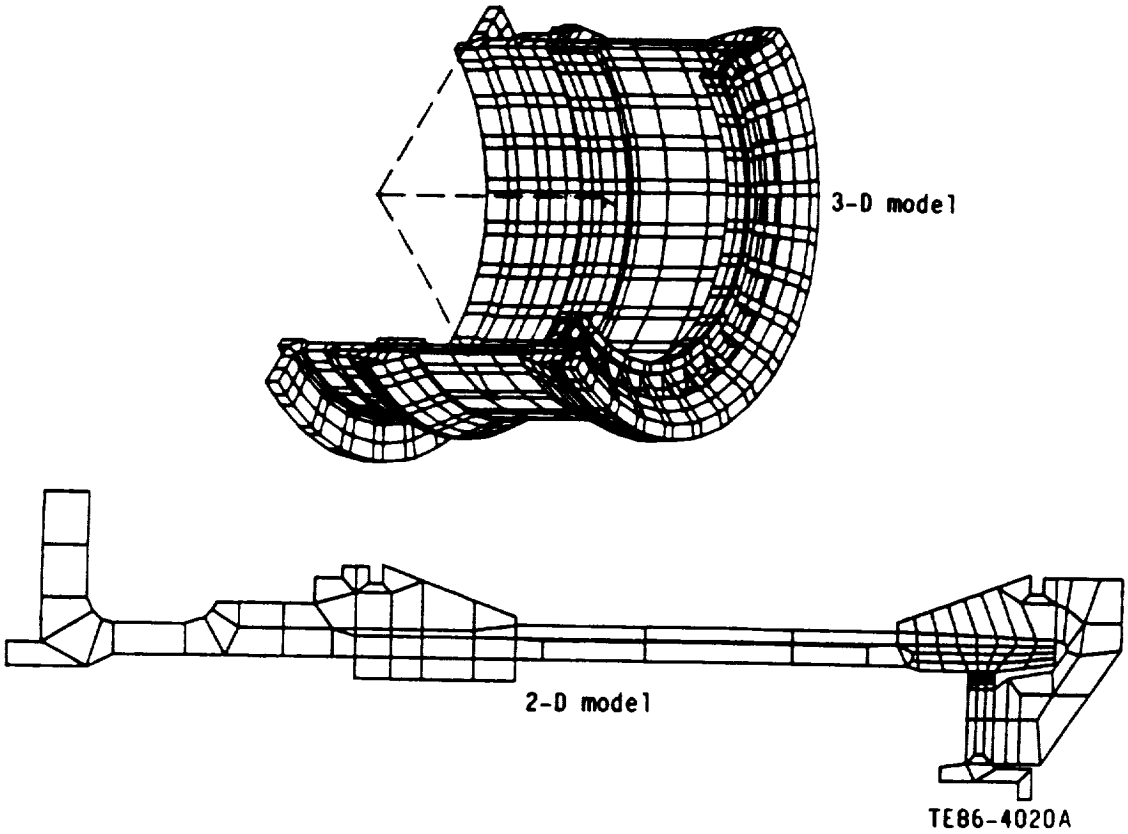

Figure 5.3-2. Prop shaft finite element models.

1) Aero--Cruise 1 x P
FN--Normal load = -2520 lb
MP--Pitching moments = 51,480 in.-lb
MY--Yawing Moment = ± 14,760 in.-lb
Thrust = +4500 lb

2) Inertial
10 G's down
2 G's forward
1 G side

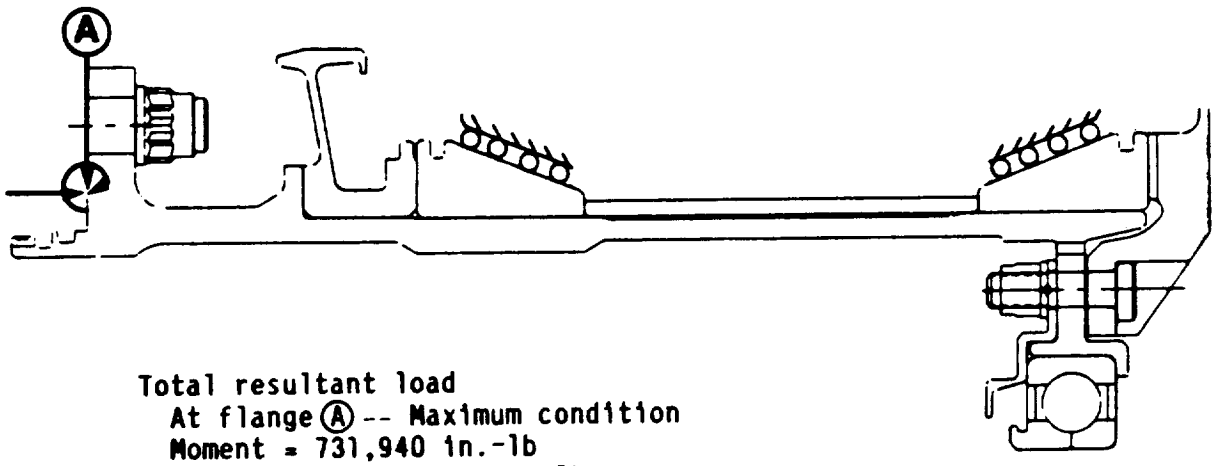

Total resultant load
At flange Ⓐ -- Maximum condition
Moment = 731,940 in.-lb
Vertical shear = 32,185 lb
Thrust = 9840 lb

TE86-4019

Figure 5.3-3. Propeller loads.

There are 11 critical stress points in the prop shaft area design: seven on the prop shaft itself, two on the flex diaphragm, and one each on the bearing spacer and the seal runner. These locations are shown in Figure 5.3-4 with stress results listed in Table 5.3-I. All values are within the capability of the AMS 6414 material.

Table 5.3-I.
Stress and margin with respect to infinite high cycle fatigue (HCF) life.

Location	Component	Equivalent stress ($lb/in.^2 \times 10^3$) ±
A	Prop shaft	0 ± 25.92
B	Prop shaft	24.49 ± 17.59
C	Prop shaft	39.50 ± 5.51
D	Prop shaft	60.75 ± 15.27
E	Prop shaft	85.29 ± 19.30
F	Prop shaft	16.05 ± 19.82
G	Prop shaft	100.28 ± 14.00
H	Flex diaphragm	79.84 ± 15.06
I	Flex diaphragm	72.66 ± 16.57
J	Bearing spacer	40.23
K	Seal runner	48.86

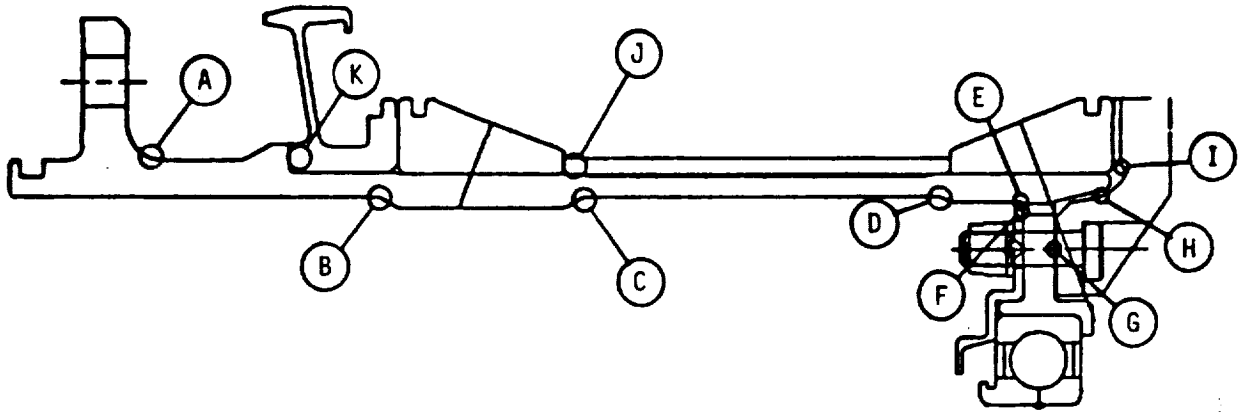

TE86-4194

Figure 5.3-4. Calculation locations.

5.3.2 Input Shaft and Sun Gear Shaft

The input shaft and sun gear shaft combination transmits the drive power from the engine to the sun gear. The input shaft is mounted on two preloaded split inner ring ball bearings. The sun gear shaft is a quill shaft supported at one end by the input shaft and at the other end by the sun gear. The sun gear shaft provides a flexible location for the sun gear. Axial location is provided by the input bearings.

Figures 5.3-5 and 5.3-6 illustrate the sun gear shaft and the input shaft with their critical stress points, respectively. Table 5.3-II lists the resulting stresses against high cycle fatigue at maximum takeoff power. Each critical point was analyzed for torsion, tension, hoop, and bending stresses with stress concentration factors included. The nonalternating stresses were combined into an equivalent mean stress by the distortion energy method. Bending stresses

Table 5.3-II.
Input and sun gear shafts stress analysis.

Critical point	Equivalent stress, lb/in.^{2} Mean	Alternating
Sun gear shaft		
1	75,750	6970
2	58,100	3660
3	54,040	13,600
4	112,300	10,400
Input Shaft		
1	82,590	13,880
2	82,340	18,060

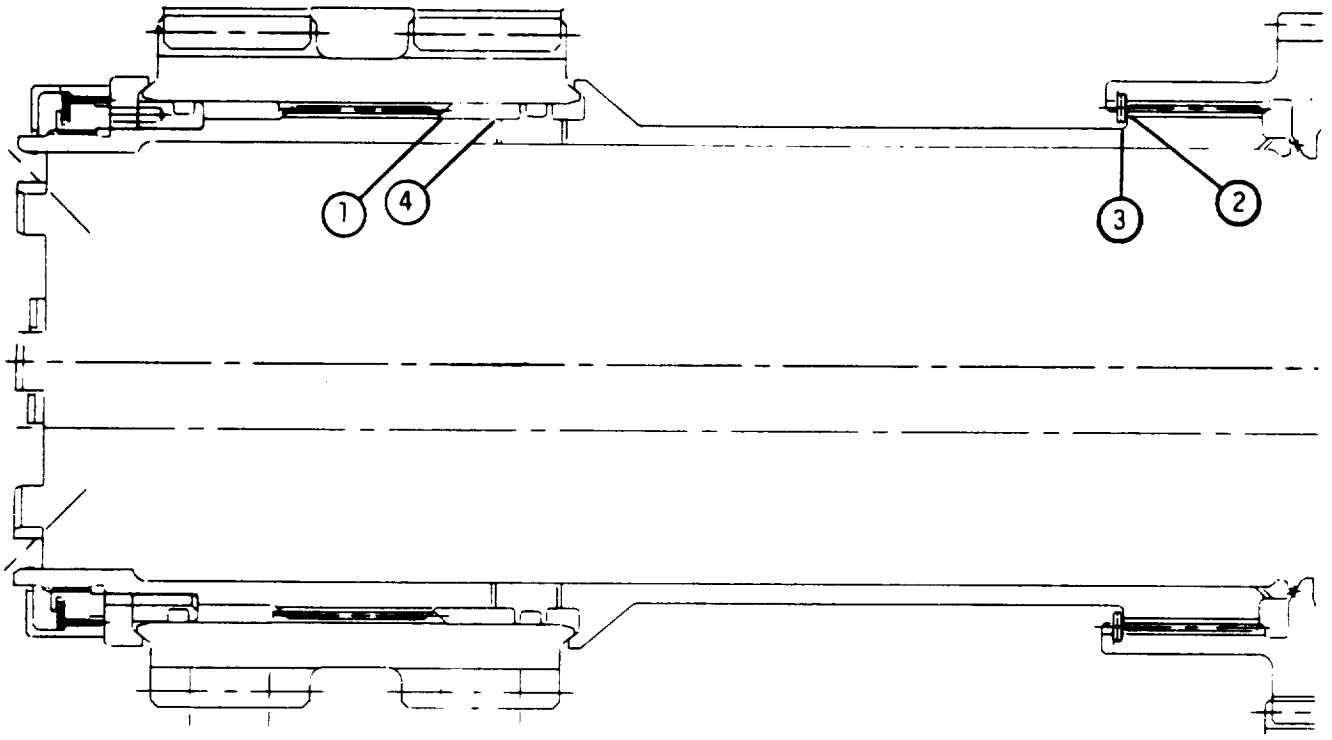

TE86-4196A

Figure 5.3-5. Sun gear shaft.

from the working splines were the alternating stresses. All stresses are torque induced and any change in torque causes a proportional change in shaft stresses.

5.3.3 Shaft Splines

There are eight splines in the AGBT gearbox. The locations of these splines are shown in Figure 5.3-7 and the operating data, at full power, for these splines are shown in Table 5.3-III.

The working splines are hardened, by either carburizing or nitriding, for long wear life. They are flooded with flow-through oil to the entire depth of the teeth to minimize fretting.

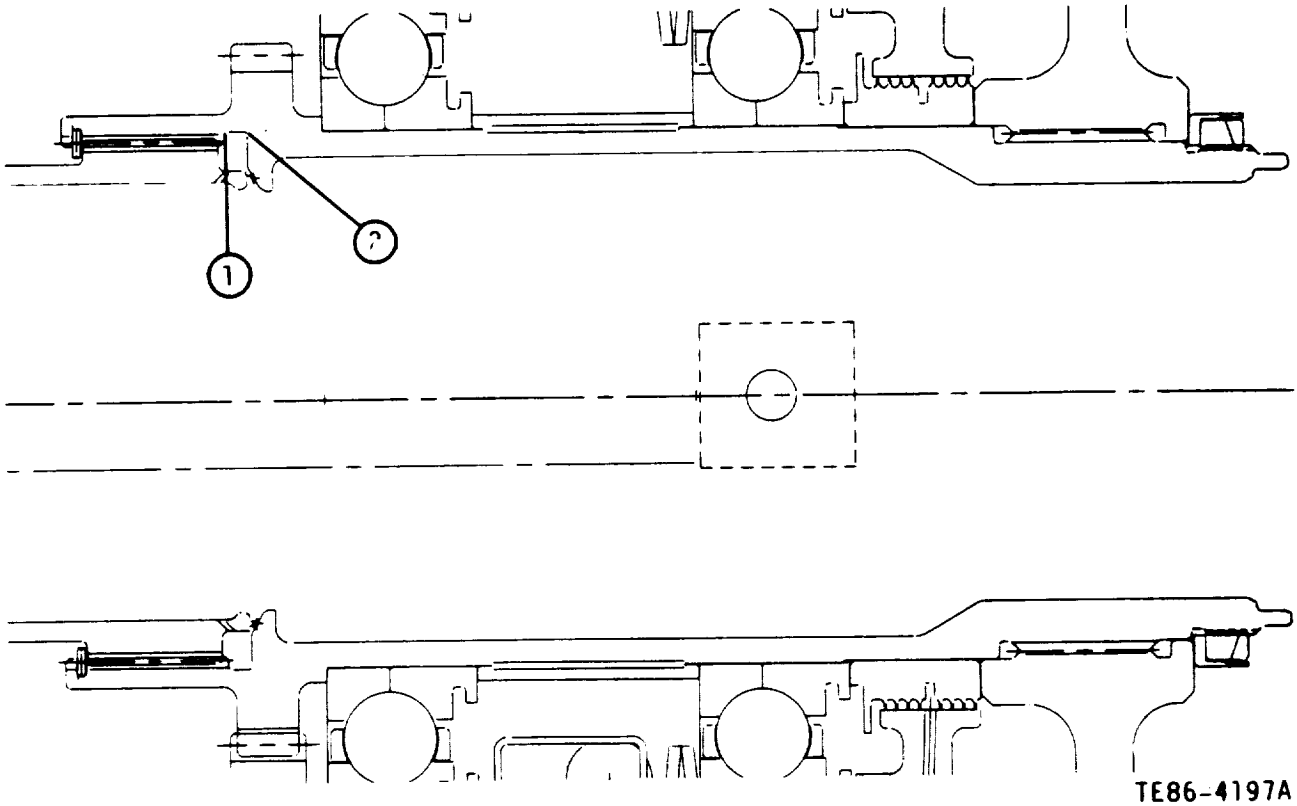

Figure 5.3-6. Input shaft.

Table 5.3-III.
Spline data.

Spline number	Number of teeth	Pitch	Contact stress (lb/in.^{2})
1. Outer output prop shaft spline	226	16/32	14,300
2.* Inner output prop shaft spline (carrier)	68	8/16	18,900
3.* Sun gear spline	70	16/32	18,600
4. Planet carrier acc gear shaft spline	218	32/64	1122
5. Input shaft to sun gear shaft spline	72	16/32	18,600
6. Carrier trunnion torque spline	104	32/64	13,600
7. Carrier trunnion nut spline (both)	156	32/64	6060
8. Carrier ball bearing spanner nut (both)	16	32/64	630

*Indicates a working (flexible) spline. All others are nonworking (fixed) or tooling splines.

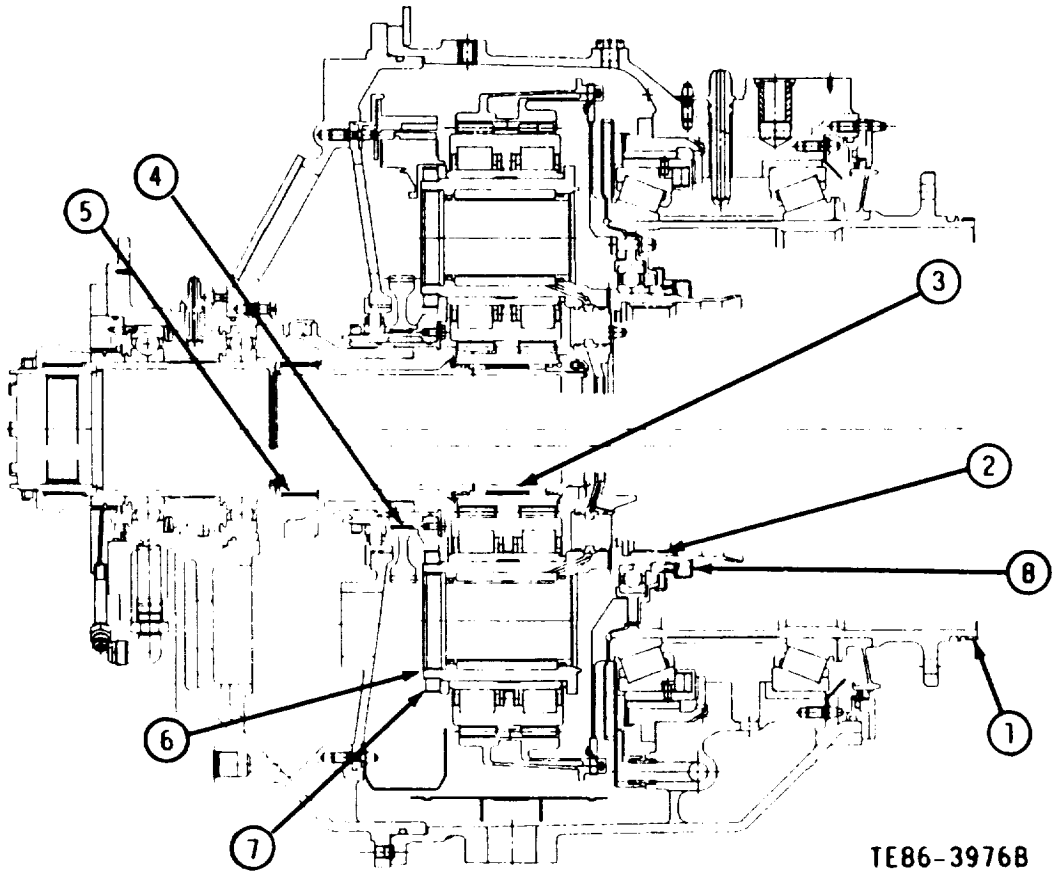

Figure 5.3-7. Spline locations.

5.4 BEARINGS

5.4.1 Prop Shaft Bearings

Trade Studies on Bearing Type and Mounting Arrangement

Tapered roller bearings were compared to the more common propeller mounting system comprised of cylindrical roller bearings for radial loads and a ball bearing for thrust load(s). Tapered roller bearings were found to offer several advantages as they can support combined radial and thrust load and, accordingly, only two bearings are required, thus increasing system reliability. Indirect mounted tapered roller bearings, designed with a steep half cup angle, provide an effective load center that is longer than their actual geometric spread to more effectively resist and reduce overhung Prop-Fan loads. In addition, tapered roller bearings can meet mounting stiffness requirements through axial preloading. Figure 5.4-1 depicts the indirect mounting arrangement of the prop shaft bearing and lists the basic features of this mounting arrangement. Initial studies of prop shaft bearing life versus bearing setting for a given 3, 4, 4.5, and 6 in. geometric spread and 20 deg contact angle (half cup included angle) indicated that a 4.5 in. geometric spread and -0.002 in. bearing setting would provide optimum bearing life. A graphical presentation of these studies is given in Figure 5.4-2. More in-depth studies concluded that a 23 deg half cup included angle and 5 in. bearing geometric spread would provide optimum bearing set life for a mounting setting range of -0.004 to +0.004 in.

Tapered roller bearings designed with ribbed cup or ribbed cone were evaluated for the subject gearbox application. Both designs provide a positive roller guidance to keep the rollers aligned, which is one of the major features unique to tapered roller bearings. The tapered roller's large diameter ends have a spherical ground surface that contacts either the cup or cone rib, based on the selected design, at a point when it is under no load. Under load, this contact area becomes elliptical and the roller rib interface geometry promotes hydrodynamic lubrication in the contact area. Ribbed cup design was selected for better lubrication of both roller large ends and cup piloted cage land.

Figure 5.4-3 shows the direction of oil jets with ribbed cup design bearing as the oil jets are introduced to the bearing at the roller small ends and forced by the roller rotational and orbital motion toward the large ends. Lower bearing heat generation and operating temperature are anticipated with this ribbed cup and outer-ring-piloted cage design. This design provides capability for extended operation under oil off condition due to the oil retained between the roller large ends and cup rib.

Selection of prop shaft tapered roller bearing size was based on prop shaft o.d. size and the selected bearing internal geometry that will meet both radial load rating and fatigue life requirements for the given prop loads/speed under various flight missions.

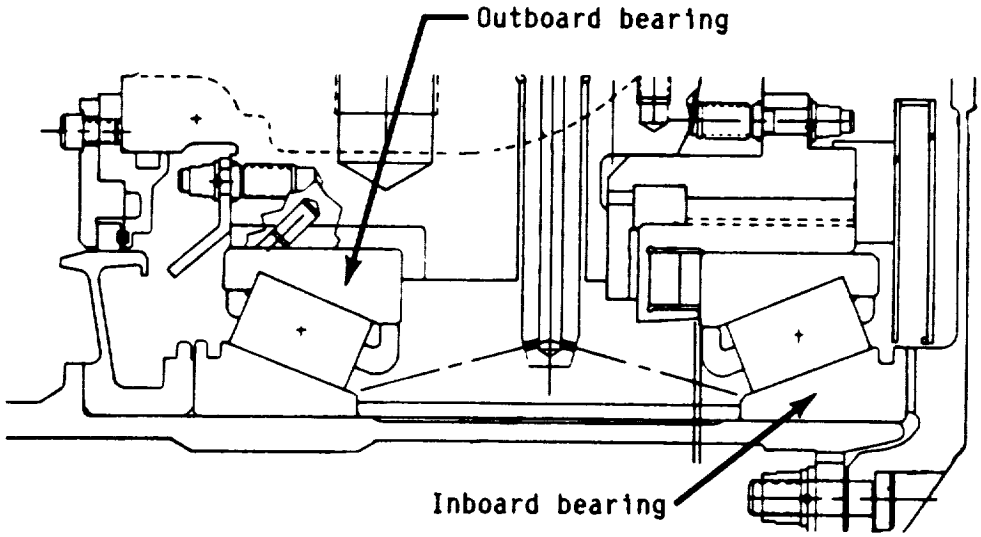

TE86-3770A

Figure 5.4-1. Indirect bearing mounting for reduced bearing loads, shorter total gearbox length, and improved mounting stiffness.

Final Design Configuration

The calculated prop shaft bearing loads along with adjusted L10 life for each flight mission are tabulated in Table 5.4-I. The calculated bearing loads and lives are based on steady-state prop loads. Table 5.4-II lists the calculated maximum Hertz contact stresses for the inboard and outboard prop shaft bearings under both normal steady state and three minutes misalignment loading conditions. The final geometry and design data of the prop shaft tapered roller bearing are given in Figure 5.4-4.

Prop Shaft Tapered Roller Bearing Under Reverse Thrust Loading

Detailed analysis of the prop shaft bearing performance during prop reverse thrust was made by Timken Company. The data in Table 5.4-III summarizes the results of this analysis for a reverse thrust loading of 19,800 lbf (same value as takeoff thrust except in the opposite direction). The prop shaft bearings are expected to function satisfactorily under reverse thrust loading.

Prop Shaft Bearings Under Maximum Transient Maneuver Loading and Eight Minutes Misalignment

Prop shaft loads under maximum transient maneuver loads that are expected to occur for a very short duration are given in Figure 5.4-5. These loads combine to form approximately 800,000 in.-lb moment load in the vertical plane at the prop flange. The calculated maximum Hertz contact stresses for the prop inboard and outboard bearings under maximum transient maneuver loads and eight

Table 5.4-I.
Calculated bearing loads and L10 lives for steady-state prop loads.

Flight condition	% time	Outboard bearing loads (lbf) Radial	Outboard bearing loads (lbf) Axial	L10 life (hr)*	Inboard bearing loads (lbf) Radial	Inboard bearing loads (lbf) Axial	L10 life (hr)*
Warmup	24.1	7340	3186	145,058	4670	2380	272,853
Takeoff	1.6	2170	22,100	9392	4690	2020	627,437
Climb 1	6.4	1930	13,950	36,943	1550	670	51.8 E6
Climb 2	27.5	2310	8900	72,177	1210	530	4.22 E6
Cruise	23.6	17,310	8650	17,061	9640	4150	90,226
Descent	16.8	2580	1120	371,927	2860	1270	322,986
	100.0						
Weighted avg L10 life (hrs)				43,118			243,252
VIMVAR material adjusted L10 life (hrs)				431,185			2.43 E6

* Calculated L10 life based on AFBMA ratings, lube film thickness (using Dowson formulation), ASME lube life adjustment factor

Table 5.4-II.
Calculated maximum contact stresses for prop shaft bearings.*

Flight condition	Bearing maximum contact stress lb/in.^{2} x 10^3 Normal steady state Inboard	Outboard	Bearing maximum contact stress lb/in.^{2} x 10^3 Three minute misalignment Inboard	Outboard
Warmup	131.0	144.0	130.3	143.7
Takeoff	155.4	186.0	156.1	186.0
First climb	106.1	164.2	107.1	164.3
Second climb	82.7	149.6	81.3	149.2
Cruise	180.8	201.9	182.5	202.5
Descent	121.8	117.4	121.1	116.7

*Values calculated for -0.003 in. bearing setting, 230°F lube oil in temperature, and MIL-L-23699 lube oil

minutes misalignment were calculated as 299 lb/in.^{2} x 10^3 and 394 lb/in.^{2} x 10^3, respectively. No bearing race brinelling damage is anticipated to occur under the above maximum contact stresses.

Table 5.4-III.
Timken's analysis for prop reverse thrust condition.

Item	Outboard Bearing	Inboard Bearing
Radial load	1765 lbf	3956 lbf
Thrust load	754 lbf	20,554 lbf
Load zone	29 deg	360 deg
Max roller load	752 lbf	1225 lbf
Max race contact stress	159,000 lb/in.^{2}	187,000 lb/in.^{2}
Lube film thickness	10.1 μ/in.	7.7 μ/in.

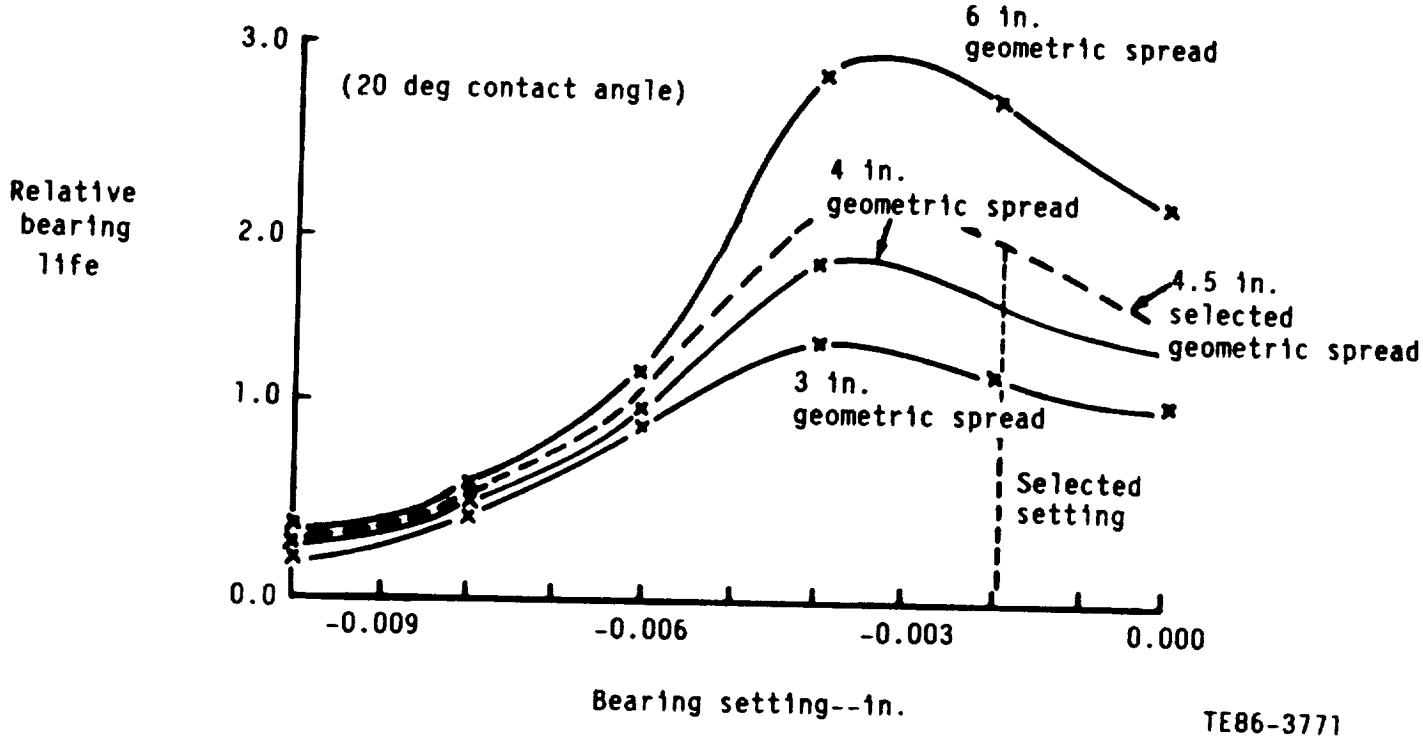

Data from Timken Co.

Figure 5.4-2. Prop shaft tapered roller bearing; relative bearing life versus mounting setting and geometric spread.

5.4.2 Carrier Support Bearings

The carrier of the AGBT planet system is supported in the front by a roller bearing and in the rear by a split inner ring ball bearing. Both bearings support light radial loads most of the time. The ball bearing was selected for the rear position to eliminate the effect of roller skewing (if the roller bearing was selected) with counterrotating races, since the ball spin speed is

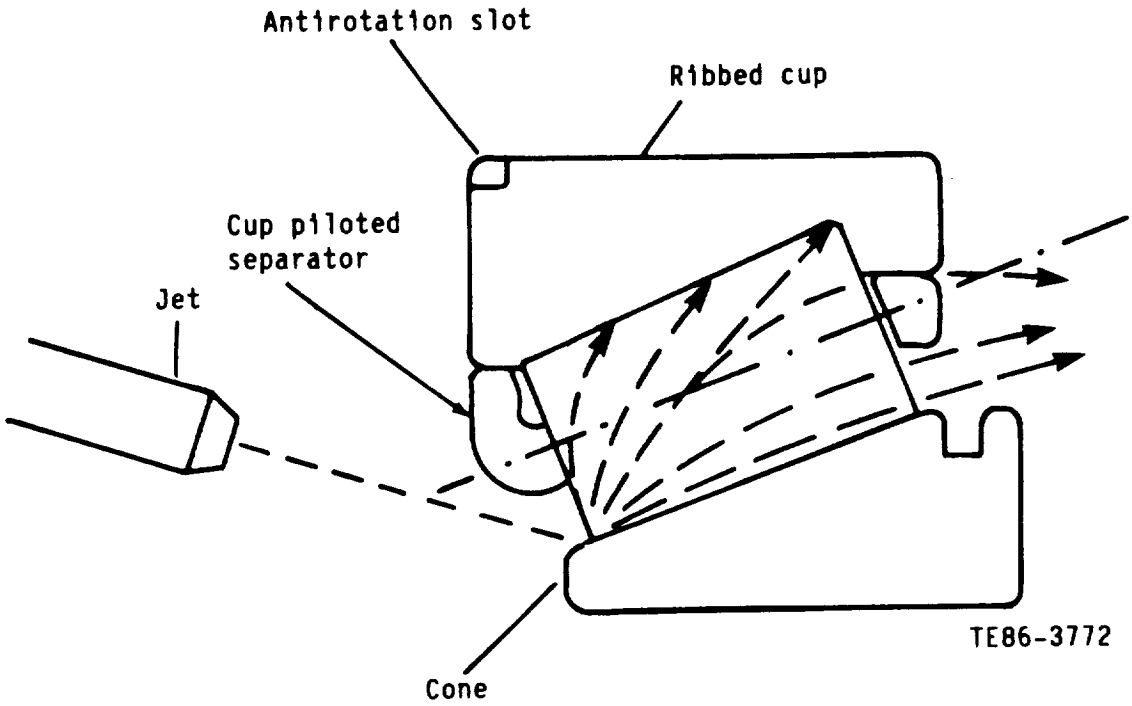

Figure 5.4-3. Placement of oil jet at cone's smaller end for more efficient bearing lubrication.

calculated to be about 19,000 rpm while its orbital speed is limited to about 60 rpm. In addition, the carrier ball bearing is designed to provide misalignment capability.

The carrier ball bearing radially supports the carrier rear end while axially locating on the carrier/planet assembly. It also supports the axial loads induced by spline thermal lock-up of the quillshaft. The preliminary study made for selecting the design of the carrier ball bearing had considered two types: (1) a split inner ring ball bearing with a single piece machined steel separator, and (2) a deep groove (conrad type) ball bearing with a two-piece riveted machined steel separator. Selection of a deep groove ball bearing would cause difficulty in assembling and disassembling the bearing without causing internal bearing damage, as the bearing is a nonseparable type. Accordingly, a split inner ring ball bearing design was selected since it has a separable two-piece inner ring and is easy to mount and remove with both inner and outer rings tight fitted (providing that the inner ring is furnished with a puller groove). In addition, a split inner ring design has the capability for under race lubrication, which is considered a desirable design feature. A one-piece machined separator is more reliable than a two-piece riveted machined separator.

Carrier Bearing Loads

Carrier bearing loads are basically radial due to the carrier component weight (1G load), which is assumed to be equally distributed between front and rear bearings. Each bearing will support about 200 lbf radial load. This load value could increase ten times (10G load) during anticipated flight maneuvers, which are expected to occur less than 0.1% of the time. The carrier rear ball

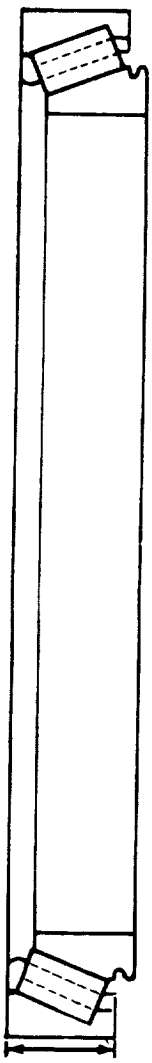

Shaft i.d.	13.50 in.
Housing o.d.	20.25 in.
Cup included angle	46 deg
Ribbed cup design	
No. rollers	50
Roller small end dia	0.8016 in.
Roller large end dia	0.8562 in.
Roller overall length	1.4477 in.
Effective length	1.2904 in.
Apex length	22.6429 in.
AFBMA dynamic load rating	125,000 lb
Bearing K factor	1.02
Cup, cone, and roller material	CBS 600
Separator	One piece machined steel (AMS 6414) silver plated and cup piloted
Tolerance	AFBMA Class 2

TE86-3773A

Figure 5.4-4. Prop shaft tapered roller bearing.

bearing locates the carrier/planet system axially and also supports the induced axial load by shaft splines (1000 lbf maximum) during both cruise and takeoff conditions. In addition, the carrier ball bearing will support a maximum axial load of 3000 lbf (estimated), as induced by spline lock-up during thermal transient conditions, for a very short duration.

Carrier Ball Bearing Design Details

The basic geometry, design data, and special design features of the carrier ball bearing are given below:

- ABEC class 5
- bearing size, mm--240 i.d. x 290 o.d. x 28.5 inner ring (i.r.) (24 outer ring [o.r.]) width

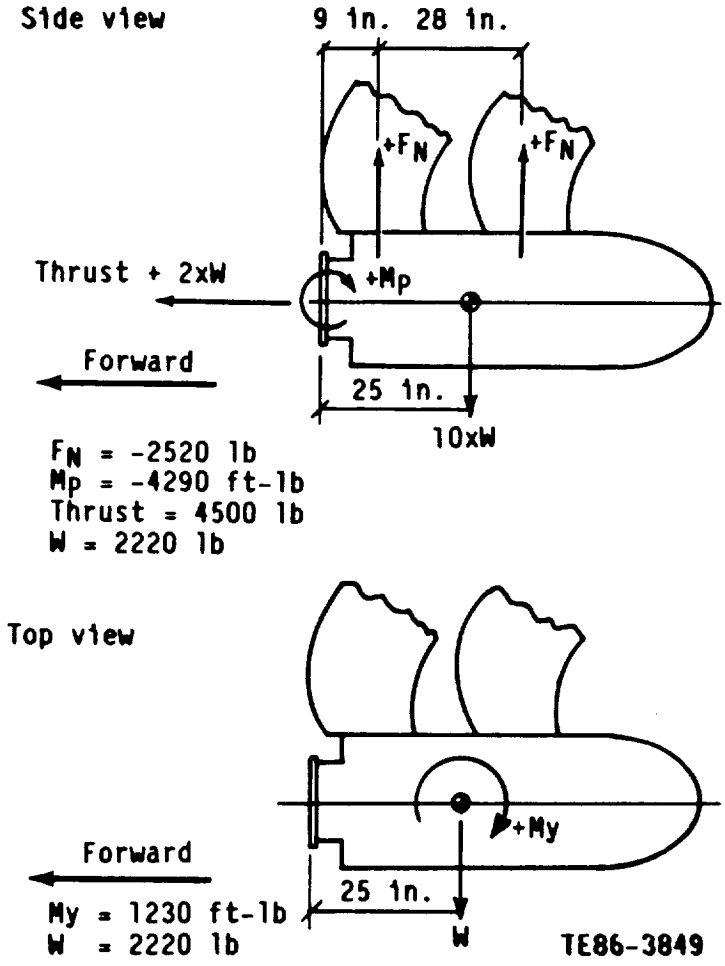

Figure 5.4-5. Prop shaft maximum transient maneuver loads.

- o ball diameter (nominal), in.--0.625
- o no. of balls--44
- o pitch diameter, in.--10.433
- o contact angle under 44 lb gage load--28 deg
- o AMS 5847 (M50-NiL) rings and AMS 6491 (M50) balls
- o race curvature (% of ball diameter)--52.5 inner, 53.5 outer
- o under race lubrication through slots between inner ring split line
- o inner ring and outer ring speed--1140 rpm (in opposite directions)
- o basic dynamic load rating lb--17,660

Basic design features of carrier ball bearings are depicted in Figure 5.4-6.

Carrier Roller Bearing Design Details

The basic geometry, design data, and special design features of the carrier roller bearing are given below:

- o RBEC class 5
- o bearing size, mm--170 i.d. x 215 o.d. x 18 i.r. (24.2 o.r.) width
- o roller diameter x length (nominal), mm--12 x 10

- o no. of rollers--20
- o AMS 6491 (M50) rings and rollers
- o ribless outer ring provides for axial freedom due to thermal growth
- o oil splash lubrication
- o inner ring speed, rpm--1140
- o basic dynamic load rating, lb--12,095

Basic design features of carrier roller bearings are depicted in Figure 5.4-7.

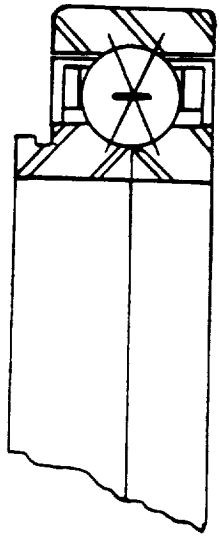

TE86-3990A

Figure 5.4-6. Cross section of carrier ball bearing.

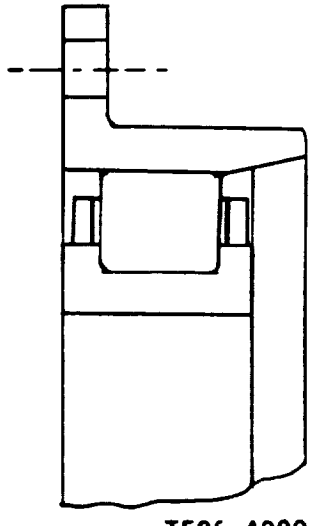

TE86-4200

Figure 5.4-7. Cross section of carrier roller bearing.

Carrier Bearing Design Analysis

The SHABERTH computer program was used to aid in design optimization of the carrier ball and roller bearings. Table 5.4-IV summarizes the result of the SHABERTH analysis. The SHABERTH computer analysis was made with the use of MIL-L-23699 lube oil at 180°F input temperature, assuming 1% lube oil in the bearing cavity.

Table 5.4-IV.
Summary of SHABERTH analysis.

Carrier bearing	Roller		Ball		
Condition	Steady state	Maneuver	Steady state	Maneuver	Thermal transient
Radial load, lbf	200	2000	200	2000	200
Thrust load, lbf (max)	0	0	1000	1000	3000
Surface finish micro-inch					
Ring raceways	5	5	5	5	5
Rolling element	4	4	2	2	2
Max Hz stress i.r./o.r. lb/in.^{2} x 10^3	120/113	284/267	154/157	263/267	301/306
EHD film thickness i.r./o.r. micro-inch	4.25/4.48	3.40/3.58	8.52/7.96	7.57/7.06	6.86/7.29
Lambda ratio i.r./o.r.	0.74/0.78	0.59/0.62	1.76/1.64	1.56/1.46	1.50/1.41
Lube film factor i.r./o.r.	0.26/0.29	0.15/0.17	1.87/1.63	1.29/0.99	1.10/0.91
Material processing factor	10	10	10	10	10
Bearing L10 life, hr	2.34 x 10^6	1110	950,000	23,635	2043
Weighted average life, hr	953,000		760,000		

5.4.3 Planet Bearing

Planet Bearing Loads

Planet bearing loads are given as follows:

- o gear tangential loads at both sun and ring gear meshes
- o gear separating forces as induced by sun and ring gears (These forces cancel each other as they are equal and in opposite direction.)
- o helical gear axial forces (These forces cancel each other as they are induced in opposite direction due to the herringbone gear design.)
- o centrifugal force due to planet mass orbital speed
- o gyro and maneuver loads

Based on the given 300 nautical mile missions profile, Table 5.4-V summarizes the planet bearing radial loads due tangential gear forces, planet gear centrifugal forces, and resultant radial loads along with planet system speed and percent time for each given mission phase.

Table 5.4-V.
Planet bearing loads/speeds for each flight mission phase.

Mission phase	Time minutes	Percent time	Planet bearing loads (per row) lbf: Radial due gear tangential forces	Radial due planet C forces	Resultant radial load	Speeds--rpm: Sun	Carrier	Planet
Warm-up	15.0	24.08	574	737	934	6000	720	3240
Takeoff	1.0	1.60	7536	1847	7759	9500	1140	5130
First climb	4.0	6.42	7446	1847	7672	9500	1140	5130
Second climb	17.1	27.45	6378	1847	6640	9500	1140	5130
Cruise	14.7	23.60	4638	1847	4992	9500	1140	5130
Descent	10.5	16.85	526	737	905	6000	720	3240
Total	62.3	100%						

Planet System's Total Induced Thrust Loads Due to Misalignment

The induced thrust loads by planet roller bearings due to misalignment of inner ring relative to outer ring were calculated by SKF Industries' computer program AE69Y001. The equation used for calculating bearing induced thrust load F_a, within the program, is given as follows:

$$F_a = 2w \sum_{j=1}^{j=\frac{Z}{2}+1} \bar{\tau}_j \theta \cos\phi_j \sum_{K=1}^{K=m} q_{1jK}$$

where:

F_a = induced thrust load lb
τ_j = roller counting factor
w = width of axial laminum in.
θ = misalignment of i.r. relative to o.r., radians
ϕ = roller azimuth, radians
Z = no. of rollers
$\tau_j = 0.5$; $\phi_j = 0, \pi$
$\tau_j = 1$; $\phi_j = 0, \pi$
q = load per unit length lb/in.

Subscripts:

j refers to roller azimuthal location
K refers to laminum
1 refers to inner raceway

A graphical presentation of the planet system total induced thrust load (lbf) versus misalignment angle (minutes) at various given flight mission phases is

included in Figure 5.4-8. The planet system's maximum induced thrust load due to four minute misalignment is about 72 lbf during the takeoff (or first climb) phase. However, under ten minutes misalignment the total induced thrust would be about 180 lbf during the takeoff (or first climb) phase. These induced thrust loads are considered to be small load values and should have no detrimental effect on planet bearing performance as they may occur for a very short duration during maneuver conditions. Most of the time the planet bearings will have no misalignment. Table 5.4-VI includes the values of the planet system-total induced thrust load due to misalignment at various mission phases.

Table 5.4-VI.
Study of planet system's total induced thrust load versus misalignment at various given mission phases.

Mission phase	Planet bearing radial load-- per row lb	Planet outer ring relative speed rpm	Planet system total induced thrust load due to misalignment of inner ring relative to outer ring-- minutes* 2	4	6	8	10
Warm-up	934	3960	9.00	18.01	27.00	36.01	44.96
Takeoff	7759	6270	36.11	72.23	108.36	145.45	180.55
First climb	7672	6270	35.71	71.43	107.14	142.84	178.53
Second climb	6640	6270	30.91	61.82	92.74	123.66	154.54
Cruise	4992	6270	23.24	46.48	69.74	92.99	116.19
Descent	905	3960	8.94	17.88	26.81	35.75	44.71

* Calculated by SKF computer program AE69Y001

Planet Bearing Lubrication

Many techniques to lubricate and cool the planet bearings were considered but the two basic schemes include: (1) a pressure fed system, and (2) a centrifugally fed system. A centrifugal system requires that the oil be fed into the bearing at the outer periphery of the bearing journal. Rotation of the bearing carries the cooling oil around the bearing. A pressure-fed system allows oil to be introduced anywhere around the bearing journal. This type system was selected for the AGBT planet bearing primarily for this reason. The details of the AGBT lubrication scheme are shown in Figure 5.6-2 and described in subsection 5.6.1.

Roller Size and Number

Each planet bearing is furnished with 18 rectangular, crowned rollers per row (36 rollers per planet). The roller length (L) and diameter (D) are 31.5 mm and 20 mm, respectively, with L/D = 1.575. The initial planet bearing design included 19 rectangular, crowned rollers per row (38 rollers per planet) with

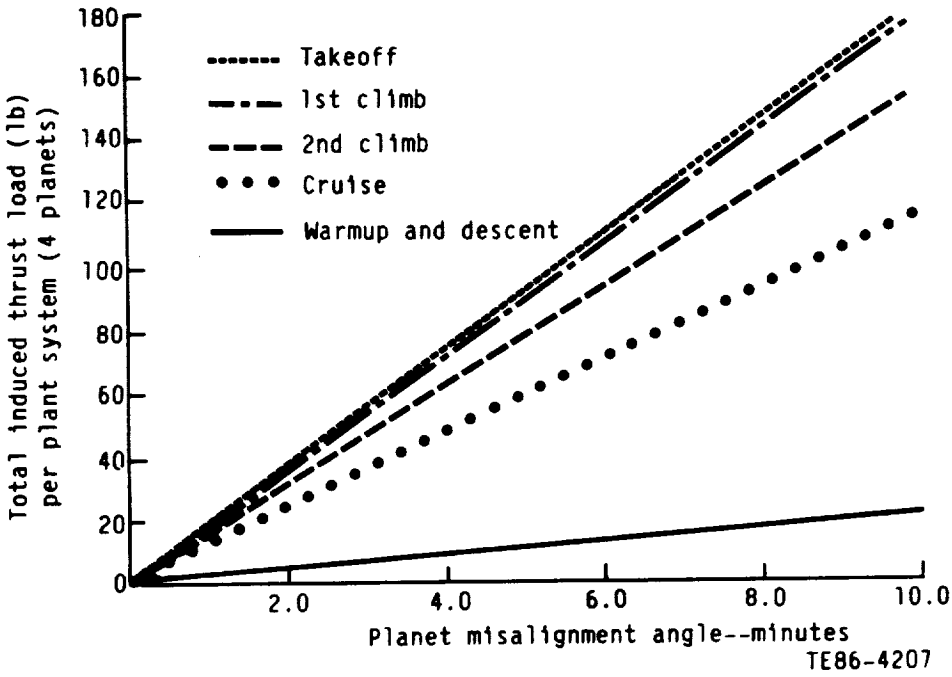

Figure 5.4-8. Planet system's total induced thrust load (lb) versus misalignment angle (minutes) for the counterrotation, AGBT at various mission phases of 3000 nautical mile mission.

roller L = 30 mm, D = 20 mm, and L/D = 1.5. However, a 19 rollers per row design resulted in a marginal separator crossbar section design particularly at separator inner diameter. Also, with 19 rollers (odd number) each separator pocket has to be machined separately, which would result in a higher bearing final cost as compared to 18 rollers (even number) where two roller pockets can be machined at a time. Changing the number of rollers per row from 19 to 18 rollers and increasing roller L/D from 1.5 to 1.575 will maintain almost the same bearing dynamic capacity. Also, the study of roller skew due to increasing the L/D ratio to 1.575 revealed minimal effect on bearing heat generation under various operating conditions.

Planet Gear Deflection Analysis

Preliminary design studies of the planet gear/bearing indicated that planet gear stiffness has a major impact on the planet bearing load distribution. A flexible planet gear creates high roller loads at the end of the load zone due to excessive gear deflection. In Ref 2, flexible planet bearing races with the proper diametral clearance were found to have better life than rigid planet gears. Results of an early AGBT study using the PLANETSYS bearing computer program indicated that an infinitely stiff planet gear was the best solution. To resolve the question of bearing stiffness, a 3-D FEM analysis of the planet gear and bearing was performed. The results are described in subsection 5.1.4. The final configuration of the planet gear/bearing resulted in a very acceptable load distribution.

Effect of Carrier Trunnion Deflection

Results of the planet carrier FEM study indicated that under full torque the trunnion would deflect 0 deg 2 min due to torsional windup in the carrier backing plates (see Figure 5.2-3). The planet bearing was analyzed with the computer program SHABERTH to determine if the misalignment would have an adverse effect on the bearing operation (see Figure 5.4-9). Fatigue life under cruise load was reduced by 36% at 0 deg 2 min misalignment. Based on these results, it was decided to intentionally misalign the trunnion during fabrication so that under heavy loads the bearing would align itself.

Planet Bearing Design Details

The basic geometry, design data, and special design features of the planet roller bearing are given as follows:

- o RBEC class 5 tolerances
- o eighteen rollers per row (36 total)
- o roller nominal size 0.7874 in. dia x 1.2402 in. long
- o roller set pitch diameter = 5.528 in.
- o internal diametral clearance = 0.0032 in. - 0.0042 in.
- o AMS 6491 (M50) inner ring and rollers
- o outer land piloted steel separator
- o outer race of each row has ribs for roller guidance and center web between outer raceways
- o ribless inner ring for axial freedom

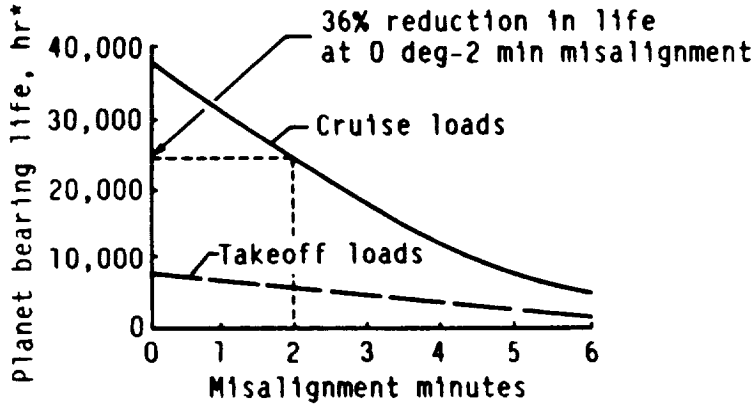

a. Effect of misalignment on planet bearing life

*Results from SHABERTH bearing computer program

TE86-3996A

Figure 5.4-9. Planet bearing misalignment.

- o outer raceway roller guidance flange layback angle to provide better hydrodynamic lubrication to roller end faces and to minimize roller skew under a controlled roller to ring end clearance
- o roller and raceways surface finish of 2 micro-in. and 4 micro-in., respectively
- o separator balance after silver plating to 0.04 oz-in.
- o inner ring axial travel capability of ±0.12 in.
- o inner ring with antirotation slot on one side to locate inner ring maximum angularity
- o pressure fed under race lubrication with MIL-L-23699 oil
- o oil inlet temperature = 180°F
- o planet speed--5130 rpm, trunnion orbital speed--1140 rpm
- o lambda ratio = 2.1 for inner race and = 2.2 for outer race*
- o rollers, loads, and speeds, separator orbital speed--3580 rpm and roller rotational speed--21,600 rpm*
- o calculated maximum Hz contact stress = 193 lb/in.^{2} x 10^3 inner race and 168 lb/in.^{2} x 10^3 outer race*
- o dynamic load rating of 102,000 lb per two rows

* Values calculated by PLANETSYS computer program with 180°F MIL-L-23699 lube oil.

5.4.4 Input Shaft Bearings

The input shaft bearings are required for testing of the gearbox in a test stand. Since these bearings were considered to be test equipment, a new bearing design was not considered. The objective was to find an existing bearing that could handle the AGBT design requirements for test purposes. This bearing was located and its details are shown in Figure 5.4-10 and Table 5.4-VII.

Table 5.4-VII.
Input shaft bearing geometry.

- o bearing type--split inner ring ball
- o bearing size, in.--4.673 i.d. x 7.173 o.d. x 1.318 width
- o pitch diameter in.--5.923
- o ball diameter in.--0.8125
- o number of balls--19
- o ratio-radius of I/O races curvature to ball diameter--0.515
- o machined steel separator
- o outer ring land riding separator
- o jet oil lubrication
- o basic dynamic load rating--18,930 lb
- o inner ring/shaft speed--9500 rpm
- o capability for carrying radial and axial loads
- o contact angle--30 deg ref
- o Vimvar M50 rings and ball material

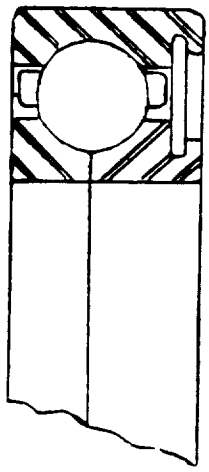

TE86-4041A

Figure 5.4-10. Input shaft bearing.

The input shaft bearings determine the axial centerline of the differential power train, as shown in Figure 5.4-11. The outboard bearing is unloaded except for a 1500 lb wave spring force that prevents skidding and stiffens the input shaft bearing system. The outboard bearing has an oil damper integrated into the housing. The bearings are jet lubricated.

Results from the computer program SHABERTH follow:

Radial load = 200 lb	lambda ratio = 2.1
Axial load = 1500 lb	Max Hertz stress = 152 lb/in.^{2} x 10^3
Shaft speed = 9500 rpm	Operating diametral clearance = 0.004
	Cage slip = 0%

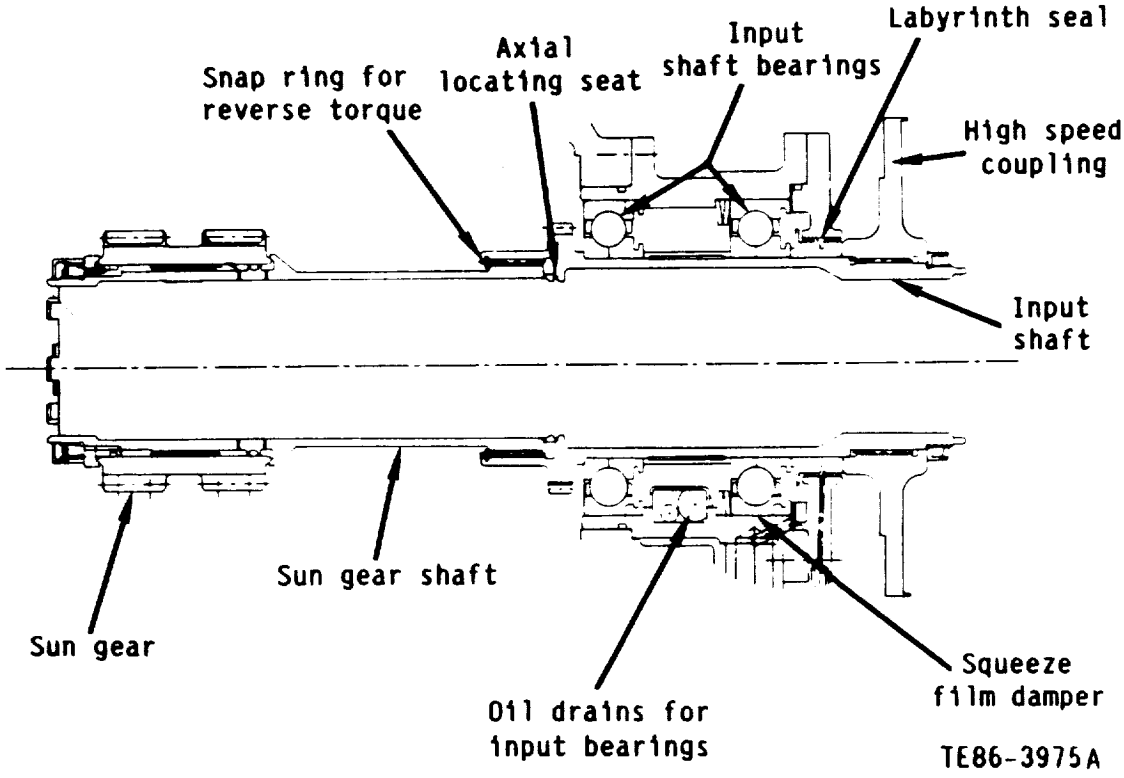

Figure 5.4-11. Input shaft bearing arrangement.

5.5 HOUSING

5.5.1 General Arrangement

The housing structure was designed to be representative of a flight gearbox so that effects of external loads on gearbox operation could be evaluated. Other aspects of the housing design were treated as test equipment. For example, there are no cored passages for transfer of oil within the walls of the housing. Considerable external plumbing is required to operate the gearbox on the test stand. This is appropriate for test purposes since it is easier to measure and modify oil flow rates to various locations in the gearbox with separate oil lines and external oil pumps.

C-355 aluminum heat treated to a T7 condition was selected for the gearbox. Aluminum was selected because of its better corrosion resistance, as compared to magnesium. Since a major goal in the gearbox design is low maintainability, it was determined that aluminum would require less maintenance than magnesium. The T7 heat treatment was selected to allow operation at elevated temperatures for approximately 100 hr. All components in the gearbox are capable of operation at an oil in temperature of 350°F. With a 50°F temperature rise, the housing must be able to withstand 400°F. Figure 5.5-1 shows the allowable operating yield stress levels as a function of time and temperature. For this design, 14.5 lb/in.^{2} x 10^3 was selected as the maximum allowable stress value.

The housing is made of three individual castings. Tight fitting pilot diameters ensure concentricity of bearing bores when the assembly is bolted together. The three finish machined castings are shown individually in Figures

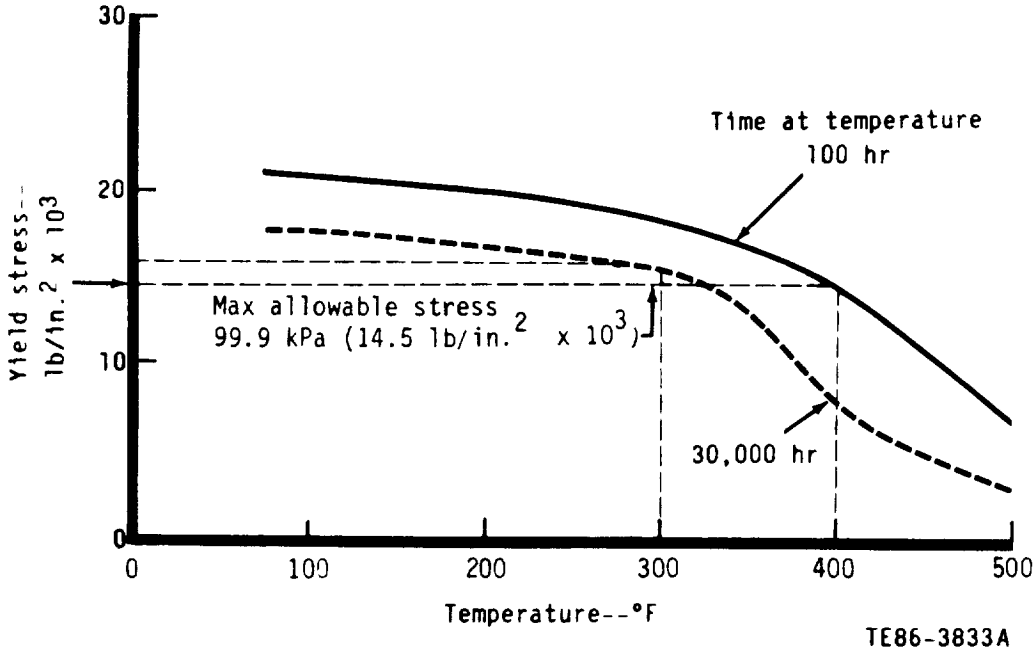

Figure 5.5-1. Allowable housing stress--3σ confidence level (99.7%).

5.5-2 through 5.5-4 and the fully assembled unit in Figure 5.5-5. One of the main objectives in the design of the housing was to minimize the distance between the externally applied load and the reaction point, the mount pads. In Figure 5.5-2, the mount pads are located directly over the prop bearings. This type of construction minimizes misalignment of the internal bearing and gear contacts since the load is carried over a very short span by a relatively heavy cross section. The balance of the casting can be lightweight since the loads outside the mount pads are low.

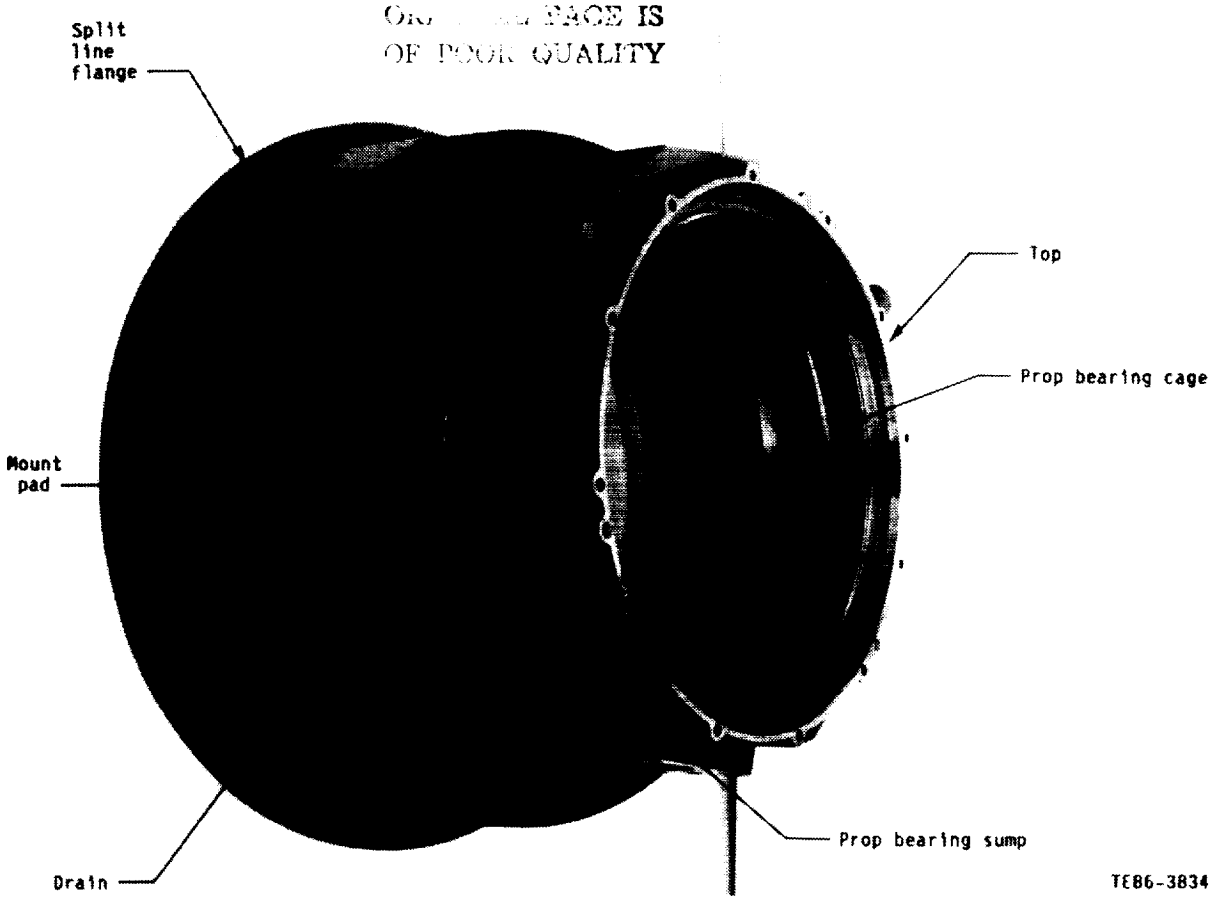

Figure 5.5-2. Main housing.

The mount pad locations are shown schematically in Figure 5.5-6. The pads are not spaced equally due to the method developed to support the gearbox from the engine. Six 1/2 in. bolts clamp a steel interface plate to the aluminum housing in four places.

Large viewports were incorporated into the cover to allow visual inspection of much of the interior of the gearbox. Pyrex glass windows are used to cover

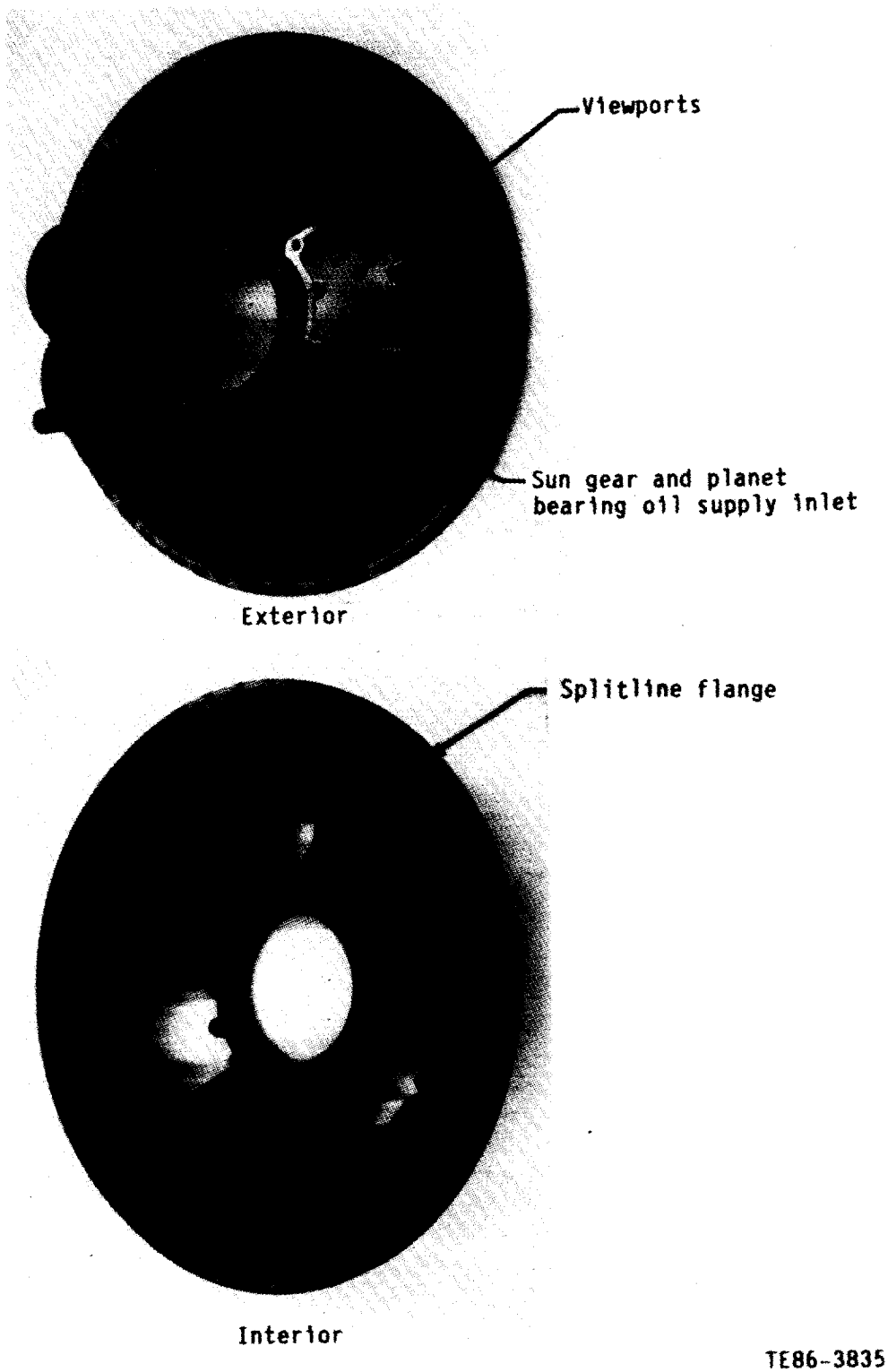

Figure 5.5-3. Cover.

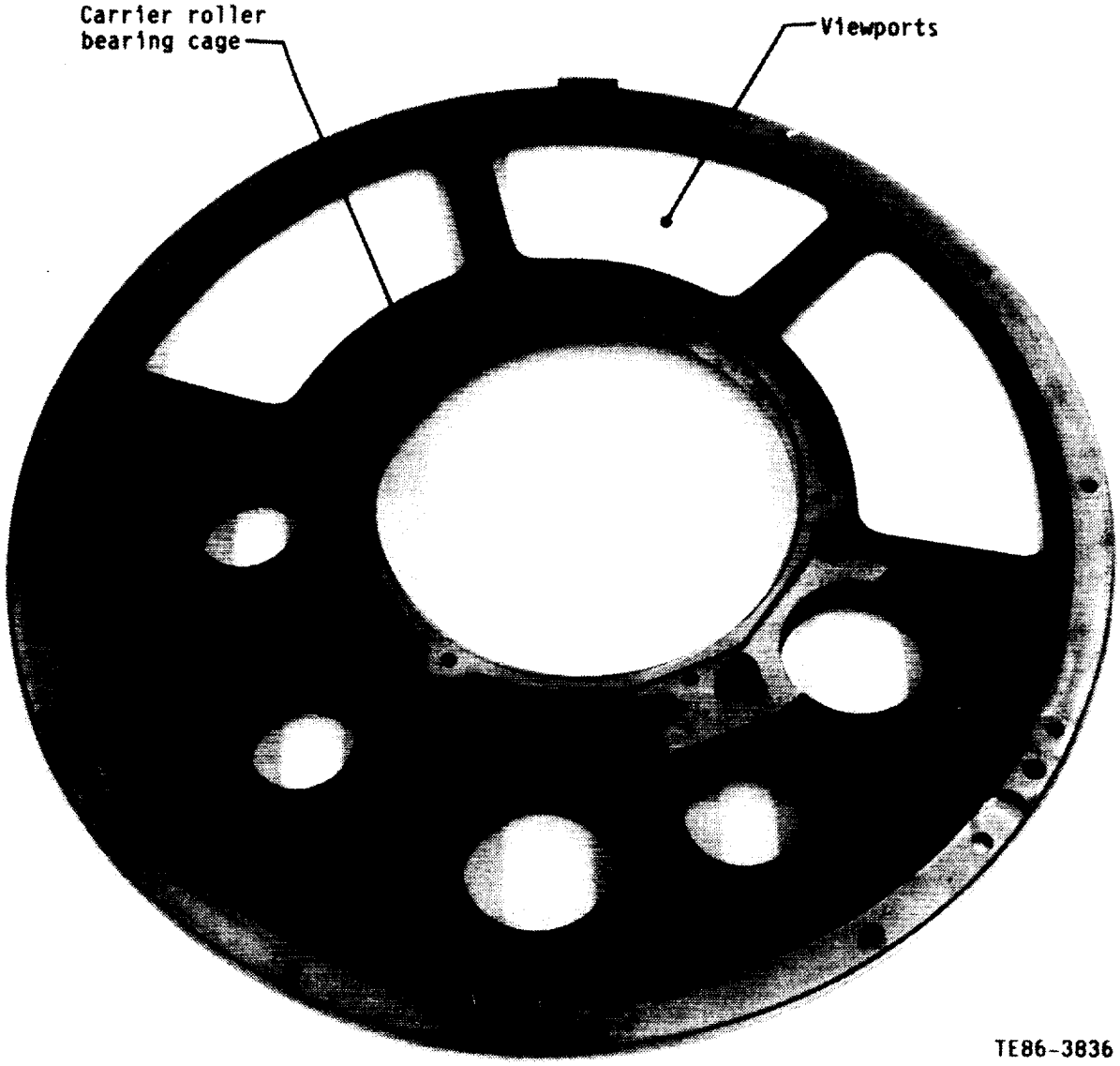

Figure 5.5-4. Inner support.

the viewports during running. Additionally, special borescope ports were included to allow examination of ring gears and prop shaft bearings. Since this gearbox will be run with extensive instrumentation, special mounting pads and wire routing holes were incorporated in the casting design.

5.5.2 Stress and Deflection

The housing was sized to maintain stresses developed under the worst case load condition below the 14.5 $lb/in.^2 \times 10^3$ allowable stress level. The design point, shown in Figure 3-3, represents a gust load situation that can occur an indefinite number of times during the life of the gearbox. Thus, the housing stresses at the design point must be below the yield stress. The design load condition will not occur frequently, however.

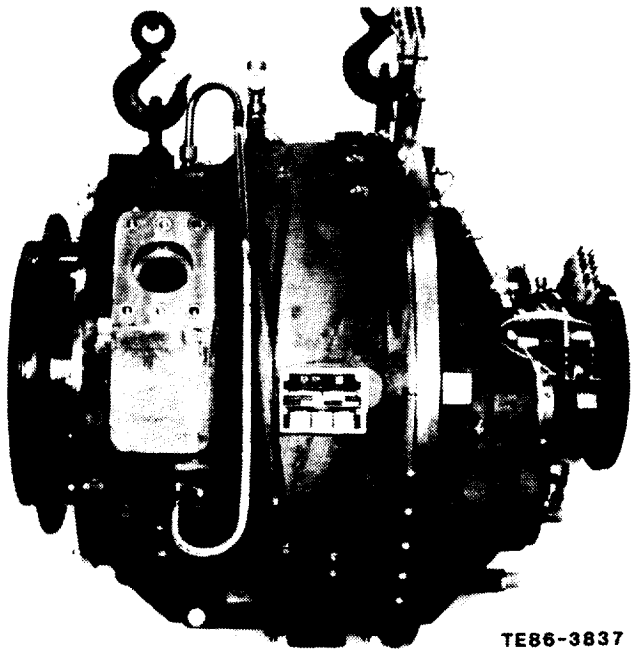

Figure 5.5-5. Assembled gearbox.

The housing was analyzed with a 3-D finite element model shown in Figure 5.5-7. A 180 deg sector analysis was performed using 20 node solid elements. The resulting stresses are shown in Figure 5.5-8. Stresses in the area shown were determined to be acceptable. Stresses in other areas of the housing are significantly lower than those shown in Figure 5.5-8 since no other loads will be applied. Deflections of the housing are shown in Figure 5.5-9.

5.5.3 Hardware

Rosan fasteners and fluid fittings were used extensively in the AGBT gearbox (see Figure 5.5-10). The major difference between Rosan fasteners and others is the locking device. A lockring, serrated on its outer diameter, engages a spline on the shaft of a stud and is forced into the aluminum housing. This provides a very rigid construction that prevents the stud from backing out of the tapped aluminum. The threaded and fluid inserts function in the same fashion. If the part must be removed, the lockring must be destroyed and replaced with another but the stud or insert can be reused. These fittings are expected to greatly aid maintainability of the gearbox.

A circumferential static O-ring seal is used to seal the main housing and cover. An AS 3085 Viton O-ring (0.21 in. thick) was selected here.

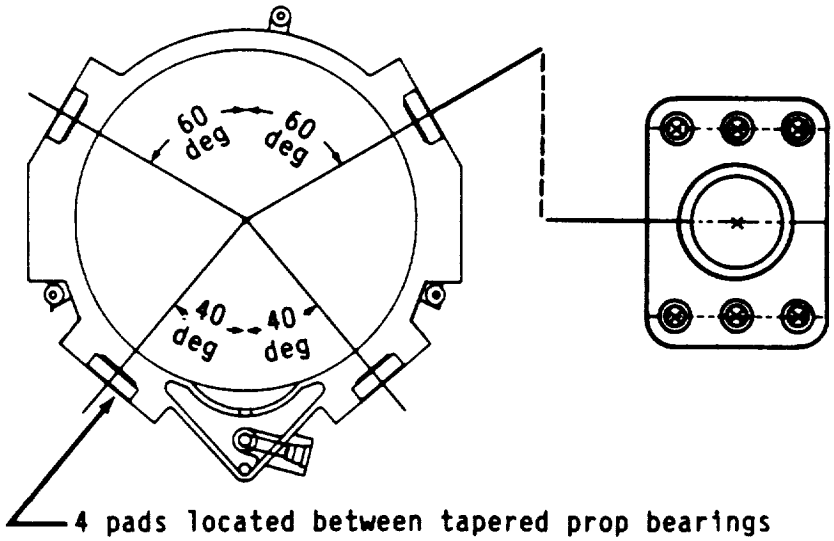

TE86-3838

Figure 5.5-6. Housing mount pad locations.

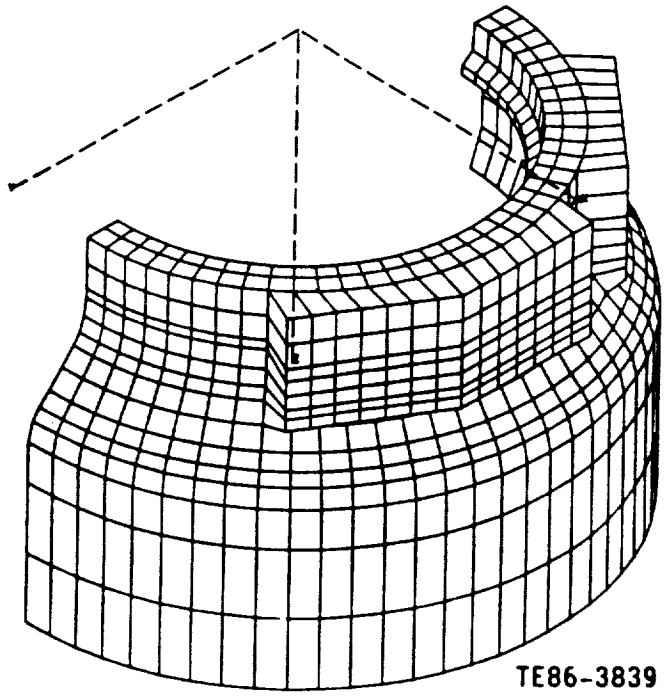

Figure 5.5-7. 3-D finite element housing model.

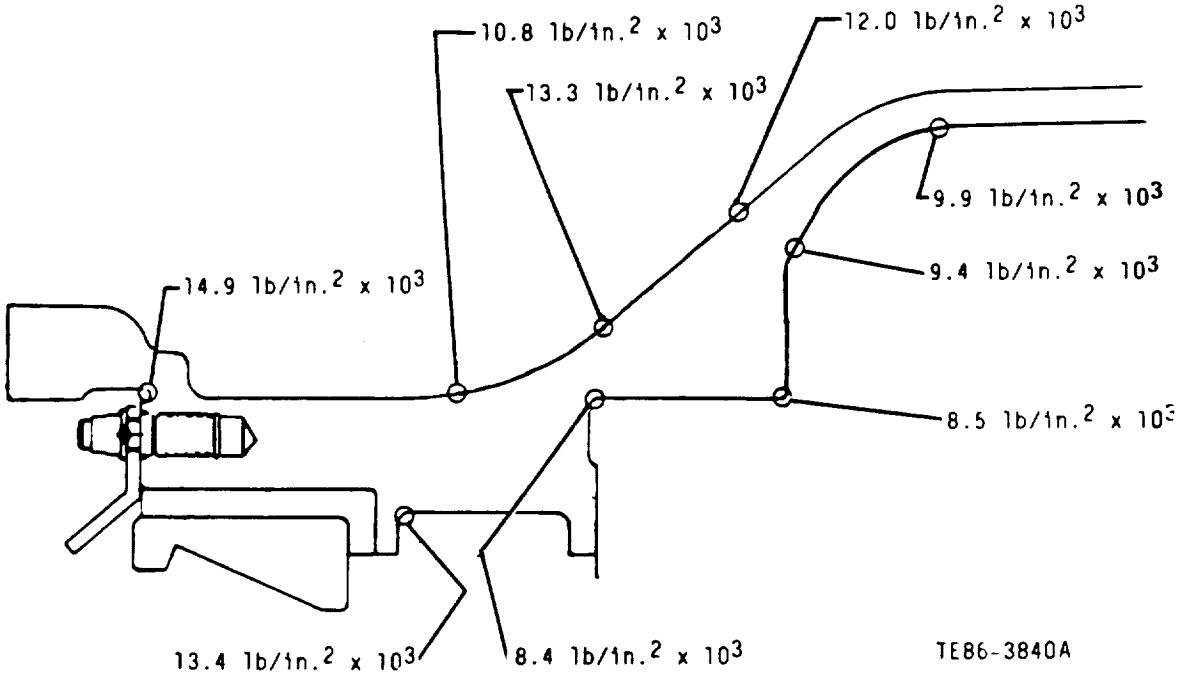

Figure 5.5-8. Maximum housing stresses.

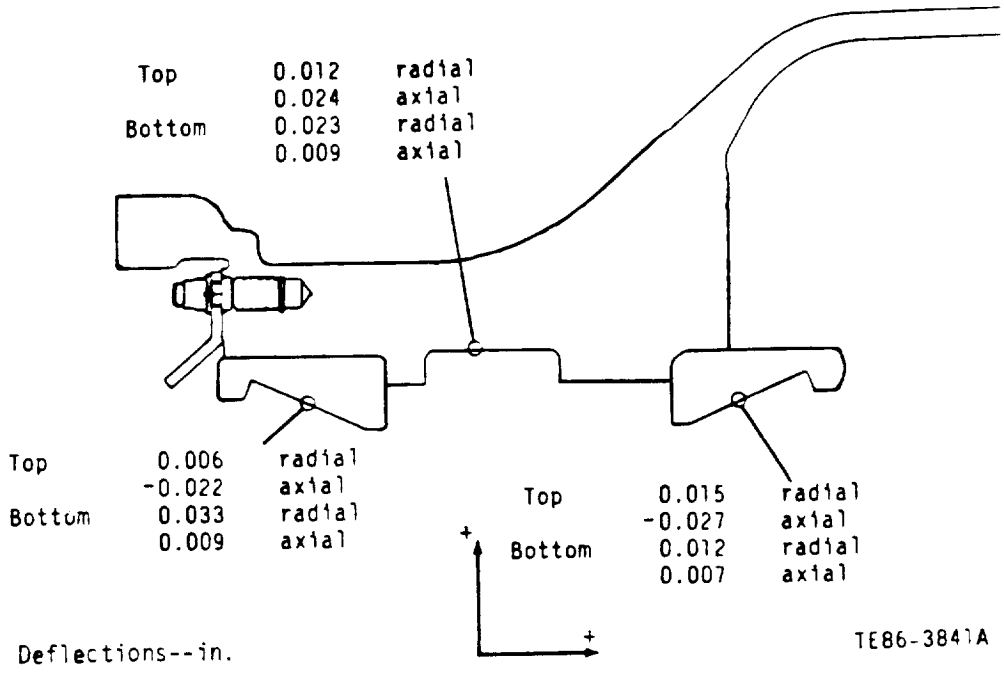

Figure 5.5-9. Maximum housing deflections.

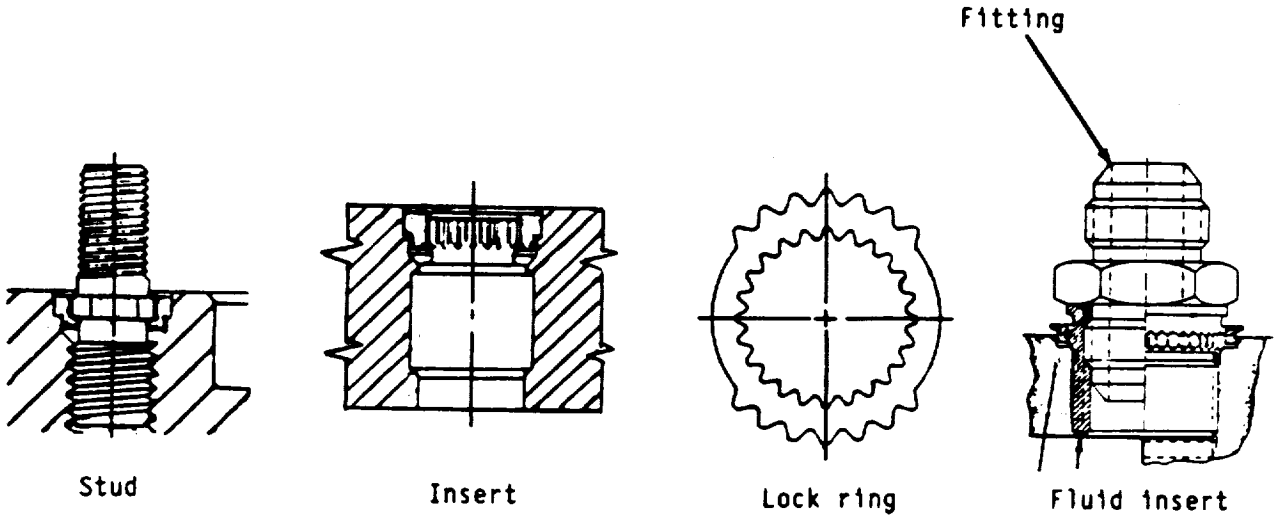

Figure 5.5-10. Rosan fasteners.

5.6 LUBRICATION SYSTEM

5.6.1 General System

Although the gear system lubrication system was designed to meet flight requirements, the actual hardware was designed as test equipment. The most obvious example of this approach is the lack of cored oil passages in the housing. Each of the eight connection points is fed independently from a distribution manifold. Oil is supplied to the manifold from a remote oil conditioning system. By providing individual lines to each area of the gearbox, flow rates can be measured directly and changed easily. Even though the hardware is not identical to the flight version, performance is the same.

The lubricant selected for this system is MIL-L-23699. Advanced oils, including high temperature (350°F oil in) lubricants, can also be used in this system. The oil pressure level is set by sun gear cooling requirements. A pressure of 100 $lb/in.^2$ at the sun gear jet is required to force oil below the pitch diameter of the sun gear at full speed (see subsection 5.6.3). Including a 20 $lb/in.^2$ pressure drop between the housing inlet and the sun gear jet, the nominal gearbox oil pressure required is 120 $lb/in.^2$.

Flow rates were selected so that all heat generated in the gearbox at full power can be removed through the oil. Convective heat loss is assumed to be zero. These flow rates reflect a 50°F rise in oil temperature.

Figure 5.6-1 shows the gearbox lubrication scheme. Table 5.6-I provides additional data at each lubricated area. The majority of the oil is transferred through oil transfer seals (see subsection 5.6.4). This passage supplies oil to the sun gear jets and the planet bearings. The seals transfer oil from the stationary supply manifold to the rotating carrier. At this point, the oil flows to sun gear supply tubes or through transfer tubes that in turn feed each trunnion supply annulus. The oil supply annulus (Figure 5.6-2) in the carrier trunnion feeds two jets per row in the planet bearing inner race. The supply jets are located off the planet bearing centerline oriented toward the center of the gearbox. One of the jets is in the load zone. This arrangement was selected so that cool oil is fed toward the center of the drive, against centrifugal force, and the inner half of the bearing is positively supplied with oil. Axially, the jets are located beneath the inboard rib of the cage. Oil must flow from the center of the gear out.

The tapered roller prop shaft bearings are jet lubricated (see Figure 5.6-3). The outboard bearing receives approximately four times the flow supplied to the inboard bearing due to the propeller thrust loads reacted there. The inboard bearing will also see thrust during landing (thrust reverse), but the duration of this maneuver is not expected to be significant. Oil is jetted below the bearing cage. The natural pumping action of the tapered bearing will move the oil through the bearing.

Figure 5.6-4 shows the lubrication technique used for the counterrotating carrier ball bearing. A split inner race bearing was selected for this location for assembly purposes. The split line has been used to supply lubricants through a series of grooves. Calculations show minimal heat generation in this bearing. Two supply lines are provided in case one becomes clogged.

Table 5.6-I.
Heat generation/oil flow rate summary.

Location	Heat gen at takeoff, hp	Pressure	Flow rate gpm
Power train gears	43.72	100	9.75
Planet bearings (tot)	20.00	70	4.48
Prop bearings (thrust/nonthrust)	9.36/2.29/	37	2.50/0.61
Carrier ball brg	0.21	70	0.56
Carrier roller brg	0.19	-	Mist
Input bearing set	4.72	100	1.05
Prop shaft seal	2.00	100	0.45

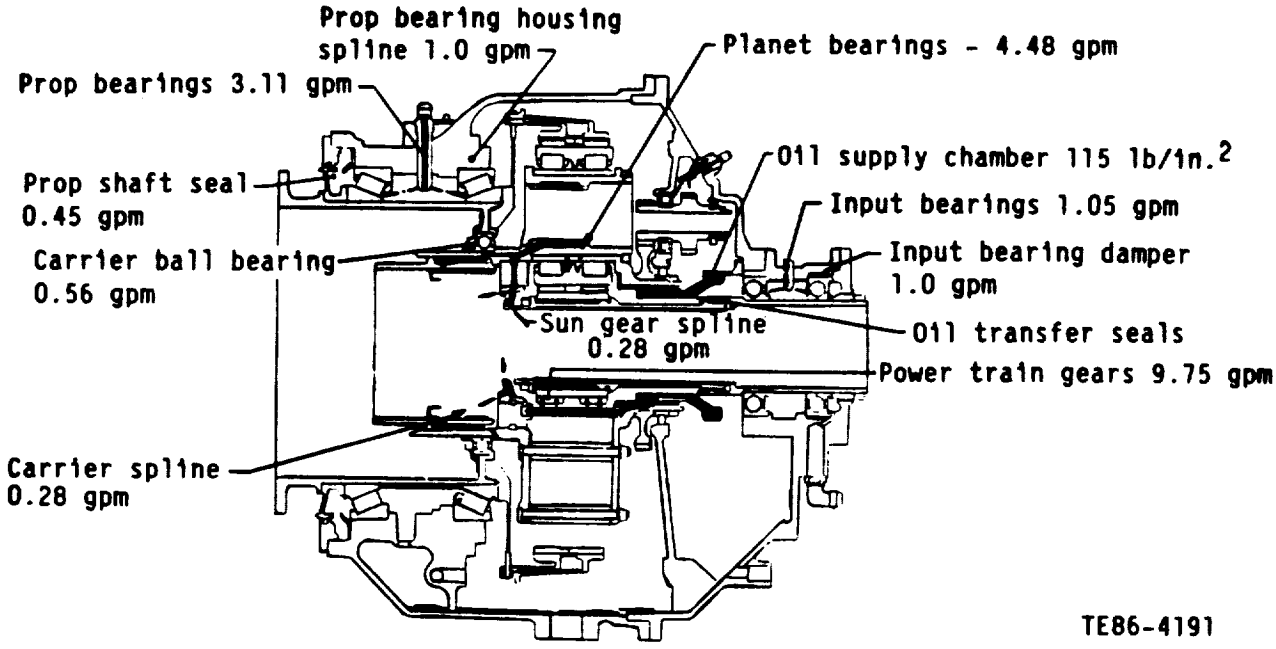

Figure 5.6-1. AGBT lubrication system.

The carrier roller bearing is loaded only by weight of the carrier assembly and any unbalance that might occur. Heat generation in this bearing was also found to be quite low. Splash lubrication occurring naturally in this area was determined to be adequate for the bearing.

The relatively high speed input bearings are jet lubricated with one jet per bearing (see Figure 5.6-5). The predominant load on these bearings is the 1500 lb preload spring force. Thrust from the sun gear is expected to be low. The jets are targeted to supply oil below the bearing cages. The outboard bearing floats on an oil squeeze film damper. The damper may be required if the high

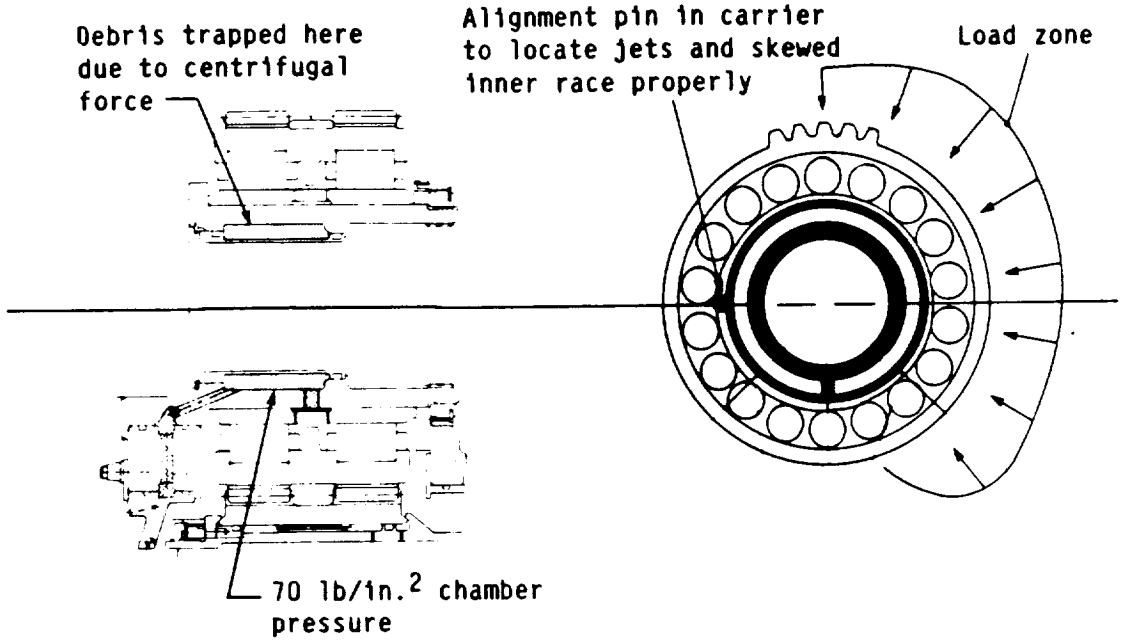

TE86-3783A

Figure 5.6-2. Planet bearing lubrication scheme.

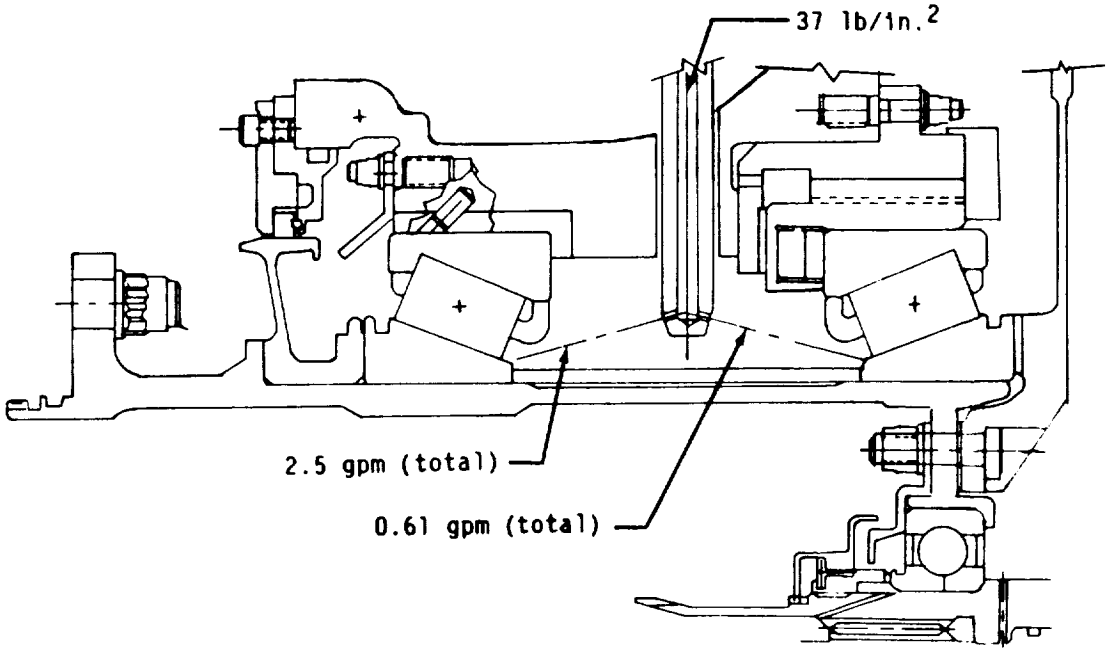

TE86-3784A

Figure 5.6-3. Lubrication of tapered roller prop shaft bearings.

speed shafting responds to predicted modes during operation. The damper requires approximately 1 gal./min of oil. The input bearing housing has its own drain that will feed back into the main housing.

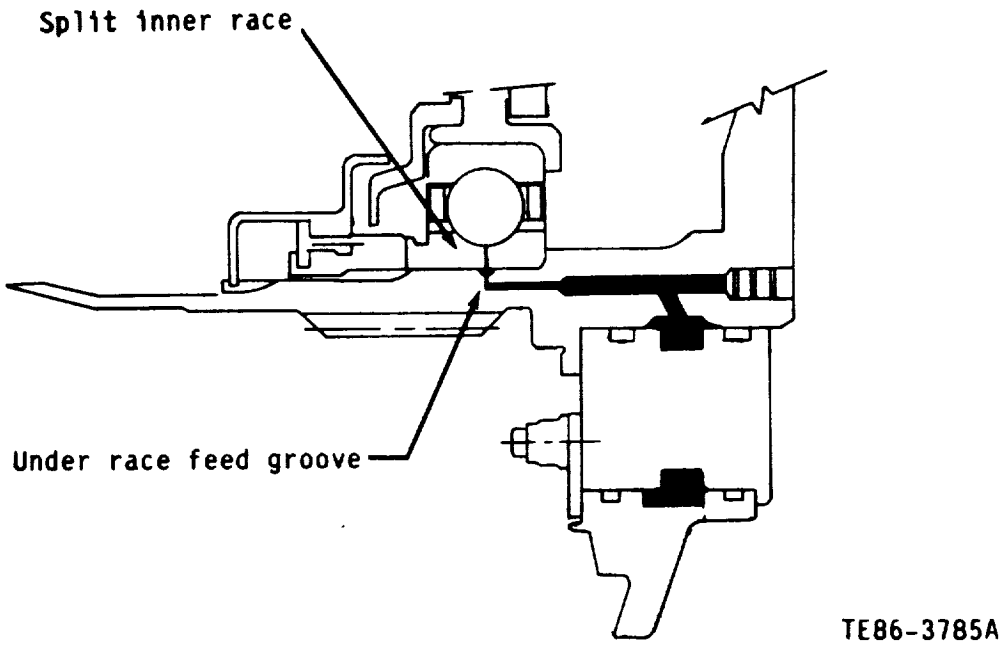

Figure 5.6-4. Lubrication of carrier ball bearing.

The prop shaft seal is expected to require oil cooling due to frictional losses. About one-half gal./min of cooling oil will be supplied to cool the seal runner in the event that this heat cannot be conducted or convected away.

A 75 gpm scavenge pump will be connected to the housing drain at the bottom of the main housing. This is the only suction line on the gearbox. Oil must either drain by gravity or be forced into the drain through the oil baffles designed to redirect the flow. The scavenge pump will provide a 3:1 ratio of scavenge to supply flow. This ratio was determined to be necessary for flight at high altitudes (35,000 ft).

Fine filtration will be implemented in this gearbox. Three micron absolute filters will be placed on the supply and scavenge oil lines to protect the gearbox and lube system. This level of filtration was found to be necessary to meet the long life requirement for propfan gearboxes.

Oil supply temperature to the gearbox was selected to be consistent with Allison experience in other gear systems--180°F. This temperature allows the formation of adequate film thickness in the bearing and gear contacts yet does not cause excessive windage and churning loss. All components were designed to operate from -65°F to 210°F (for short periods of time).

5.6.2 Efficiency

Gear power loss was calculated with a technique based on the Anderson/Loewenthal spur gear efficiency calculation method (Ref 3). In these calculations, a gear mesh friction coefficient developed by Southwest Research Institute was used (Ref 4). Bearing loses were calculated with several large scale computer

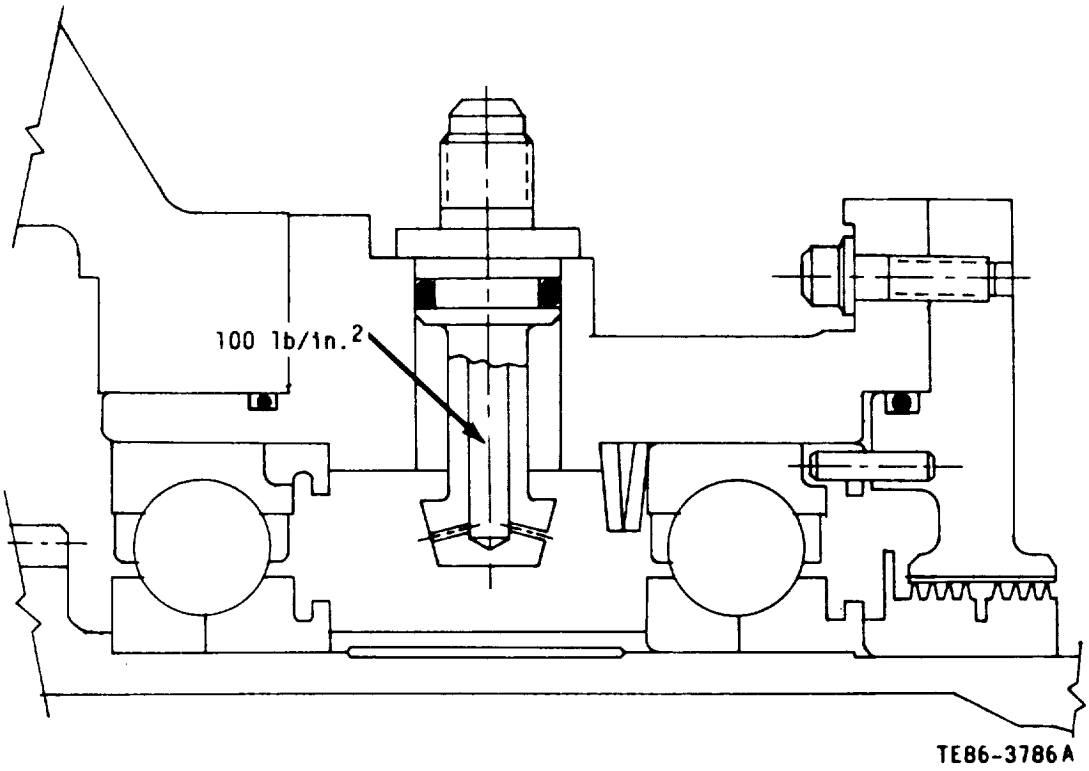

Figure 5.6-5. Input bearing lubrication and damper.

programs such as SHABERTH, BD43, and BD44 (Allison owned SKF computer programs). Data from the suppliers of the bearings, Timken and Fafnir, were also used. Simple estimates were made for power loss in the seals and oil pumps. Since these bearing computer programs do not run well under no load conditions, tare power loss for bearings was calculated with methods described in Ref 5 and 6.

Figure 5.6-6 illustrates a typical helical gear mesh with two teeth in contact. The Anderson/Loewenthal method for spur gear power loss calculations uses geometry in the transverse plane to evaluate the power loss parameters. In a spur gear, these parameters are constant across the face width of the gear. In a helical gear, the contact line is skewed across the tooth as shown in Figure 5.6-6. In order to properly evaluate parameters such as sliding and rolling velocity at each contact point on the skewed line, the equivalent point in the transverse plane must be determined. This is accomplished by reflecting points on the line of contact in the normal plane such as point H down to its equivalent point on the line of contact in the transverse plane.

In Figure 5.6-7, a helical gear mesh situation at a given roll angle, θ, with three teeth in contact, is shown. The start of contact in the transverse plane occurs at point 1 and ends at point 6. Sliding and rolling velocities vary as shown in the transverse plane. Contact load is determined by summing the lines

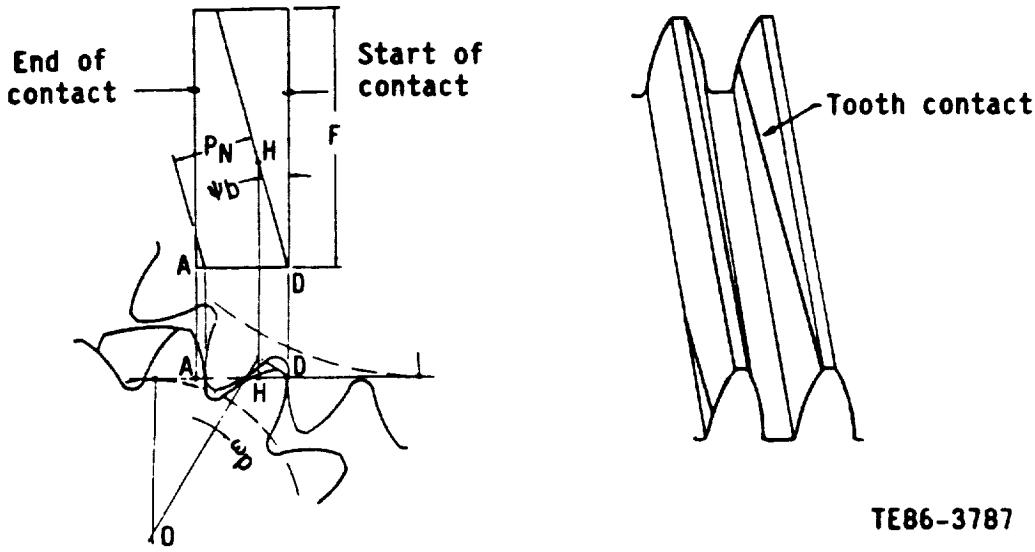

Figure 5.6-6. Helical gear geometry for efficiency calculation.

of contact and assuming equal load distribution on all teeth. The instantaneous loss at this roll angle is determined by integrating the sliding and rolling loss equations for each tooth in contact and summing the results. Windage loss is included but does not vary as a function of roll angle. As the roll angle progresses, the contact lines shown in Figure 5.6-7 change position, creating changes in the meshing parameters until finally the initial mesh situation is repeated. Thus, in a helical gear, power loss is a function of roll angle. To obtain the average mesh loss, the computer program divides this mesh sequence into 20 steps and calculates the overall average.

This type of analysis was performed on the AGBT gears, taking into consideration the differential planetary action of both the internal and external meshes. The results are shown in Table 5.6-II along with all other losses considered. Two points are shown--cruise and takeoff. Steady-state propeller loads at these conditions were included in the tapered bearing analysis. The two largest losses occur at the sun/planet gear mesh and the planet bearings. Oil pump losses are also quite significant due to their low efficiency (25%). Oil churning loss was not included in this analysis. Churning loss will occur if cooling oil cannot easily exit from a gear mesh. The same type of analysis was performed on the Allison T56 gearbox and found to match test data (see Ref 7). The exit area in the AGBT gearbox is at least twice that in the T56 planetary gearset. For these reasons, churning losses are expected to be low.

Table 5.6-III shows tare (no-load) losses for the gearbox. The biggest difference in this analysis technique is that bearing losses were calculated with less sophisticated prediction techniques. The T56 analysis done in the same manner showed excellent correlation with test data. The data in Table 5.6-III is plotted in Figure 5.6-8.

5.6.3 Gear Lubrication

In order to adequately cool a gear mesh, oil must penetrate to at least the pitch diameter of the gear. Out-of-mesh lubrication provides the best cooling

Table 5.6-II.
Gearbox power loss under load.

	Cruise (8000 HP)	Takeoff (13,000 HP)
Gears		
Sun/planet mesh	18.56	29.08
Planet/ring mesh	6.38	9.26
Windage--gears and carrier	5.39	5.39
Total	30.33	43.73
Bearings		
Planet bearings	18.16	20.00
Prop bearings	4.52	6.58
Sun gear thrust bearings	4.72	4.72
Carrier ball bearing	0.21	0.21
Carrier roller bearing	0.19	0.19
Total	23.28	25.12
Seals		
Prop shaft	2.00	2.00
Oil transfer gland	0.50	0.50
Total	2.50	2.50
Oil Pumps		
Supply	6.14	6.14
Scavenge	3.35	3.35
Total	9.49	9.49
Grand Total	65.60 HP	80.84HP
Efficiency	99.18%	99.38%

since it sprays the gear surface with cool oil as soon as mesh action is completed. It then flings off the oil before its next mesh cycle. Out-of-mesh lubrication has been shown to reduce power loss. This technique has been used successfully for many years in the T56 gear system and has been implemented in the AGBT gear system as well.

The planet/ring gear mesh does not have jet lubrication for two reasons: (1) losses in this contact are quite low, and (2) the ring gears will be bathed in oil as centrifugal force carries the sun gear and planet bearing oil out. After the oil is forced out axially, it will flow through the opening in the ring gear (flex fingers) to the housing. Due to the rotation, this oil will rotate around the housing until it is diverted to the drain.

Table 5.6-III.
Gearbox tare (no-load) losses.

	Gearbox power loss, HP				
	Percent speed				
	10	25	50	75	100
Gears					
Sun/planet mesh	0.11	0.40	0.98	1.60	2.22
Planet/ring mesh	0.10	0.42	1.11	1.87	2.65
Windage--gears and carrier	0.02	0.11	0.77	2.40	5.38
Total	0.23	0.93	2.86	5.87	10.25
Bearings					
Planet bearings	0.24	1.14	4.00	8.80	15.89
Prop bearings	0.20	0.78	2.20	4.05	6.23
Sun gear thrust bearings	0.11	0.38	1.01	1.83	2.82
Carrier ball bearing	0.20	0.20	0.20	0.20	0.20
Carrier roller bearing	0.20	0.20	0.20	0.20	0.20
Total	0.95	2.70	7.61	15.08	25.34
Seals					
Prop shaft	0.20	0.50	1.00	1.50	2.00
Oil transfer gland	0.10	0.25	0.50	0.74	0.99
Total	0.30	0.75	1.50	2.24	2.99
Oil Pumps					
Supply	0.61	1.54	3.07	4.61	6.14
Scavenge	0.34	0.84	1.68	2.51	3.35
Total	0.95	2.38	4.75	7.12	9.49
Grand Total	2.43	6.76	16.72	30.31	48.07

5.6.4 Oil Transfer Seal

The largest portion of the gear system oil flow requirement, 15.1 gpm, must be supplied to the rotating planet carrier through the oil transfer seal. Several oil transfer schemes were considered--carbon seals, journal bearing with controlled leakage, and Teflon seals. The latter concept was adopted in the AGBT gear system.

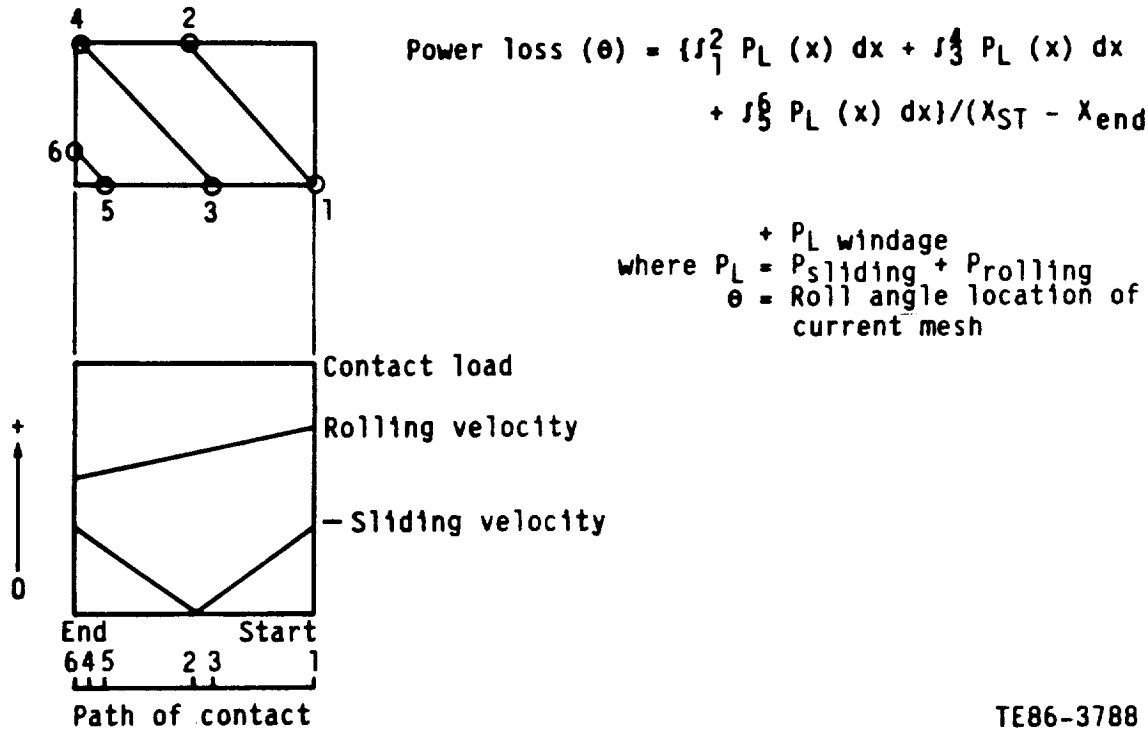

Figure 5.6-7. Evaluation of helical gear power loss.

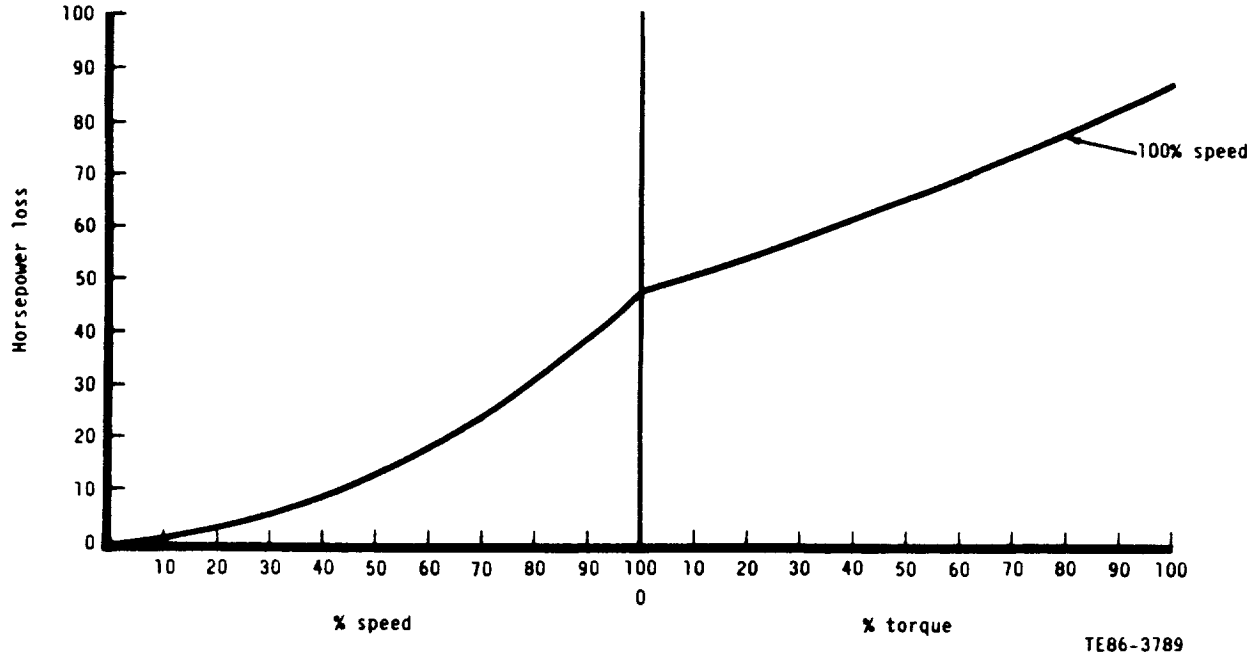

Figure 5.6-8. Predicted AGBT power loss.

5.7 SEALS

5.7.1 Prop Shaft Seal

Requirements for the prop shaft seal are difficult to meet with standard seal designs. The combination of high surface velocity (5400 fpm), large diameter, and long life rule out lip seals of any type. A concept developed by the Stein Seal Company, the Hydro-Load circumferential seal (Figure 5.7-1), was used in the AGBT design.

This seal, made of matched segments of carbon, has overcome many problems found in sealing oil with a circumferential carbon seal. The Hydro-Load seal uses the negative lift concept where a series of pockets machined into the carbon seal surface creates a suction force when the shaft rotates. This force pulls the carbon toward the shaft and eliminates the problem encountered with solid carbon segments--that of lifting due to creation of an oil film between the rotating and stationary parts. The suction force can be very high. To prevent excessive frictional power loss, a series of pressure reducing grooves are machined into the pockets to maintain pressure at proper levels. Another feature important in the AGBT design is the ability to remove the seal without disassembling the gearbox. The entire seal assembly slides over the prop shaft flange after removing the retaining nuts.

Each carbon segment has a lapped joint surface to allow repositioning as the negative lift force is developed. This mechanism provides a flexible seal surface that can accommodate runout and thermal expansion. The segments are

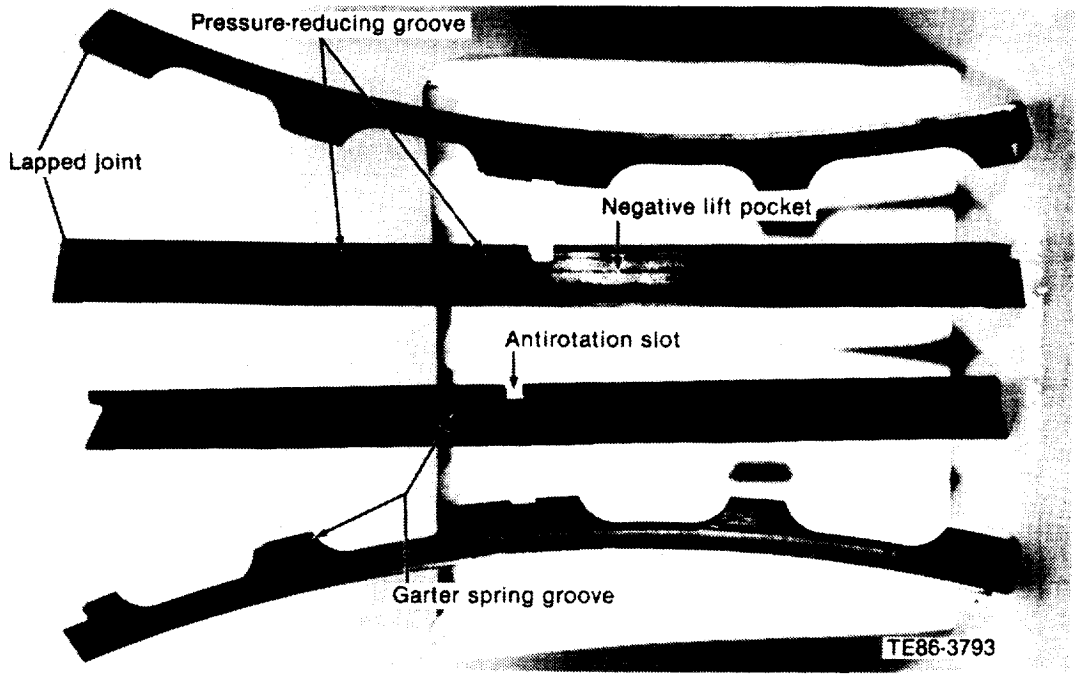

Figure 5.7-1. Hydro-Load seal ring segment.

surrounded by a garter spring that provides a light radial load. The primary purpose of this spring is to prevent leakage when there is little or no rotation. An antirotation slot prevents spinning of the carbon segment with the shaft.

Figure 5.7-2 shows the Stein Hydro-Load seal in the AGBT configuration. In this view the axial compression springs can be seen. A series of 30 small springs keeps the carbon segments preloaded against the vertical seal surface to prevent leakage along that surface. The carbon segment rides on a ground tungsten carbide surface (approximately 8 micro-inch rms). Results of testing other Hydro-Load seals show that wear on these contact surfaces is very low. An oil deflector was incorporated in the AGBT design to prevent direct impingement of prop bearing exit oil on the carbon segments. This seal cannot prevent leakage when oil is flowing directly toward the seal. Assuming a friction coefficient of 0.05, the power loss is estimated to be 2 hp. The seal is capable of sealing to ± 2 lb/in.^{2} with up to 0.01 runout of the seal runner surface.

5.7.2 Input Shaft Seal

An input shaft seal was designed to allow operation of the gearbox on the test stand. In flight systems this area is not normally sealed from the engine. A labyrinth seal pressurized with filtered shop air was selected for the AGBT gearbox. The configuration selected and pertinent design data are shown in Figure 5.7-3. The parameters selected are consistent with Allison design practice based on previous labyrinth seal designs.

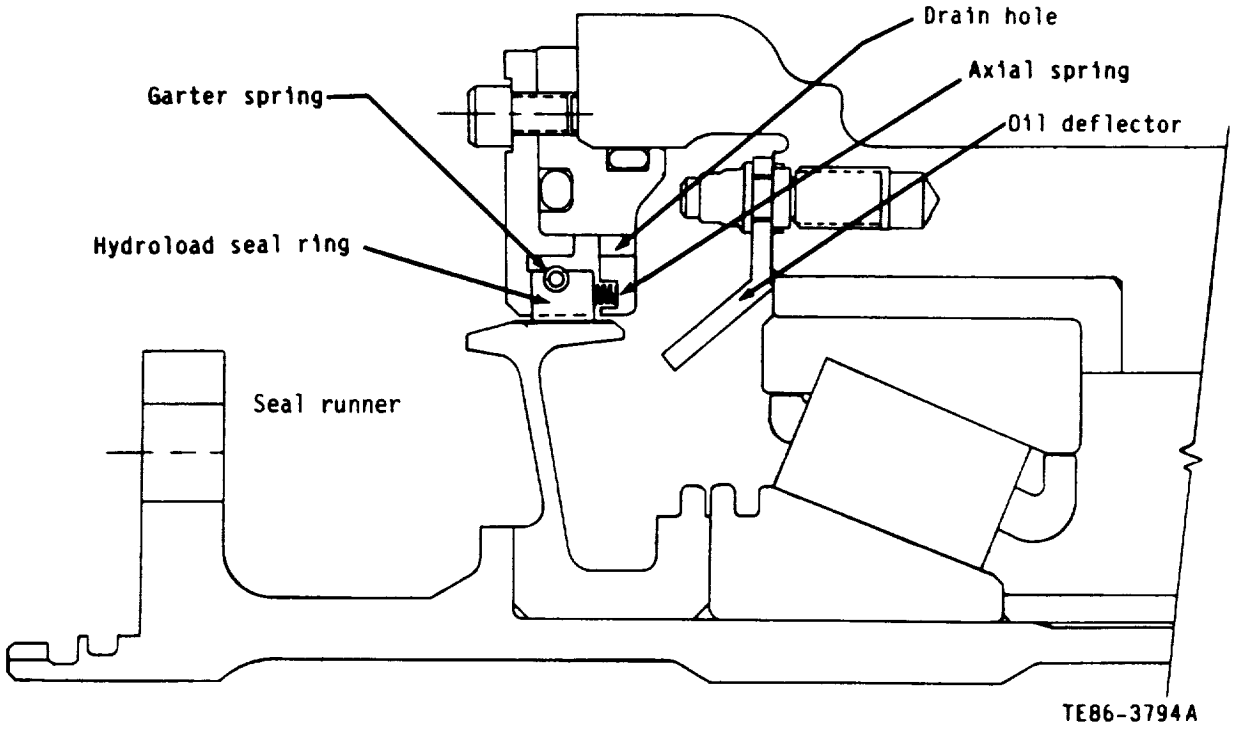

Figure 5.7-2. AGBT prop shaft seal arrangement.

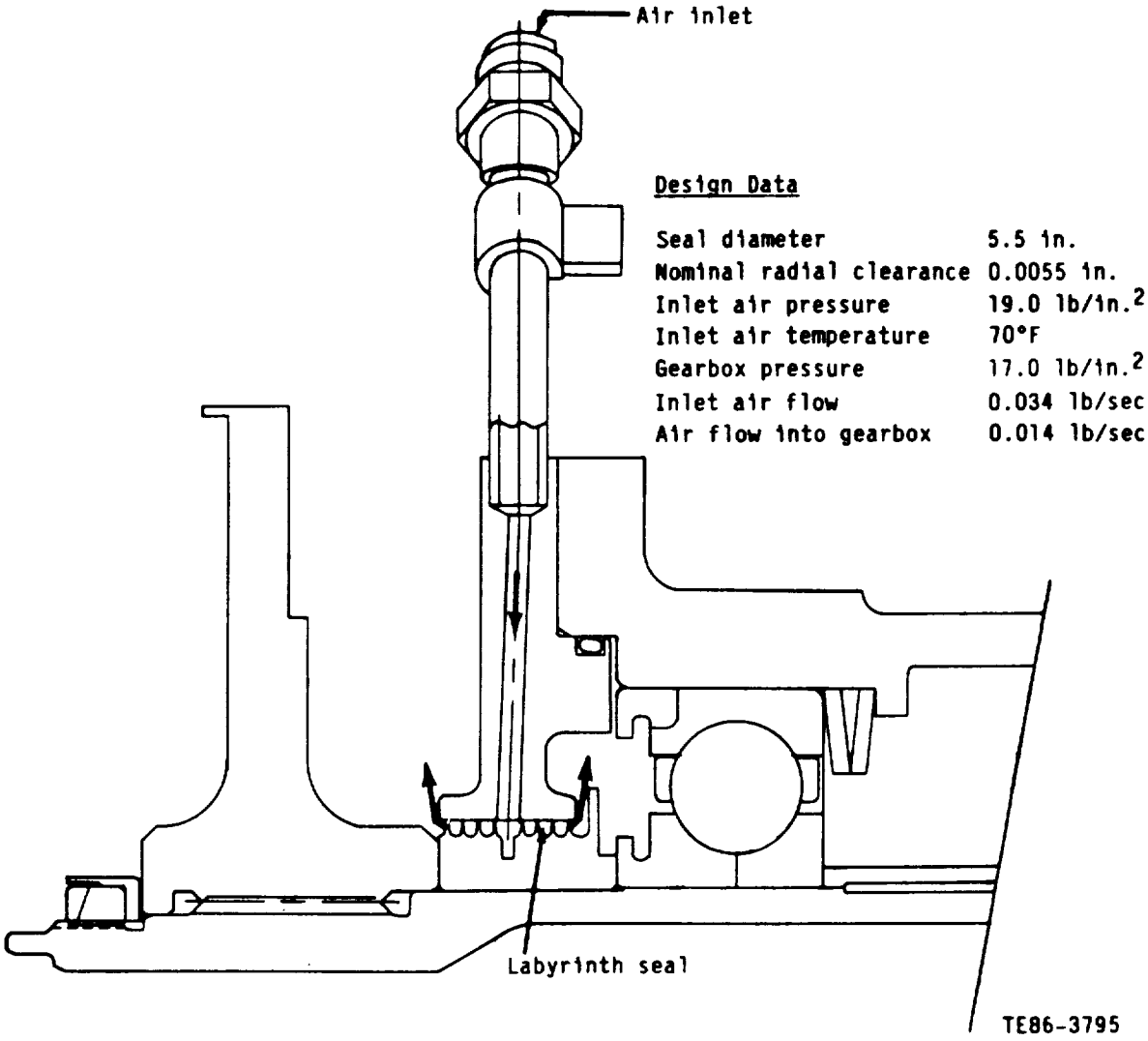

Figure 5.7-3. Input shaft labyrinth seal.

5.8 MATERIALS

The AGBT gear system includes advanced materials for critical components such as the sun and planet gears, the propshaft roller bearings, and the carrier support bearing races. Ring gears and several shafts were manufactured from a British standard steel that has been used for 20 years in Allison turbine engine components. The remaining components were made of standard aerospace quality materials commonly used by the aerospace industry. Steel components were nitrided or carburized for fatigue, wear, or fretting resistance. A cross section of the gear system showing the materials used is given in Figure 5.8-1.

Sun and Planet Gears

CBS 600 steel, carburized and hardened to 60 HRC surface hardness, was used for the sun and planet gears. This steel is one of several advanced gear steels developed to provide high hot hardness for improved scoring resistance and bending and pitting fatigue strengths for higher operating temperatures. CBS 600 was selected for the gear applications after an extensive literature review of advanced gear steels that included CBS 1000M, Vasco X2M, Pyrowear 53, and M50-NiL. The properties of each candidate steel were ranked using 9310 steel for minimum property requirements, as shown in Table 5.8-I. CBS 600 proved to have the best combination of rolling contact fatigue resistance, hot hardness, fracture toughness, and potential for property improvement with process optimization for the sun and planet gear applications.

Table 5.8-I.
Rankings of various steels considered for sun and planet gear applications.

Hot hardness

1. Vasco X2M
2. CBS 1000M
3. Pyrowear 53 and CBS 600
4. 9310 and M50-NiL (no data)

Fracture toughness

1. Pyrowear 53
2. 9310
3. CBS 600
4. CBS 1000M
5. Vasco X2M and M50-NiL (no data)

Rolling contact fatigue

1. CBS 600 and M50-NiL
2. 9310
3. Pyrowear 53
4. Vasco X2M and CBS 1000M

Note: Ranked in order of best to worst. Results are generated from literature data.

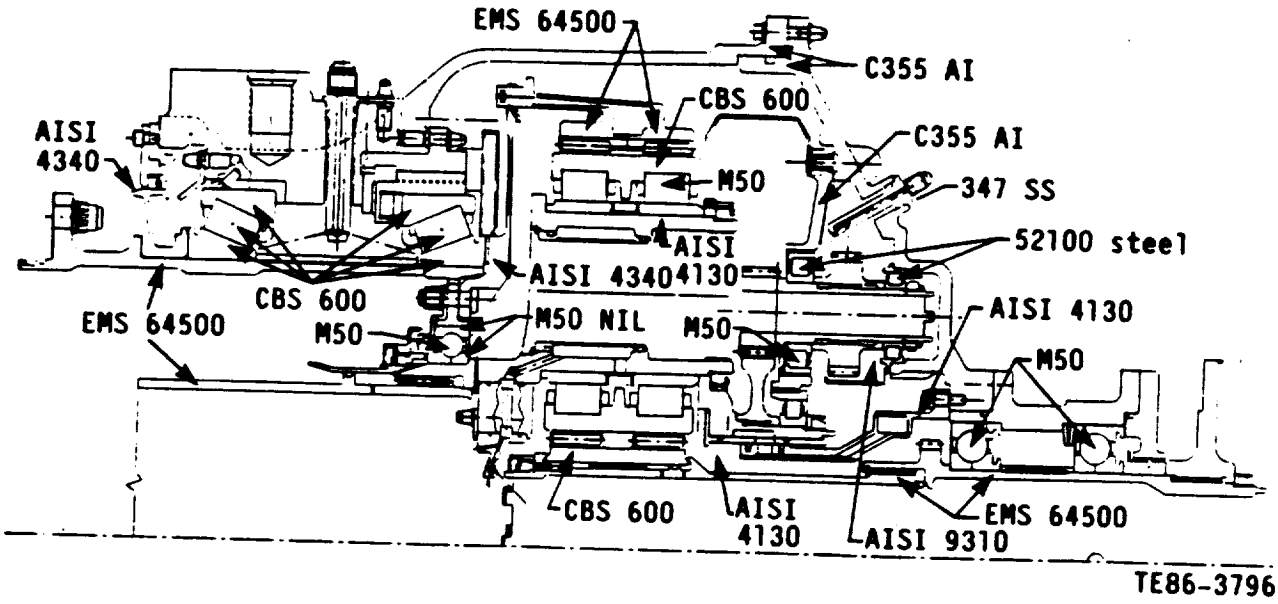

Figure 5.8-1. Cross section of the gear system depicting primary material selections.

Carburizing studies were performed to determine processing parameters for the CBS 600 sun and planet gears. Preoxidation of the parts was found to be a necessary process step. Some difficulty was encountered in consistently attaining the 60 HRC minimum surface hardness specified, but further process development should eliminate this situation. An Allison process specification was written to control the heat treatment of CBS 600 sun and planet gears.

AGBT Ring Gears

Ring gears were made from EMS 64500, a British standard medium carbon Cr-Mo-V steel. The gears were through-hardened and tempered to a uniform 36-40 HRC strength level and nitrided to 60 HRC minimum surface hardness for additional scoring/pitting/bending fatigue resistance in the teeth. Nitrided ring gears were preferred over carburized gears for this gearbox for low thermal distortion during heat treatment of these close tolerance, moderately stressed parts. A summary of the factors that were considered in choosing EMS 64500 is shown in Table 5.8-II.

Main Housing, Cover, and Inner Support

Cast aluminum alloy C-355 in the T7 heat treatment condition was chosen for the main housing, cover, and inner support components. C-355 aluminum is used in all Allison aircraft production engines and is easier to cast and less expensive than higher strength aluminum alloys. The T7 heat treated condition (overaged) was selected over the T6 condition to provide dimensional stability when operating above the T6 aging temperature. (One gearbox design criterion was the ability to withstand 400°F exposure for 100 hr.)

Table 5.8-II.
Summary of materials selection factors for the AGBT ring gears.

Material selected: First choice--EMS 64500 nitrided

Primary factors affecting decision:

A. Gear operates in a low medium stress application
B. Carburizing would require quench dies to control distortion--part is too large for in-house capacity
C. EMS 64500 has been selected as Allison standard shaft material
   1. Heat treat procedures have been established
   2. High core hardness for increased strength (HRC 40-45)
   3. Through hardened gear may be acceptable for testing (HRC 36-40 or HRC 38-42)
   4. More clean-up stock available on nitrided surface than other nitrided alloys (0.0050 in. versus 0.0025 in.)
   5. Material data package available for design
D. Core hardness of nitralloy is HRC 33-37 (limited in-house material data for design)
E. 18% Ni maraging steel cost is two to three times EMS 64500

Shafts

Shafts were made from EMS 64500 steel or SAE 4340 steel, depending on the strength level and nitriding capability required. These materials are widely used in Allison development and production engines. EMS 64500 steel was used for highly stressed shafts containing working splines that were nitrided to achieve a 60 HRC minimum case surface hardness. SAE 4340 was chosen for moderately stressed shafts containing splines that required only a 50 HRC or lower cased surface hardness.

Bearings

Bearing materials selected included currently used through-hardened materials and experimental materials that were carburized and hardened to provide better fracture toughness and increased bearing life. The prop shaft bearings were made from CBS 600 steel, carburized and hardened to 60-64 HRC surface hardness and manufactured by the Timken Company. The inner and outer races of the carrier support bearings were manufactured from M50-NiL steel by Fafnir Bearing Division, Textron Corporation. M50-NiL is a low carbon modified version of M50 steel that can be carburized and core hardened to produce a high surface hardness like M50, but it has a lower core hardness to provide better fracture toughness. All other bearings were made from M50 steel or 52100 steel, as shown in Figure 5.8-1. The 52100 and M50 steels are widely used in all development and production engines at Allison. A summary of the bearing materials used in the AGBT gearbox is shown in Table 5.8-III.

Table 5.8-III.
Summary of bearing materials used in AGBT.

Standard bearings, 52100
M50 bearings
M50-NiL bearings
CBS 600 bearings

- o Standard bearings are existing designs available at Allison
- o M50 bearing material is used in all development and production engines at Allison
- o M50-NiL is a modified M50--carburized, better fracture toughness, increased life
- o CBS 600--carburized, better fracture toughness, increased life

Miscellaneous Component and Materials Summary

The planet carrier and other steel details were made from 4130 steel, speed controlling gears from 9310 steel, and stainless steel parts from 347SS. All of these parts and those not specifically mentioned were manufactured from aerospace quality materials with which Allison has considerable experience. A summary of all materials used in the AGBT gearbox is shown in Table 5.8-IV.

Table 5.8-IV.
Summary of materials used in the AGBT gear system.

Planet gears and sun gear	CBS 600
Speed controlling gear train gears	AISI 9310
Ring gears	EMS 64500
Planet, carrier, and input bearings	M50 and M50-NiL
Prop shaft bearings	CBS 600
Speed controlling gear train bearings	Existing
Housing, cover, and inner support	C355.0-T7
Planet carrier	4130
Shafts	EMS 64500 and 4340
Flexible diaphragm	4340
Miscellaneous alloy steel details	4130
Miscellaneous stainless steel details	347SS

5.9 WEIGHT

All gearbox components were either weighed or their weight calculated. The results of this tabulation are shown in Table 5.9-I. The design task did not include a significant weight reduction effort, in fact, in many cases the hardware was to be designed as if it was test equipment.

Table 5.9-I.
Gearbox weight summary.

(Weights listed are measured weights unless noted.)

Gears**	Qty	Unit Weight	Total Weight
Sun	1	8.938	8.938
Planet gear and bearing assy	4	16.040	64.160
Ring-long	1	25.200	25.200
Ring-short	1	23.550	23.550
			121.848
Housing assemblies***			
Main	1	99.522	99.522
Cover	1	49.428	49.428
Inner support	1	12.411	12.411
Input bearing and seal	1	47.282	47.282
			208.643
Carrier assy** (including spacers)	1	115.028	115.028
Bearings**			
Prop	2	45.298	90.596
Planet (rollers/cage/inner race)	4	12.730	50.920
Carrier-ball	1	7.270	7.270
Carrier-roller	1	4.120	4.120
Input	2	6.592	13.184
			166.090
Shafting**			
Prop	1	64.400	64.400
Input	1	10.540	10.540
Sun gear	1	8.511	8.511
Flex diaphragm	1	27.275*	27.275
			110.726

Total gearbox weight - all fasteners + misc = 875.775

*Calculated weight
**Flight weight components
***Not representative of flight weight hardware

5.10 ADVANCED DESIGN TECHNIQUES

Computer analysis was used extensively in the AGBT gearbox design, as shown in Table 5.10-I. Many of these analyses are routine in gearbox or structural analysis, but several represent novel approaches. The planet gear FEM analysis, for example, was used to determine the load distribution within the bearing by modeling the integral bearing and roller. Bearing rollers were approximated with a series of radial springs. Loads were applied to the gear teeth and reacted at the carrier trunnion. Results showed that deflections in the gear were acceptable and that the stiffening rib at the center of the gear not only corrected a resonance problem but also provided a better load distribution within the bearing.

Table 5.10-I
Computer analysis of the AGBT gearbox.

Computer programs	Finite element analysis
Gears	Sun gear
Bearings (SHABERTH, BD-43, BD-44)	Planet gear
Efficiency	Ring gears
Rotor dynamics	Flex diaphragms
Gear dynamics (natural frequencies)	Carrier
	Housing
	Prop shaft
	Trunnion locknut

In another FEM analysis, the ring gear and ring support (flex fingers) were optimized in a series of models that attempted to restrict gear tooth movement to a uniform expansion side-to-side. Since the gear and its support are very flexible, it is not difficult to create misalignment. The final model predicts no more than a 0.002 difference in radial deflection across the tooth.

Prediction of gearbox efficiency has been very difficult in the past due to the lack of a model that can account for the many gear parameters that create differences in gears. A method was developed to predict helical gear efficiency based on a spur gear prediction technique that has been verified with T56 gearbox test data. This technique uses the common gear tooth parameters, combines them with lubricant properties, and provides a power loss estimate at any operating condition.

Many analyses were combined in this design effort to attempt to prevent development problems. Interactions of one model with another were controlled by carefully specifying the boundary conditions at these junctions. As with any new design, the models must be verified with test data. The test plan for this program includes verification.

6.0 TEST FACILITY, HARDWARE, AND INSTRUMENTATION

6.1 TEST FACILITY DESCRIPTION

The counterrotating AGBT gearbox system was tested in-house in a newly constructed back-to-back test facility. Back-to-back gearbox testing can most simply be defined as operating two gear trains of equal ratio in opposition to each other. With the input and output shafts connected, one gearbox operates as a speed increaser and the other as a reducer. In this case the reducer is the test gearbox. By introducing torque into the system, power will recirculate between the two gearboxes.

The schematic drawing in Figure 6.1-1 demonstrates this method of testing. A set of test gears is interlocked through both shafts with interconnecting shafting to a separate set of gears (slave) of equal ratio. A separately mounted source of power is used to rotate the gears to the required speed. A device to provide a relative twist in the system for loading the gears can be located in either of the interconnecting shafts. The gear loading device (torque applier) can be as simple as two bolt flanges on the end of a two-piece colinear shaft, twisted to the desired torque and locked prior to rotation. More complex mechanical, electrical, and hydraulic methods of applying the torque while the gears are rotating have been successfully employed at Allison.

The biggest advantage of the back-to-back gear test technique is the economy and simplicity of operating high capacity gearing under full load. Only 5% of the rated engine power is required to drive the back-to-back rig. The

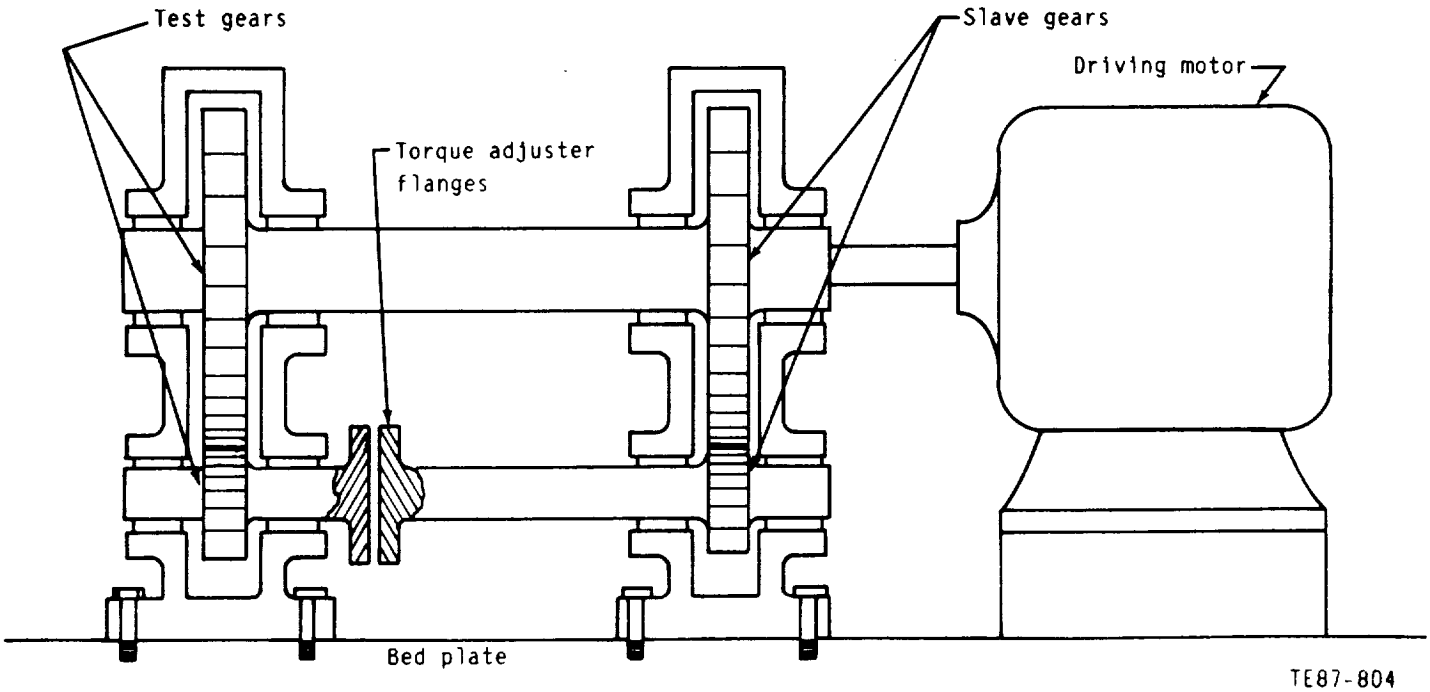

Figure 6.1-1. Back-to-back gear testing.

power requirement is equal to the power to overcome only motoring and frictional losses in the two gear trains. Other advantages of back-to-back testing compared to engine/absorber testing include the following:

- o Accelerated test programs can be performed with powers above the rammed power setting of the engine.
- o The gear system can be developed independently of the power section.
- o Rigs have the flexibility to permit the simultaneous performance of other forms of testing, such as flight maneuver prop shaft load testing, accessory loading, test lubrication, bearing tests, etc., in conjunction with gear loading.

A new facility was constructed in 1985 for development testing of Prop-Fan gear systems. The counterrotating Prop-Fan gearbox test stand arrangement is shown in Figures 6.1-2 and 6.1-3. As shown, the facility is capable of running geared systems up to 16,000 hp. The power to drive the back-to-back rig was supplied by two 500 hp motoring dynamometers. Because the maximum speed of the dynamometers is 3000 rpm, the output of the dynamometers drives through a 5:1 speed increaser gearbox into the torque applier. The torque applier gearbox reduces the speed internally by 2.6:1 ratio to drive two Rotac hydraulic torque appliers (maximum operating speed of 5000 rpm) and then steps the output (two concentric output shafts) back up by the same ratio. The two output shafts of the torque applier are connected to the input shafts of the test and slave gear systems. With the test and slave systems coupled to the outputs of the torque applier gearbox, the torque loop of the back-to-back gear rig is completed. A schematic diagram of the torque loop is shown in Figure 6.1-4. The interconnecting shafting is shown in Figure 6.1-5.

The slave gearbox is mounted rigidly to the torque applier while the test gearbox is cantilevered from the slave. Collars are mounted to the test and slave gearbox housing mount pads. Hydraulic rams between the two collars are used to apply thrust, moment, and side loads as shown in Figure 6.1-6. The prop load system was designed to apply loads of 750,000 in.-lb moment, 40,000 lb thrust, and 15,000 lb vertical and horizontal side loads. Figure 6.1-7 shows a schematic of the ram system.

Because the AGBT gearbox is a differential planetary system, a method was required to fix the two output shaft speeds. (The differential fixes the torque split between the two output shafts.) A speed coordinating gear train was built into the slave accessory housing that connects the input sun gear shaft to the planet carrier. When these two shafts are properly connected, the ring gear (outer prop shaft) must rotate at the same speed and in the opposite direction to the carrier (inner prop shaft). In addition to fixing the two prop shaft speeds, the speed coordinating gear shaft was instrumented with a torque bridge to measure the amount of power required to make the prop shafts run at equal speed. This speed control torque was then used as a health monitor of

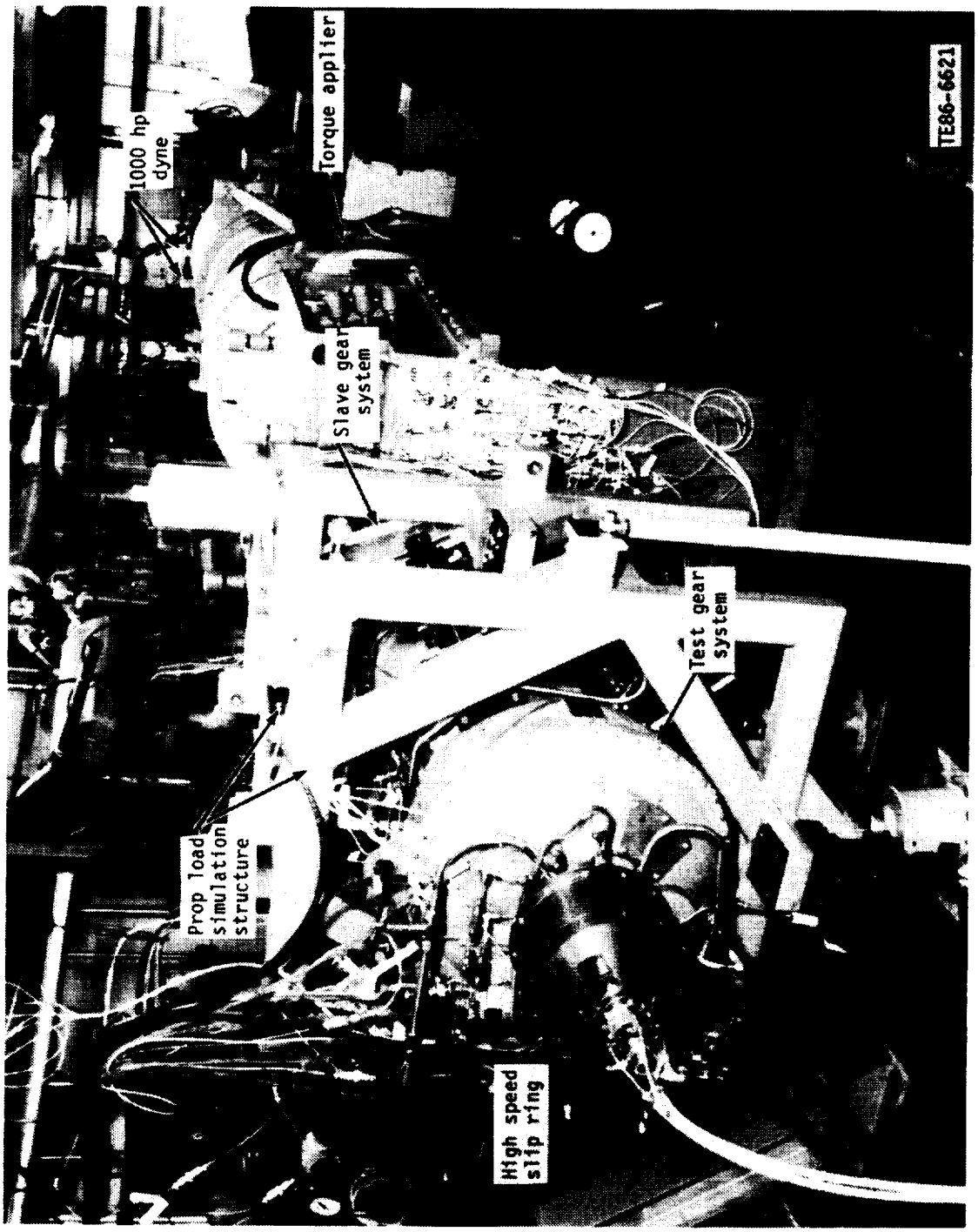

Figure 6.1-2. Counterrotating Prop-Fan gearbox test stand.

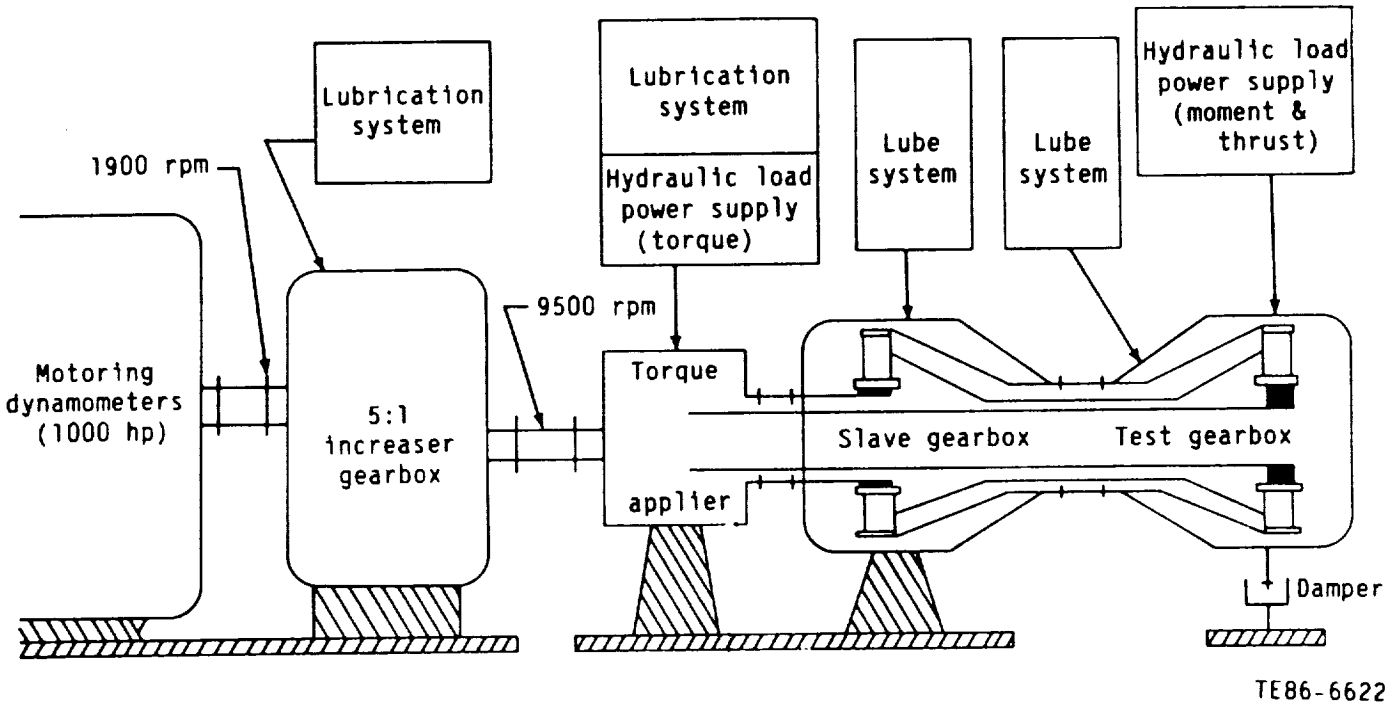

Figure 6.1-3. Schematic diagram of the counterrotating Prop-Fan gearbox rig.

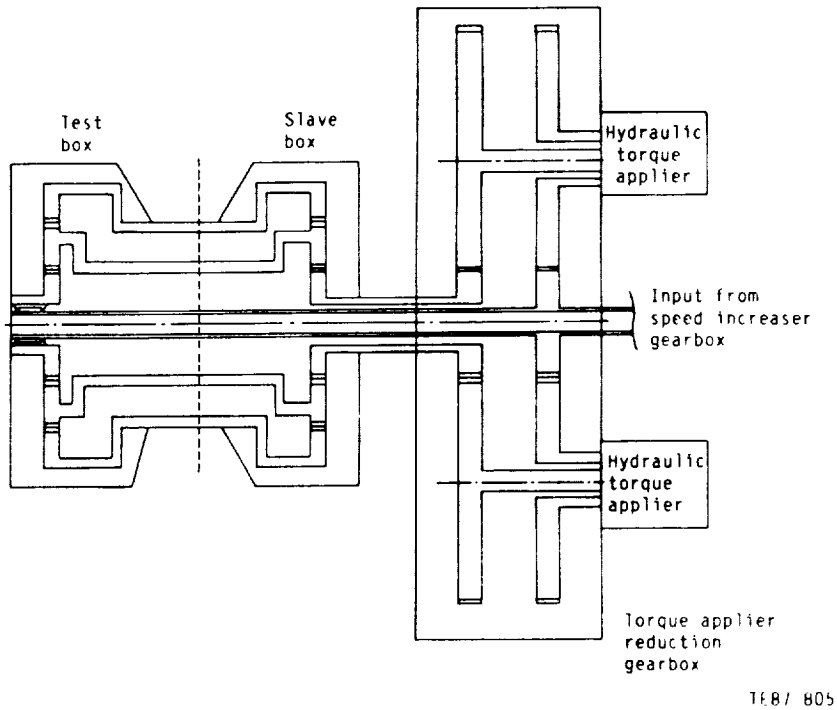

Figure 6.1-4. Torque applier schematic diagram.

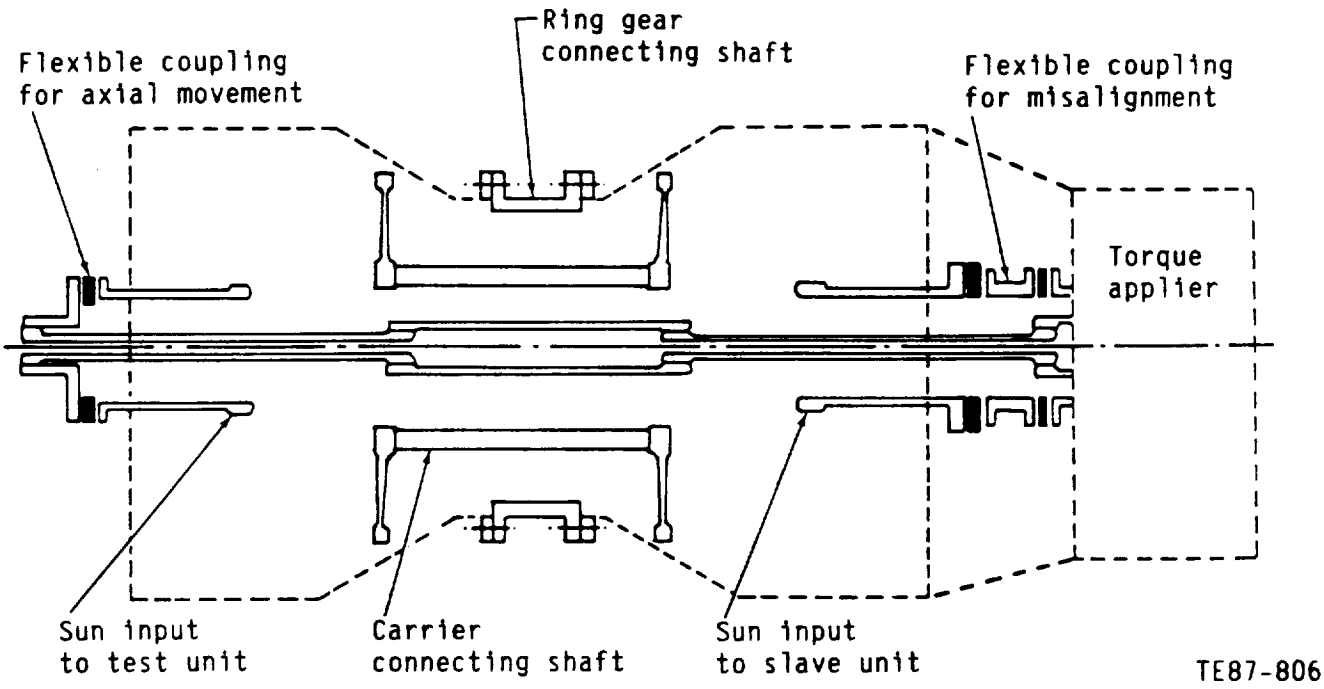

Figure 6.1-5. Test rig shafting.

the test and slave gear systems throughout the testing. A schematic of the test rig with the speed coordinating gear train is shown in Figure 6.1-8.

The test and slave gear systems were lubricated with remote oil systems. These systems are shown in Figure 6.1-9. Special features of the lubrication systems included the following:

- o oil flow rate--30 gpm
- o oil temperature control--80°F to 250°F
- o oil pressure control--0 to 200 psig
- o 3 μ abs. filtration (supply and scavenge)
- o lubriclone air/oil separator
- o quantitative debris monitor (QDM) system

The oil distribution plumbing for the test and slave gear systems was totally external. The oil supply to each area of the gearbox could be controlled by changing orifices (Lee jets) upstream of the internal oil jets.

6.2 TEST HARDWARE

The test hardware used in this test has been described in detail in section 5.0. The test gearbox was modified to allow installation of instrumention primarily by drilling thermocouple or wire holes in low stress areas. The slave gearbox was only modified for stationary instrumentation.

Partial assemblies were made, as required, to allow flow checks of all lubrication lines. Since most supply lines were externally fed, pressure to each

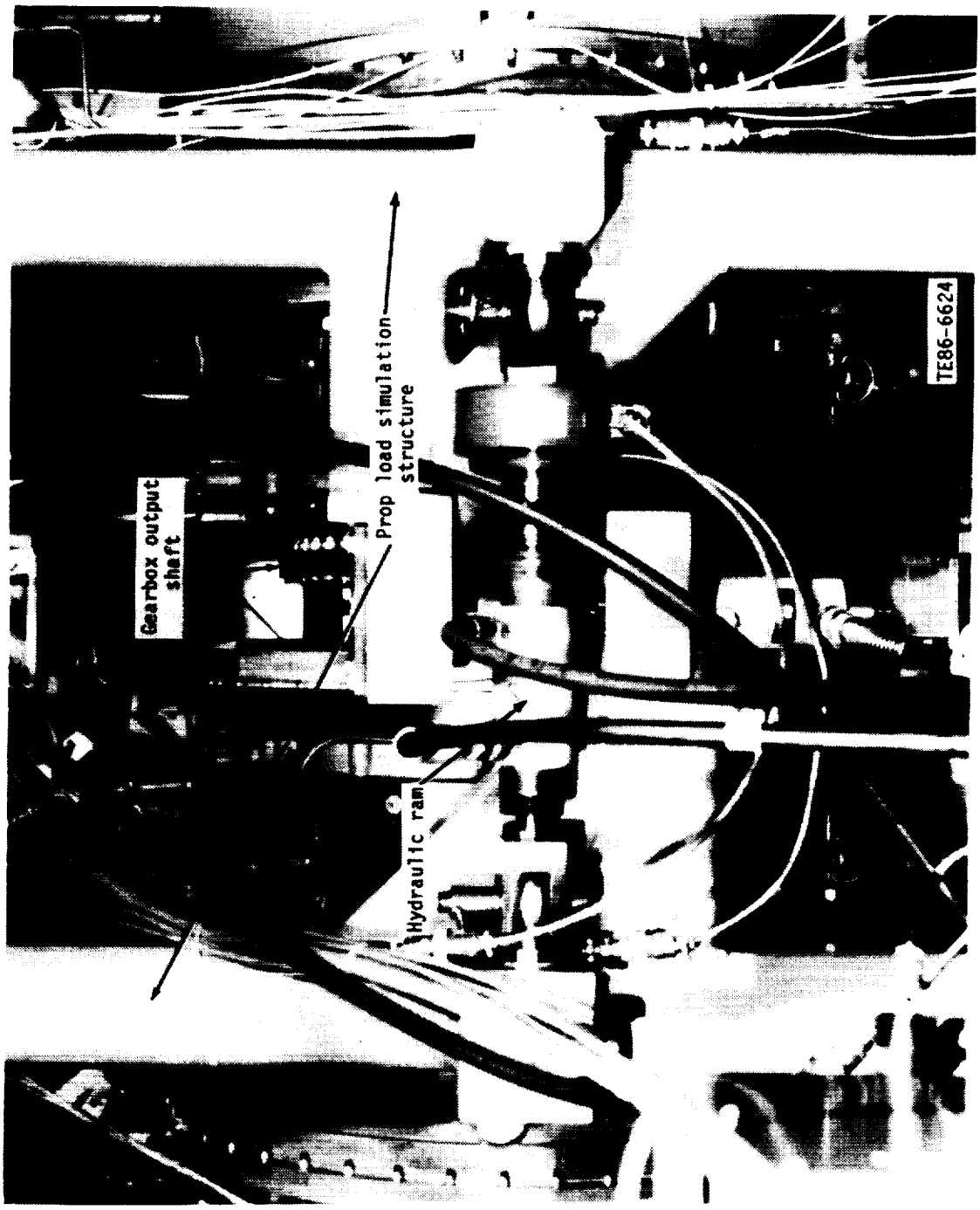

Figure 6.1-6. Prop load ram system.

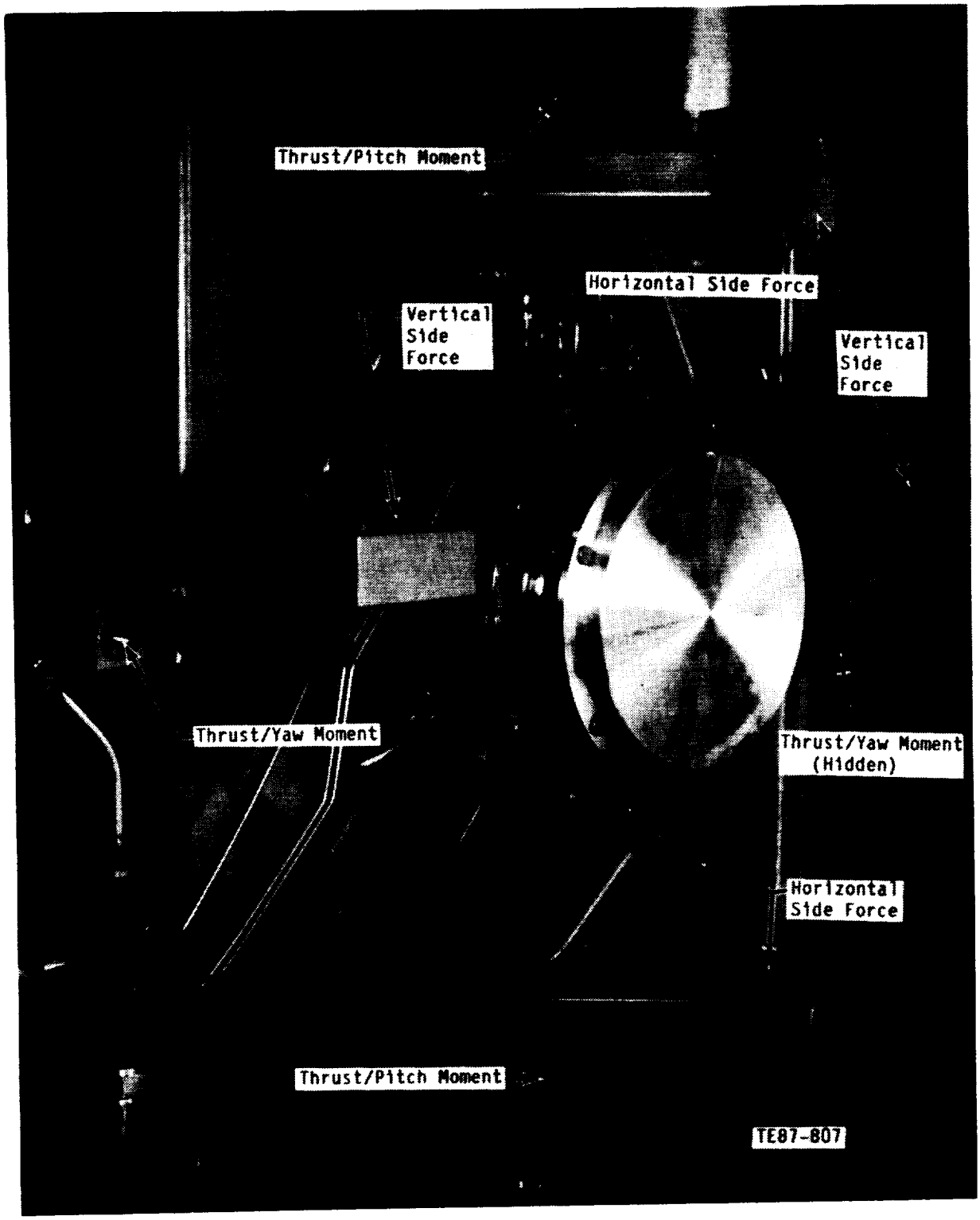

Figure 6.1-7. Schematic diagram of prop load ram system.

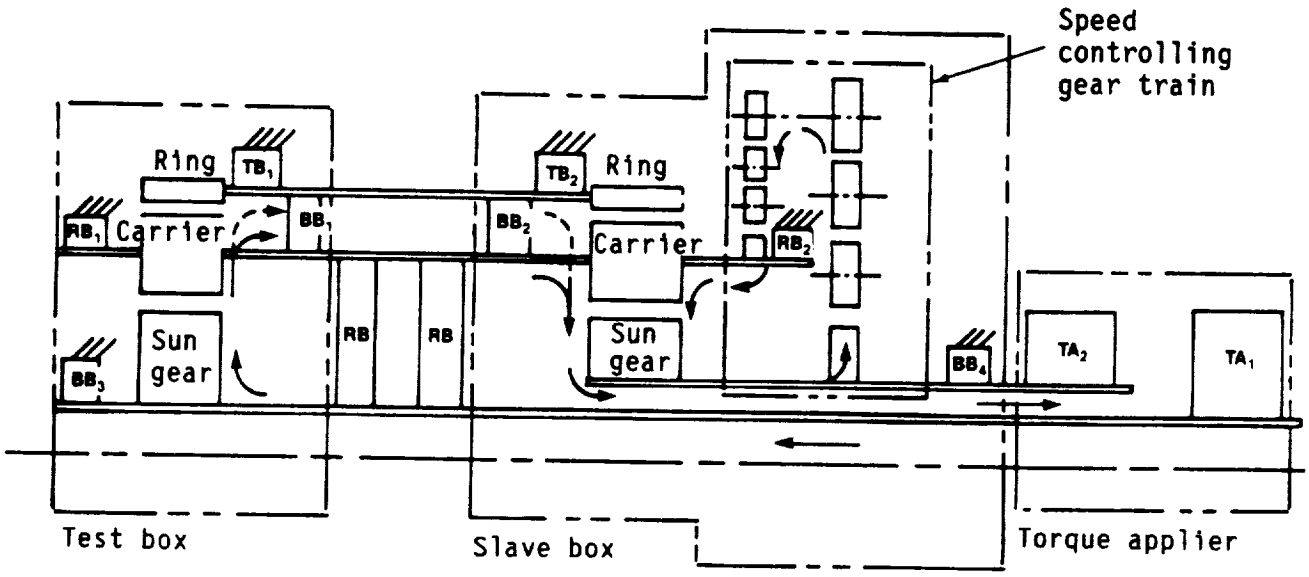

Figure 6.1-8. Schematic diagram of the test rig and speed control gear train.

location could be adjusted independently. All oil jets were target-checked to ensure that oil would reach the intended areas.

As the gearbox was assembled, measurements were taken to check the part stack-up in close fitting areas. All pilot and bearing fits were checked. Finally, all bolted or clamped assemblies were measured to ensure complete seating of all parts.

6.3 INSTRUMENTATION

The overall objective of this test was to verify the gearbox structural integrity and to provide a comparison of test data to performance predicted during the design phase. To support these objectives, an instrumentation package was incorporated into the test gearbox design. The following is a description of the instrumentation.

6.3.1 Thermocouples

Thermocouples were routed to each bearing inner and outer race in the test gearbox, except for the planet bearing outer race (planet gear) due to its combined rotational and orbital motion. Outer race thermocouples frequently will not provide an indication of bearing distress until damage has already occurred. The difference in outer and inner race temperature is also important in determining bearing operating clearances. The slave gearbox had outer race thermocouples only. Key bearing outer race temperatures in the torque applier and dynamometer system were also monitored. Since each piece of

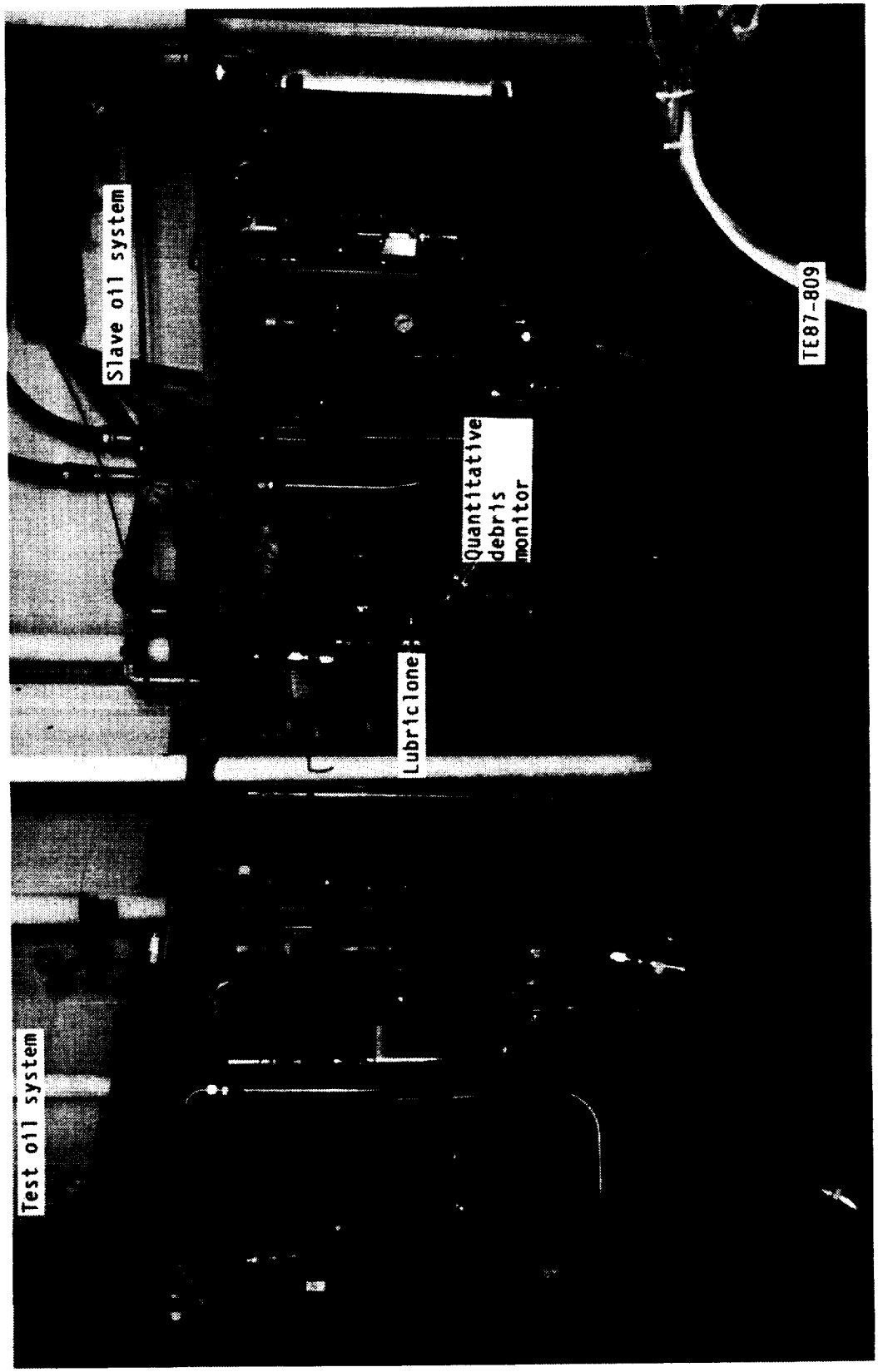

Figure 6.1-9. Gearbox lubrication system.

hardware in this test rig had its own lubrication system, many additional thermocouples were required to monitor oil temperatures.

6.3.2 Strain Gages

A total of 26 locations were monitored for strain--all in the test gearbox. Most of these gages were used to detect the onset of vibration in the lightweight ring gears or flexible diaphragm. Others were used as follows:

- o load sharing between the two ring gears
- o prop shaft bending stress
- o housing bending stress
- o flexible diaphragm bending stress

6.3.3 Vibration

The test and slave gearboxes were monitored for vibration in three directions at both input and output shaft areas. Accelerometers were located above bearings to obtain direct transmission of vibratory information. Accelerometers were also located at various points on test equipment.

6.3.4 Displacement

The test gearbox was fitted with eight proximity probes to detect (1) ring gear radial movement, (2) flex diaphragm axial movement, (3) carrier axial movement, and (4) input shaft radial and axial movement. Most of these measurements were intended to detect dynamic system response. The ring gear probe was used to measure flexure of the ring due to planet gear passage. The carrier probes were positioned to detect deflection in the carrier backing plate due to bending of the trunnions under load.

Several other proximity probes were positioned to monitor radial and axial whip of the interconnecting, high-speed shafting and couplings to check for rotor dynamic response.

6.3.5 Speed

Gearbox speed was monitored at the dynamometer location with a magnetic speed pickup.

6.3.6 Torque

Gearbox input torque was monitored through a torsion full bridge applied directly to the input shaft. The resulting transducer was then calibrated using fixtures with a calibration traceable to the National Bureau of Standards (NBS). Speed control torque was also measured through a torsion full bridge, but the output was converted to torque by calculation rather than through laboratory calibration.

Due to the large number of rotating sensors, four data transfer systems were required--two telemetry systems and two slip rings. Telemetry system I was used to record data from strain gages on the ring gear, flexible diaphragm, and prop shaft as well as rotating bearing race temperatures in the planet

carrier and prop shafting. Telemetry system II was used to measure planet bearing temperatures. Slip ring system III was used to record the input torque, sun gear bulk temperatures, and input bearing race temperatures. Slip ring system IV was used to measure speed coordinating gear train torque.

In total, more than 140 parameters were continuously recorded throughout the test program. A schematic of the test rig instrumentation is shown in Figure 6.3-1.

6.3.7 Data Monitoring/Recording

An objective in this test was to monitor key parameters during the test so that the hardware would not be damaged if a problem were to occur. To provide this on-line information, video displays, oscilloscopes, high speed and x-y chart recorders, and frequency spectrum analyzers were utilized. Dynamic measurements were also recorded on magnetic tape for later data reduction. Steady state data were recorded digitally by taking 25 samples at one reading per second and then averaging.

6.4 TEST DESCRIPTION AND PROCEDURES

The counterrotating gear system was designed to operate at 9,500 rpm input speed (1,140 rpm propeller speed) and 13,000 hp (7,190 ft-lb input torque). Testing has included the following operating conditions:

- o steady state speed and load conditions (0-11,000 rpm [115%] input speed and -500 to +7200 ft-lb input torque)
- o steady state speed and load conditions with propeller loads added (prop loads included -15,000 to +15,000 lb of thrust and 100,000 in.-lb of moment load)
- o transient conditions that included accelerations and decelerations to and from 10,000 rpm input speed with loads from -500 ft-lb to +2000 ft-lb input torque.

Figure 6.4-1 tabulates the steady state speed and torque operating conditions.

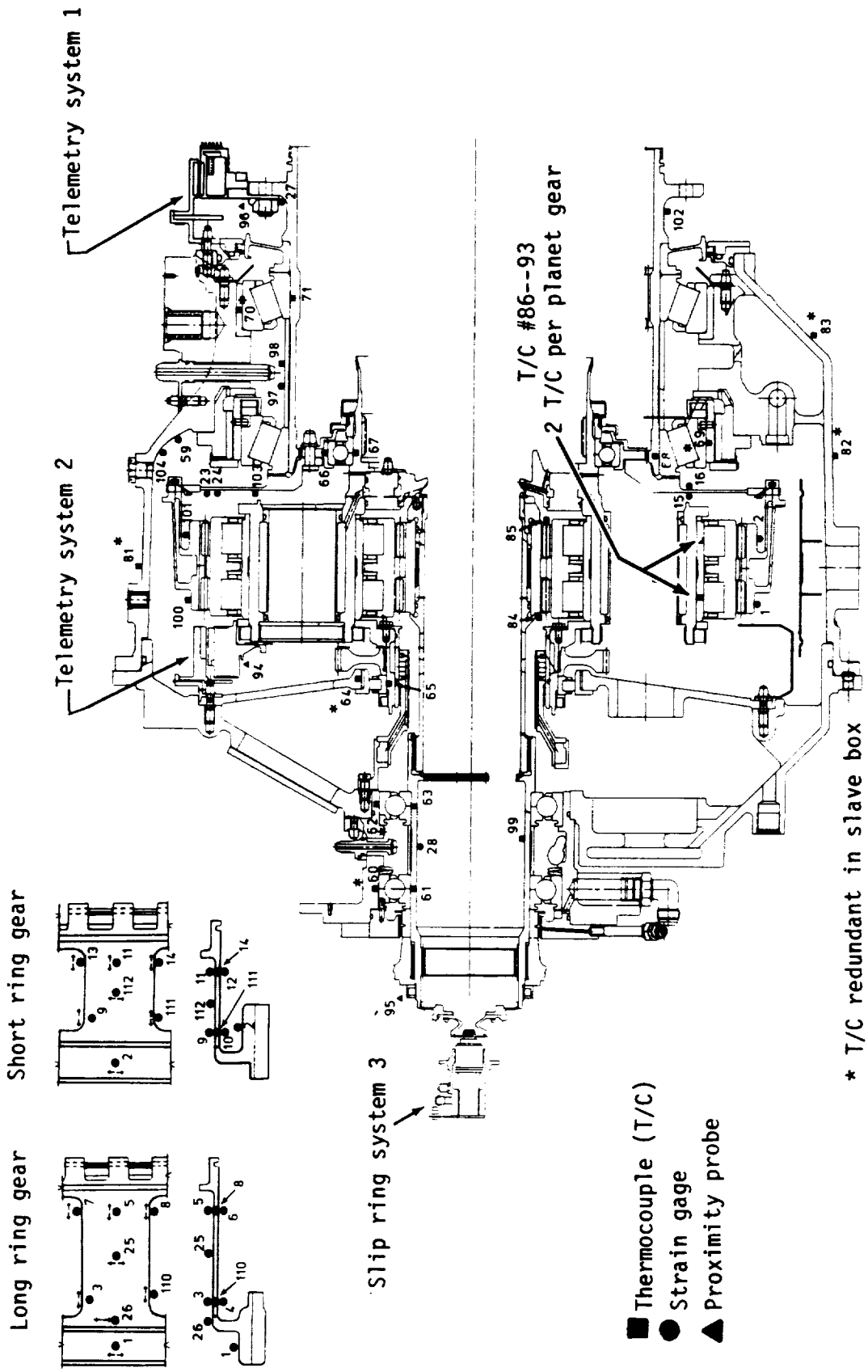

Figure 6.3-1. AGBT Instrumentation diagram.

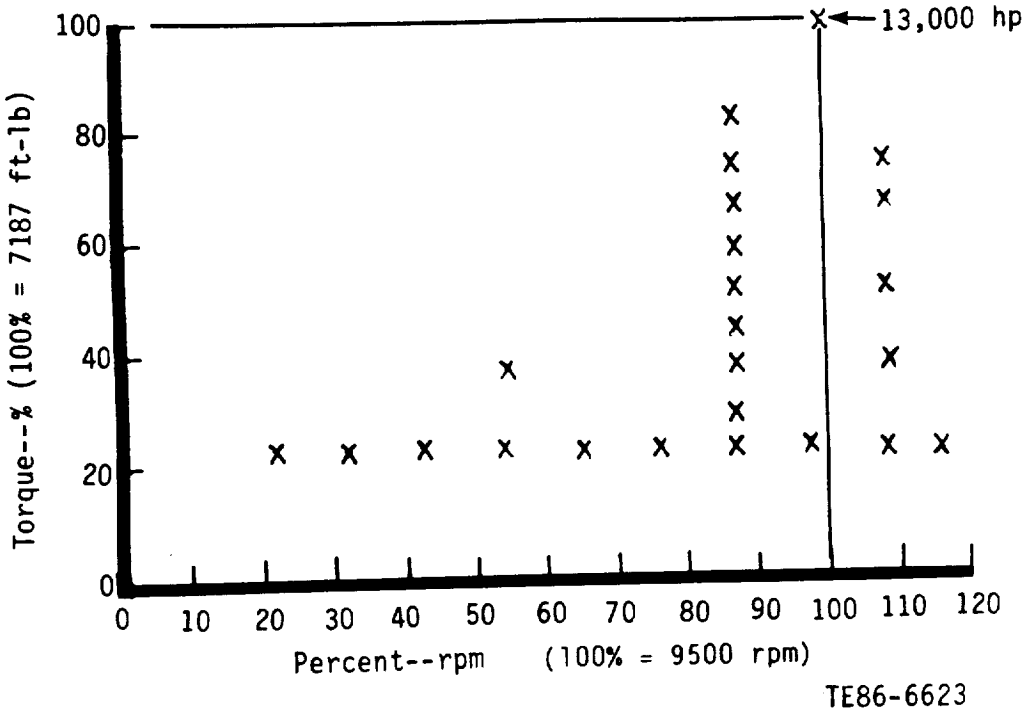

Figure 6.4-1. Steady state test points.

7.0 TEST RESULTS AND DISCUSSION

The test results discussed in this section cover back-to-back tests of the AGBT gearboxes. These tests were run with extensive stationary and rotating instrumentation to document temperatures, stresses, vibration levels, internal motion, and efficiency. Test results verified that the performance of the new gearbox design met the requirements.

A considerable amount of data was recorded during testing. To simplify this discussion, only the test gearbox data will be presented. Slave gearbox performance was very similar to that of the test unit. Characteristics and operational data obtained under various speed and torque conditions, without any prop loads applied, are presented in subsections 7-1 through 7-5. The effect of prop loads will be discussed in subsection 7.6.

7.1 GEARBOX TEMPERATURES

Gearbox temperatures were well behaved as shown in Figure 7.1-1 and 7.1-2. (Oil-in temperature was controlled to 180°F.) Temperatures are shown as a function of speed since they did not change appreciably with torque. Table 7.1-I shows these temperatures at full design power, 13,000 hp at 9500 rpm. The maximum temperature at any of these locations at full design power was 223°F.

Table 7.1-I.
Gearbox temperatures (°F) at full power (13,000 hp).

Oil-out temperature	223	
Average housing temperature	217	
Bearing temperatures		
Bearing	Inner race	Outer race
Inboard prop	-	211
Outboard prop	193	199
Carrier ball	209	-
Carrier roller	218	219

Data from telemetry system II was unusable due to a transmitter malfunction. This system included the planet bearing temperatures and carrier ball and roller bearing inner race temperatures. Observations during the test indicated that these temperatures were similar to those in Figure 7.1-1.

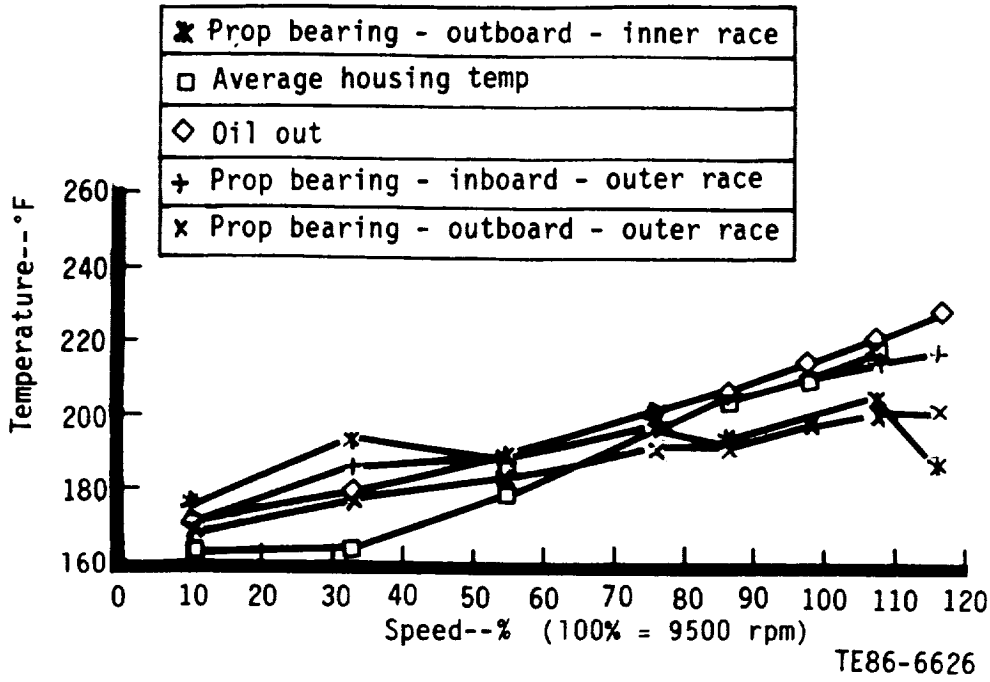

Figure 7.1-1. Prop bearing, housing, and oil temperatures as a function of speed.

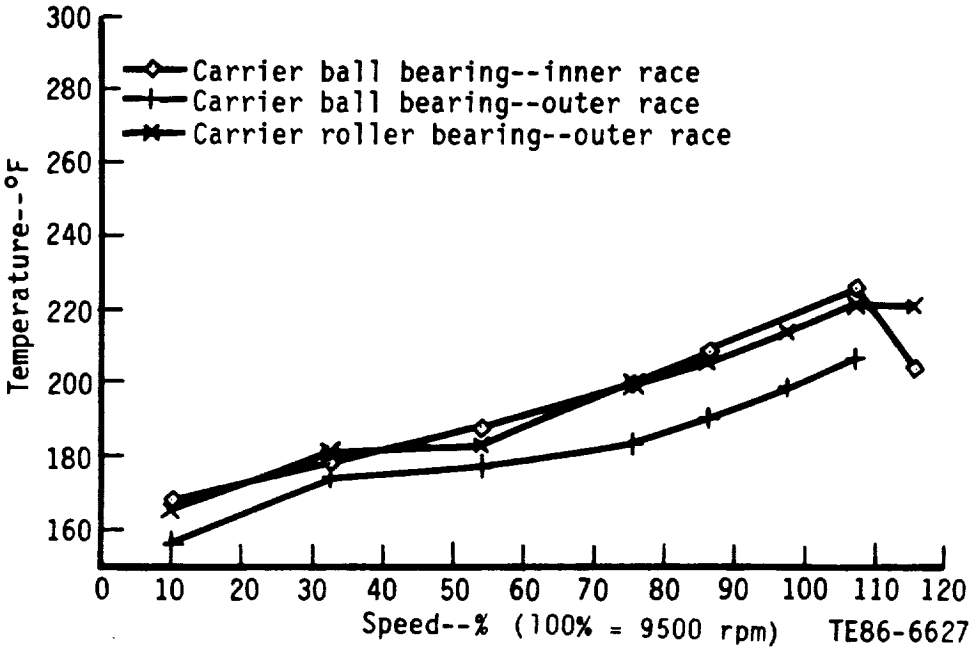

Figure 7.1-2. Carrier ball and roller bearing temperatures as a function of speed.

7.2 GEARBOX VIBRATION

Figure 7.2-1 shows the average gearbox vibration level at six locations on the test gearbox housing as a function of speed. These levels are quite low and represent smooth operation. Vibration levels were primarily a function of speed just as were the temperatures. Vibration as a function of torque is shown in Figure 7.2-2 at an input speed of 10,290 rpm. The dominant frequencies correspond to input and output shaft rotational speeds. Vibration levels at the AGBT design point, 13,000 hp, are shown in Table 7.2-I.

Table 7.2-I.
Gearbox vibration levels (in./sec--avg) at full power (13,000 hp).

Input housing	
Vertical	0.31
Lateral	0.28
Axial	0.14
Main housing	
Vertical	0.23
Lateral	0.20
Axial	0.21

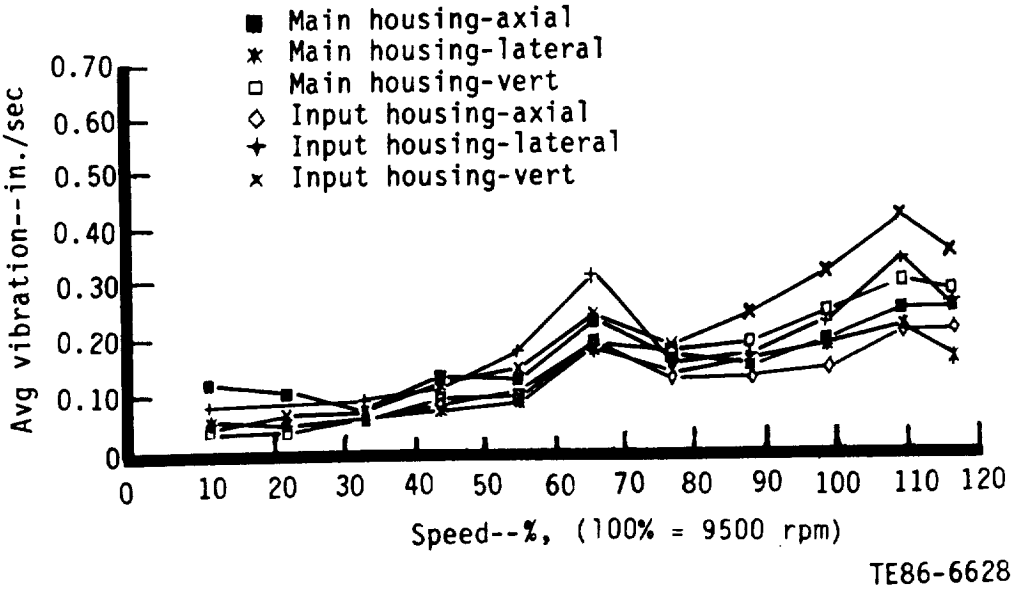

Figure 7.2-1. Gearbox vibration as a function of speed.

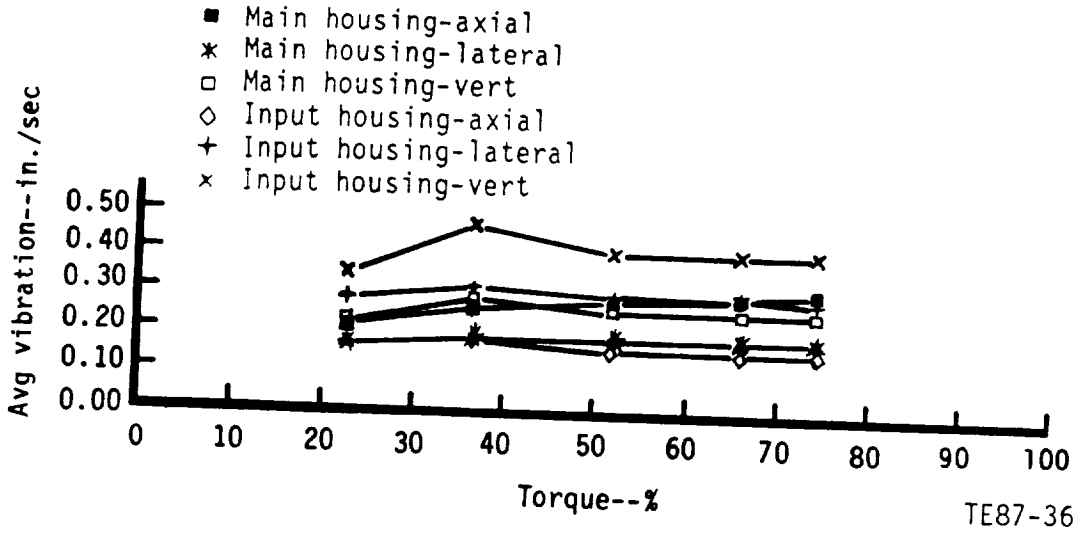

Figure 7.2-2. Gearbox vibration as a function of torque at 10,290 rpm.

Figure 7.2-3 shows a comparison of vibration levels at discrete frequencies in various Allison gearboxes. The gear mesh frequency, which is the most objectionable type of vibration, was quite low in this gear system. The use of double helical gearing significantly reduced gear mesh vibration by improving the meshing action, i.e., contact ratio. This was one of the main objectives in the AGBT design.

7.3 GEARBOX STRESS

Stress levels at 26 locations were monitored on-line during this test. Figure 7.3-1 shows the ring gear strain gage installation. A schematic diagram of the long ring gear gage locations is shown in Figure 7.3-2. The stress levels measured during the test and in a more thorough analysis afterwards indicated that all components were functioning as predicted. This data validates the finite element models used to design these critical parts in the gearbox and helps to substantiate the 30,000 hr life requirement set forth in the design phase.

Maximum stress on the long ring gear occurs at the gage number 26 location. This cyclic stress is primarily due to the planet gear loading. Figure 7.3-3 shows the output of this gage at 13,000 HP, 9500 rpm. For each revolution of the planet carrier there are eight stress pulses. The stress values measured here agreed with the finite element prediction to within 15%.

These gages were also used to detect modal vibration response in the ring gears and flex diaphragm. Data taken during an acceleration from 20% to 100%

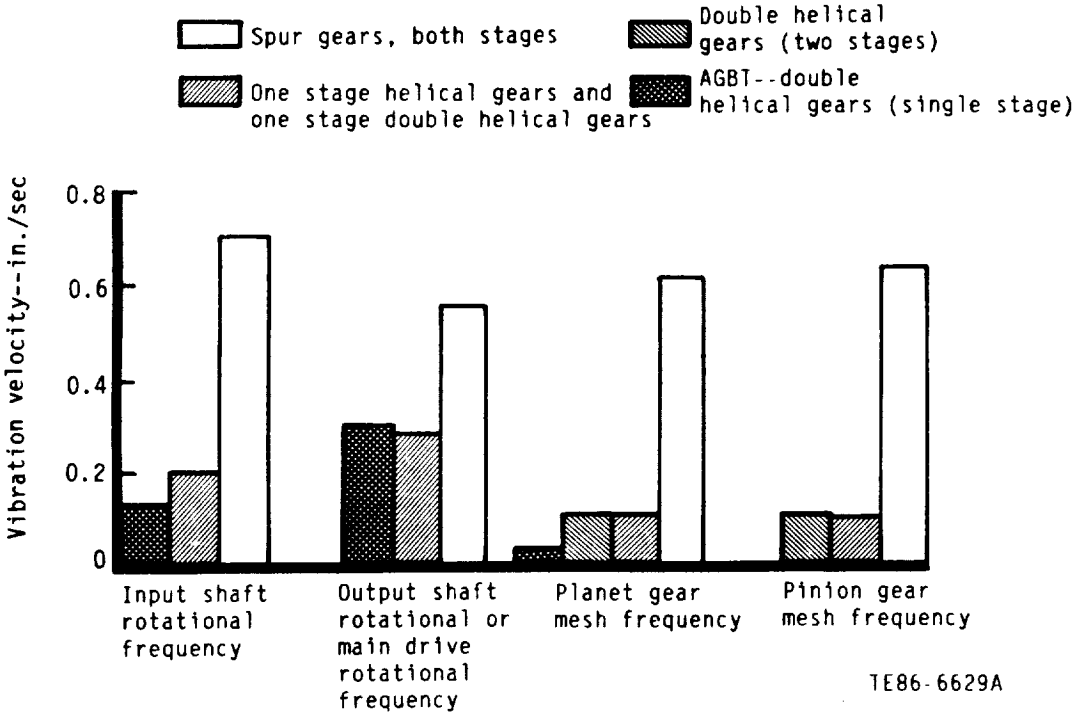

Figure 7.2-3. Vibration levels for large Allison gear systems.

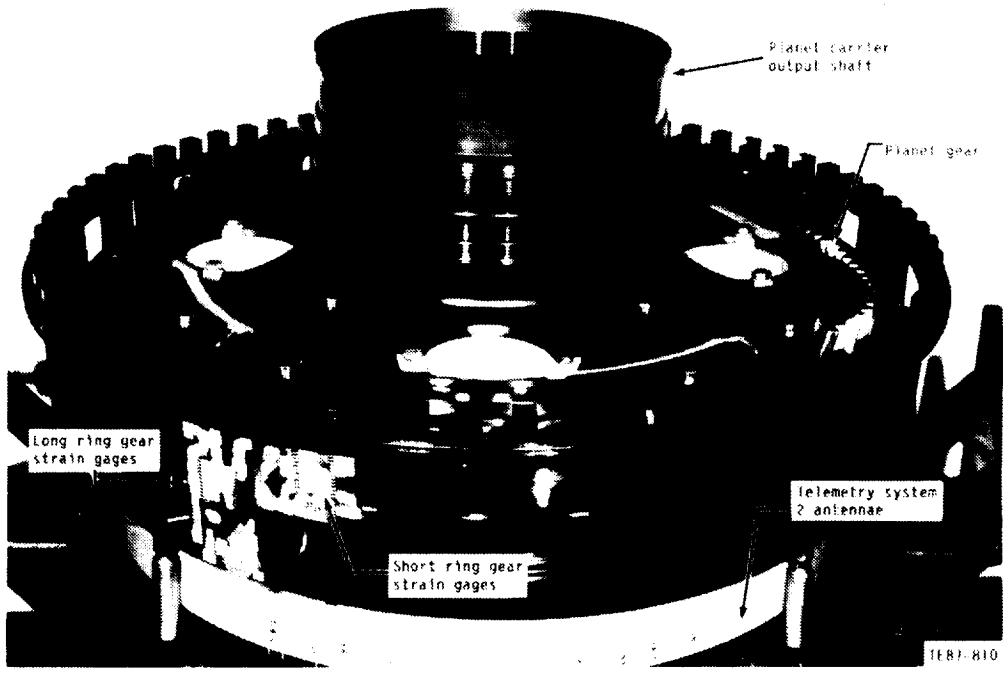

Figure 7.3-1. Ring gear strain gage installation.

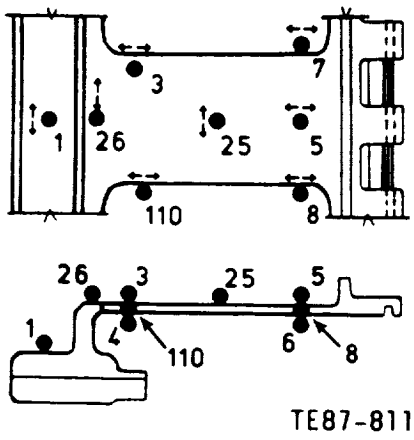

Figure 7.3-2. Strain gage locations--long ring gear.

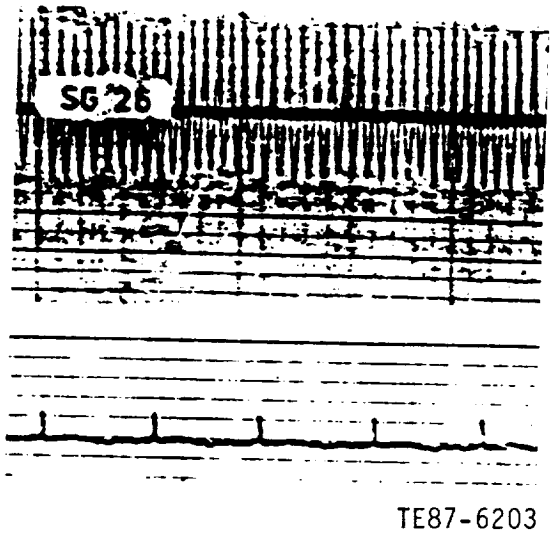

Figure 7.3-3. Long ring gear strain gage response at location 26.

speed are shown in Figure 7.3-4. These "waterfall" plots show both frequency and approximate amplitude content as well as vibratory trends through the speed range. A resonant condition would show high amplitudes usually over a well defined speed range. These data show constant low strain levels that are a function of speed (since all responses change frequency as the speed changes). Similar results were found for the short ring gear.

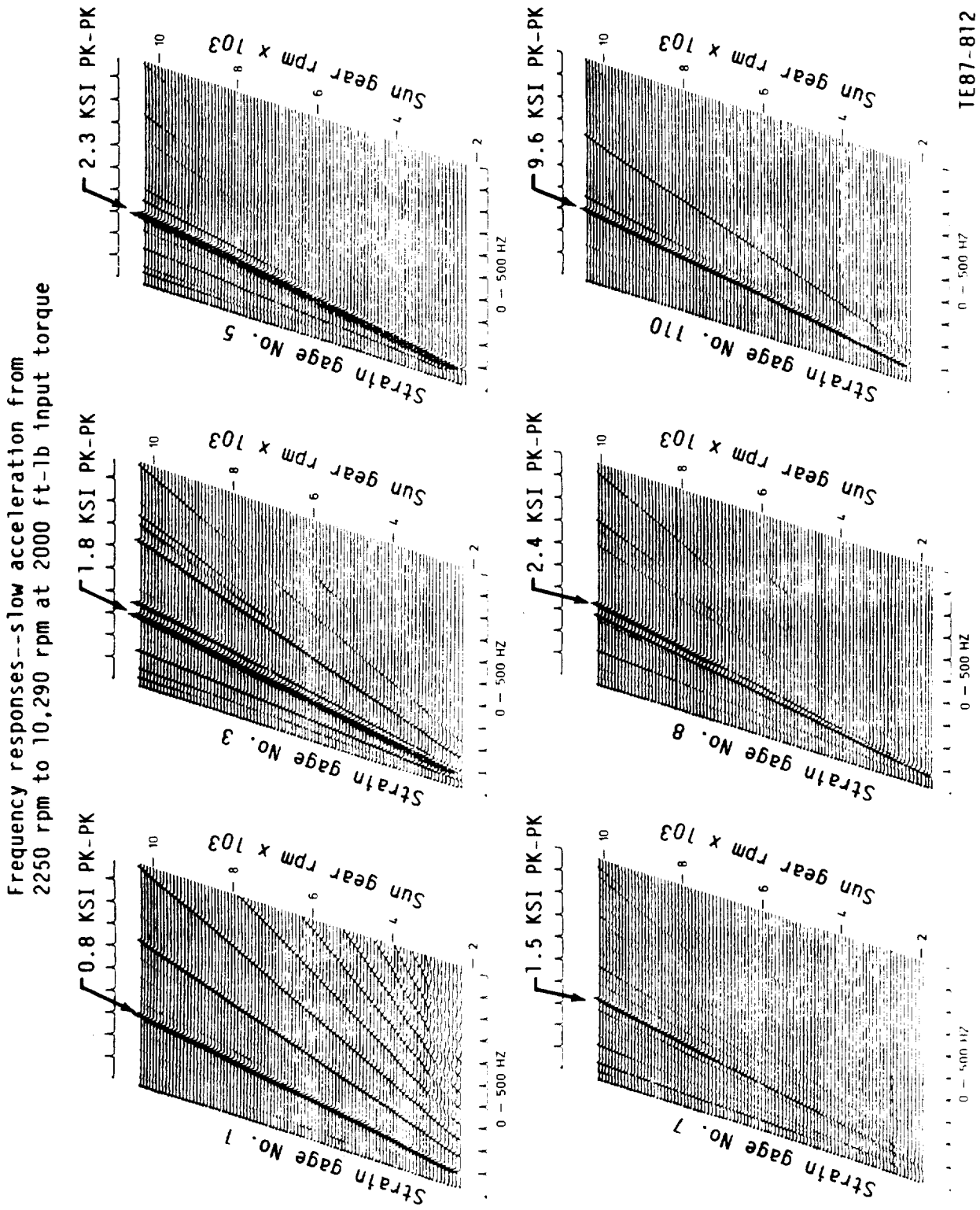

Figure 7.3-4. Response of ring gear strain gages during acceleration from 2250 rpm.

The flex diaphragm gages showed a slight response at about 7000 rpm during the 20-100% acceleration as shown in Figure 7.3-5. These gages are located at the base of the flexible diaphragm as shown in Figure 7.3-6. The stress levels shown here are well within the material allowable limits and pose no problem to the gearbox operation.

7.4 GEARBOX DEFLECTIONS

As described previously, proximity probes were located in a number of locations to monitor movement of the high speed drive shaft and several internal gearbox components. Figure 7.4-1 shows shaft movement at several locations as a function of speed. Apart from a slight increase in test gearbox shaft whip at 60% speed, motion was limited to runout. The shaft movement at 60% speed is related to the increase in flex diaphragm stress described previously. A similar response was seen in the flex diaphragm and ring gear movement.

7.5 GEARBOX EFFICIENCY

Gearbox power loss was determined by calculating the heat transferred to the oil. This technique is valid if convective heat transfer from the housing is low and if mass flow rate of the oil, specific heat of the oil, and temperature rise are known accurately. The gearbox housings were not insulated in these tests, but convective losses were determined to be low. Using the highest convective heat transfer coefficient applicable to this situation, 3 Btu/hr ft^2 °F, 1.7 hp would be lost to the atmosphere at the peak housing temperature. Compared to the total power loss at 13,000 hp (90.0 hp) this is a small percentage. Oil flow rates were determined with turbine type flowmeters calibrated with MIL-L-23699 oil at 180°F, which corresponds to the test conditions run in this test. Temperature rise is thought to be valid due to the repeatability of these measurements.

Specific heat was evaluated at the average of oil in and oil out temperature. A sample of the test lubricant was analyzed to determine specific heat. This value was then used to establish a specific heat/temperature relationship for the range of average oil temperature found in the test.

The results of these calculations are shown in Figure 7.5-1 as gearbox efficiency as a function of torque at an input speed of 10,290 rpm. Also, shown are the predicted values corresponding to takeoff (99.3%) and cruise (99.1%) power levels of the future Allison Prop-Fan demonstrator system--the 578 DX and the AGBT design point (99.4% @ 13,000 hp @ 9500 rpm). The maximum measured CR gearbox efficiency was 99.3% at the 13,000 hp design point. The high power points agree well with the predicted values. Part power efficiency was lower than predicted due to higher tare (no-load) losses. It is thought that oil was not being effectively removed from the housing during this test due to the remote location of the test equipment scavenge pump.

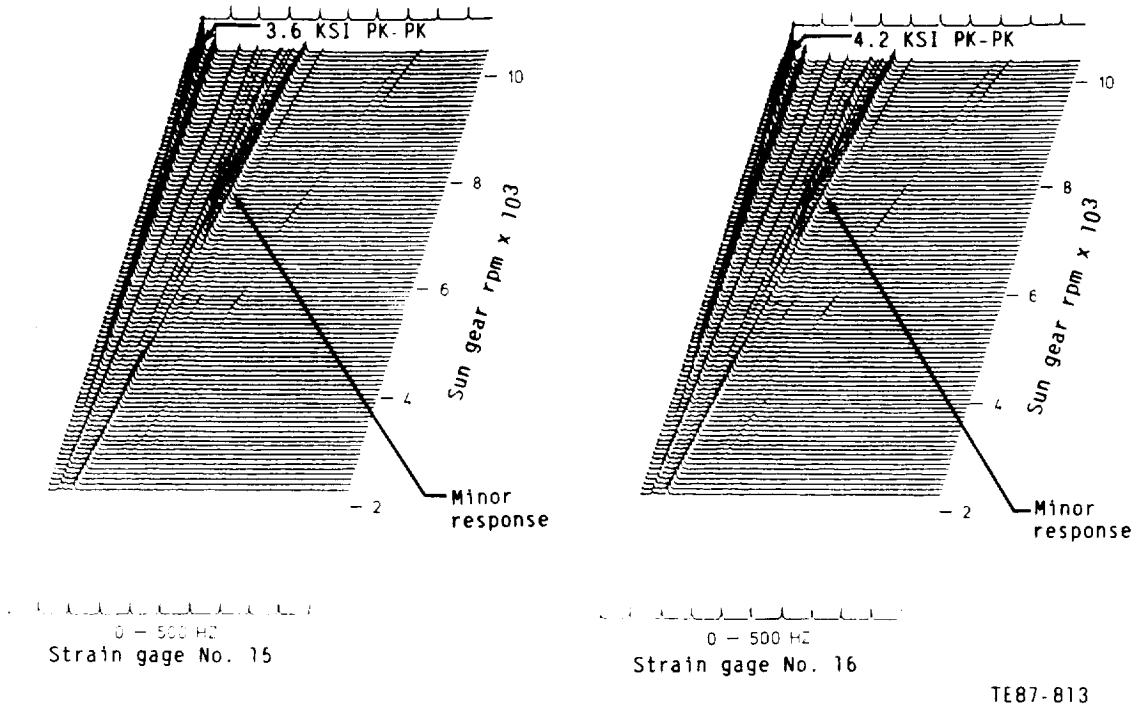

Figure 7.3-5. Flexible diaphragm strain gage response during an acceleration from 2250 rpm.

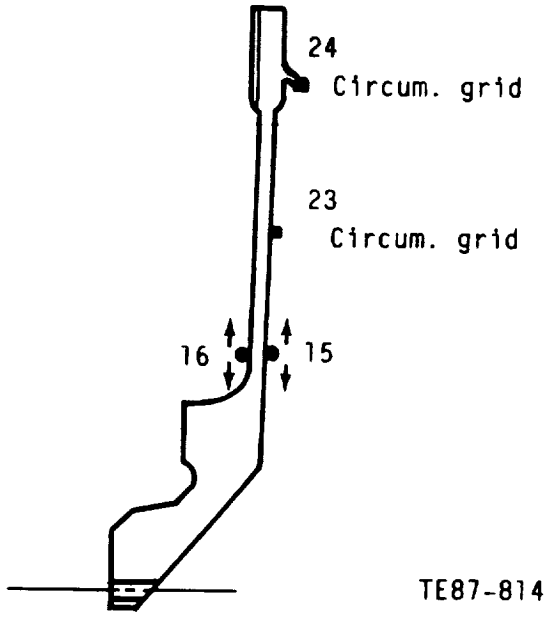

Figure 7.3-6. Flexible diaphragm strain gage locations.

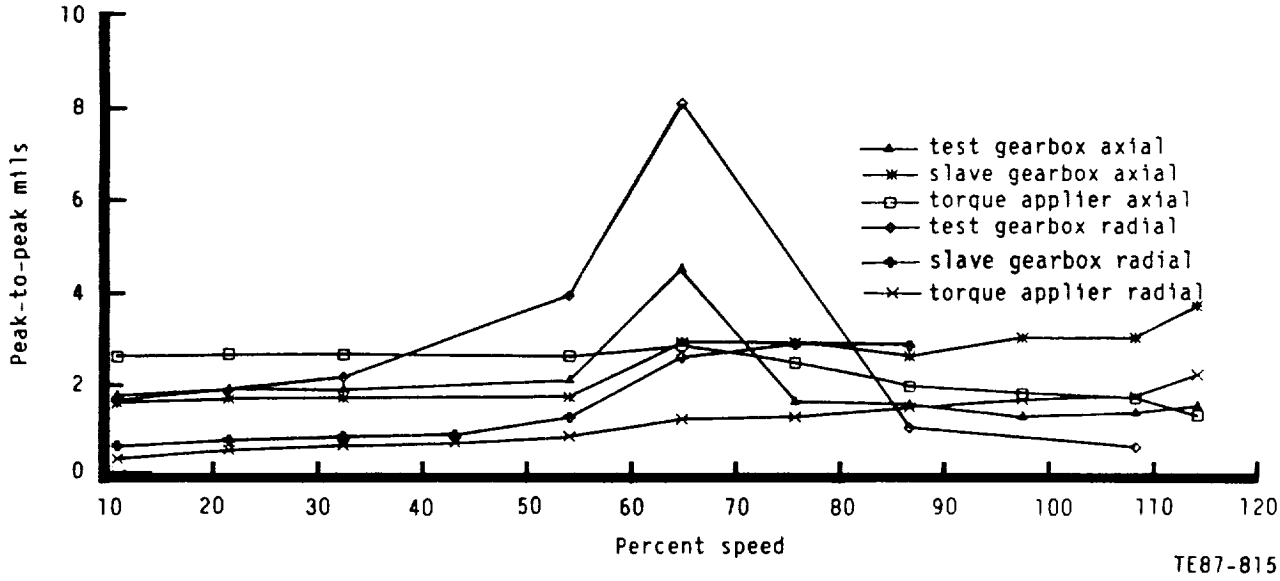

Figure 7.4-1. High speed drive shaft movement.

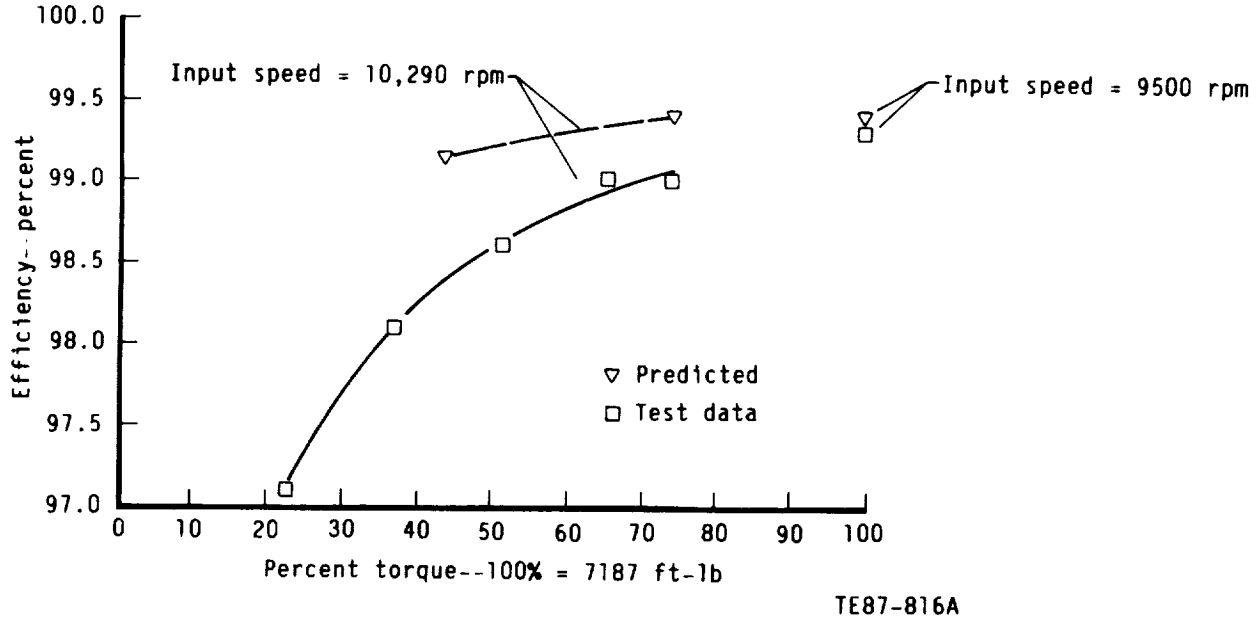

Figure 7.5-1. Gearbox efficiency as a function of torque.

7.6 EFFECT OF PROP LOADS ON GEARBOX

Prop loads were applied to the gearbox at two operating speeds while transmitting approximately 50% power. The test conditions are shown in Table 7.6-I. Temperatures and average vibration levels were affected more by the change in speed than prop loads. The maximum temperature increase at any location due to these loads was 6°F. The only exception was a 25°F increase at the inner race of the outboard tapered roller bearing due to the 15,000 lb thrust load at 110% speed. Most vibration levels varied by no more than 0.1 in./sec as the prop loads were changed.

In this test, strain on both the housing and prop shaft was monitored to determine the effects of these external loads on the structure. The thrust load applied in this test reached approximately 50% of the design value while the moment of 100,000 in.-lb represents 15% of the design point. The resulting strain values were very low and difficult to measure accurately. These values indicate that the housing stress is low and the prop shaft stress is somewhat higher than expected.

7.7 GEARBOX CONDITION AFTER TEARDOWNS

The condition of the gearbox at teardown was excellent. Contact patterns on the gear teeth were good. The sun and planet gear had full tooth contact. The planet bearings were like new except for a few circumferential scratches on several rollers. The tapered roller prop bearings had a milky appearance around the roller track. This is representative of a poor λ ratio due to either lack of oil film or rough surface finish. The 8 μ in. RMS surface finish will be improved to alleviate this condition.

Table 7.6-I.
Prop load test conditions.

Test	% Speed	% Power	Thrust--lb	Moment--in.-lb
1	87	45	15,000	-
2	110	54	15,000	-
3	87	45	-10,000	-
4	87	45	10,000	50,000
5	87	45	10,000	100,000
6	112	53	10,000	100,000

100% Speed = 9,500 rpm

100% Power = 13,000 hp

100% Torque = 7,187 ft-lb

8.0 SUMMARY OF RESULTS

8.1 CONCEPTUAL DESIGN

The conceptual design configuration studies served to place the AGBT detailed design effort on a well focused path. The conceptual design work evaluated many technologies, selected the most appropriate for the near-term AGBT design, and recommended others for further study. The selected design consists of the following:

Configuration -	differential planetary--simplest, lightest, and most easily controlled
Gear configuration -	double helical--low vibration
Planet bearing -	double row cylindrical--most capacity and compatible with double helical gears
Gear material -	CBS 600--high hot hardness and good fatigue life EMS 64500 (ring gear)--stable in heat treat
Prop shaft mount	tapered bearings--high capacity and minimum envelope
Housing material	aluminum--best for test rig

A number of alternate design approaches were considered and are recommended for further study:

Housing material -	Steel housings should be evaluated for reduced weight and the long life characteristics of low creep and low corrosion
Planet configuration -	Single helical planet gears mounted on tapered roller bearings could offer reduced production cost at the expense of additional development effort. Ring gear and sun gear thrust loads would have to be reacted.
Gear material -	CBS 1000 and M50-NiL should be evaluated further to determine their advantages in advanced production gear systems.

8.2 DETAILED DESIGN

The gearbox design was heavily influenced by the 30,000 hr mean time between unscheduled removal (MTBUR) life requirement. Since it is not economically practical to demonstrate a life of this magnitude through rig testing, design stress limits were kept low and extensive analysis was performed to document stresses and deflections. Three dimensional finite element analyses were performed on the following components to further define their operating characteristics: sun, planet and ring gears, housing, prop shaft, and planet carrier. Large scale computer programs were utilized to predict performance and optimize the design of all bearings.

The gear and bearing design concluded with a high degree of assurance that the life goal of 30,000 hr can be met. The required life is inherent in the design. Load sharing, which is critical in double helical gearing, was calculated to be within 13% of perfect balance. This was accomplished without having to impose selective fitting of parts.

The materials selected for the bearings and gears not only support the long life requirement, but also provide protection in an oil loss situation. CBS 600, M50, M50 NiL and EMS 64500 are all high hot hardness materials that will resist damage in a high temperature, high sliding situation.

Structural components were designed to keep external loads generated by the Prop-Fan away from gear and bearing contacts. These loads are carried directly to the mount pads. Deflections that do occur will not affect the gearset due to the flexibility of the diaphragm and the misalignment capability of the carrier ball bearing.

8.3 TESTING

The AGBT gearboxes were tested in a new Allison Prop-Fan gearbox test facility. This recirculating power rig loads one unit acting as a speed reducer against another acting as an increaser. Separate, external three micron absolute lubrication systems supplied clean, cool oil to the two gearboxes. Prop-Fan loads were applied to the housings to simulate flight conditions through a series of pneumatic rams.

The highly-instrumented advanced CR gearbox was successfully tested to design speed and power (13,000 HP), and to a 115% overspeed condition. CR gearbox efficiency was 99.3% at the design point. The unique rotating instrumentation operated satisfactorily and verified smooth, efficient gearbox operation.

Parametric tests demonstrated the predicted low vibration characteristics of double helical gearing, proper gear tooth load sharing, low stress levels, and the high load capacity of the prop tapered roller bearings. Vibration and temperature levels were primarily a function of speed. Applied external prop thrust and moment loads did not significantly affect gearbox temperature, vibration, or stress levels.

Both the test gearboxes and the test equipment performed quite well in these tests. The hardware was found to be in excellent condition after disassembly.

9.0 CONCLUSIONS

The AGBT program supports the following conclusions:

- o The AGBT design concept was proven satisfactory in a series of parametric tests.
- o The low vibration characteristics of double helical gearing were demonstrated.
- o Gear tooth load sharing, critical in double helical gearing, was achieved through the use of a flexible ring gear and diaphragm.
- o The 30,000 hr life prediction is supported by validation of stress levels predicted by finite element models.
- o Gearbox efficiency matches predicted values at high power levels.
- o CBS 600 was used successfully in the main power gears.
- o Tapered roller bearings functioned well as prop shaft bearings.

APPENDIX A

LIST OF SYMBOLS

2-D	two dimensional
3-D	three dimensional
APET	Advanced Prop-Fan Engine Technology
CR	counterrotating
F_N	normal force
FBD	free body diagram
FEA	finite element analysis
FEM	finite element model
HCF	high cycle fatigue
HCR	high contact ratio
HRC	hardness, Rockwell C scale
i.r.	inner ring
L/D	length/diameter
LH	left-hand
LP	low pressure
M_P	pitching moment
MTBUR	mean time between unscheduled removal
o.r.	outer ring
PTA	Prop-Fan test assessment
PTO	power takeoff
RH	right-hand
S/N	stress versus number of cycles

REFERENCES

1. R. D. Anderson, J. A. Korn, and D. V. Staton, "Advanced Prop-Fan Engine Technology (APET) Definition Study" (NASA CR168115--Allison EDR 11283), July 1985.
2. Y. P. Chiu and J. Y. Liu, "Analysis of a Planet Bearing in a Gear Transmission System," ASME Journal of Lubrication Technology, January 1976, pp 40-46.
3. N. E. Anderson and S. H. Loewenthal, "Design of Spur Gears for Improved Efficiency," ASME Journal of Mechanical Design, Vol. 104, October 1982, pp 767-774.
4. H. J. Casper, P. M. Ku, H. E. Staph, "Gear Tooth Scoring Investigation," USAAMRDL-TR-75-33, July 1975.
5. T. A. Harris, "Rolling Bearing Analysis," John Wiley and Sons, Inc., 1966, pp 446-450.
6. D. C. Witte, "Operating Torque of Tapered Roller Bearings," ASLE Transactions, Vol. 16, No. 1, January 1973, pp 61-67.
7. N. E. Anderson [redacted] S. H. Loewenthal, "An Analytical Method to Predict Efficiency of Aircraft Gearboxes," NASA TM83716, AIAA-84-1500, USAAVSCOM TR-84-C-8. (Presented at the Twentieth Joint Propulsion Conference cosponsored by AIAA, SAE, and ASME, Cincinnati, OH, June 11-13, 1984.)

1. Report No.	2. Government Accession No.	3. Recipient's Catalog No.
CR-179625		

4. Title and Subtitle	5. Report Date
Advanced Gearbox Technology (AGBT) Final Report	June 1987
	6. Performing Organization Code

7. Author(s)	8. Performing Organization Report No.
N. E. Anderson, R. W. Cedoz, E. E. Salama, D. A. Wagner	EDR 12909
	10. Work Unit No.

9. Performing Organization Name and Address	11. Contract or Grant No.
Allison Gas Turbine Division, GM Corp. P.O. Box Box 420 Indianapolis, IN 46206-0420	NAS3-24341
	13. Type of Report and Period Covered Contractor Report Aug. 84 thru Jan. 87

12. Sponsoring Agency Name and Address	14. Sponsoring Agency Code
NASA-Lewis Research Center 21000 Brookpark Rd. Cleveland, Ohio 44135	RTOP 535-03-22

15. Supplementary Notes

NASA Project Manager - D. C. Reemsnyder
Published in part and presented at the June 1987 AIAA/SAE/ASME/ASEE 23rd Joint Propulsion Conference in San Diego, CA

16. Abstract

An advanced 13,000 HP. counterrotating (CR) gearbox was designed and successfully tested to provide a technology base for future designs of geared propfan propulsion systems for both commercial and military aircraft. The advanced technology CR gearbox was designed for high efficiency, low weight, long life, and improved maintainability. The differential planetary CR gearbox features double helical gears, double row cylindrical roller bearings integral with planet gears, tapered roller prop support bearings, and a flexible ring gear and diaphragm to provide load sharing.

A new Allison propfan back-to-back gearbox test facility was constructed. Extensive rotating and stationary instrumentation was used to measure temperature, strain, vibration, deflection, and efficiency under representative flight operating conditions. The tests verified smooth, efficient gearbox operation.

The highly-instrumented advanced CR gearbox was successfully tested to design speed and power (13,000 HP), and to a 115% overspeed condition. Measured CR gearbox efficiency was 99.3% at the design point based on heat loss to the oil. Tests demonstrated low vibration characteristics of double helical gearing, proper gear tooth load sharing, low stress levels, and the high load capacity of the prop tapered roller bearings. Applied external prop loads did not significantly affect gearbox temperature, vibration, or stress levels. Gearbox hardware was in excellent condition after the tests with no indication of distress.

17. Key Words (Suggested by Author(s))	18. Distribution Statement
Advanced Gearbox Gearbox - Turboprop Gearbox - Aircraft	[redacted]